

X28271952X



2805241909

1

**ATROPHY IN MULTIPLE SCLEROSIS: MEASUREMENT
AND CLINICAL IMPLICATIONS**

Nicholas Andrew Losseff

A thesis submitted for the degree of Doctor of Medicine to The University
of London, 1997.

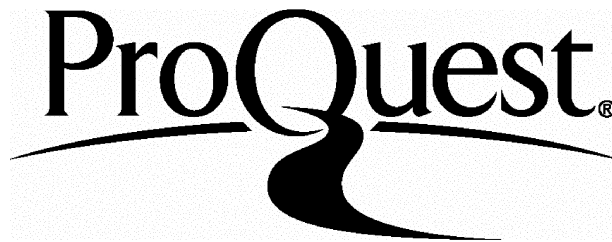
ProQuest Number: U642901

All rights reserved

INFORMATION TO ALL USERS

The quality of this reproduction is dependent upon the quality of the copy submitted.

In the unlikely event that the author did not send a complete manuscript and there are missing pages, these will be noted. Also, if material had to be removed, a note will indicate the deletion.



ProQuest U642901

Published by ProQuest LLC(2016). Copyright of the Dissertation is held by the Author.

All rights reserved.

This work is protected against unauthorized copying under Title 17, United States Code.
Microform Edition © ProQuest LLC.

ProQuest LLC
789 East Eisenhower Parkway
P.O. Box 1346
Ann Arbor, MI 48106-1346

Abstract

This thesis describes the development and application of new magnetic resonance imaging techniques to characterise and quantify underlying tissue changes in multiple sclerosis (MS) that are responsible for or associated with disability. Characterisation, measurement of such changes and their relationship to other quantitative parameters of disease activity or progression may yield important information on the pathophysiology of disability in MS. They would also be of considerable value in evaluating a putative treatment.

The work described focuses on the measurement of spinal cord and cerebral atrophy. The development and evaluation of new highly reproducible quantitative techniques are described. The results of cross-sectional and longitudinal clinical studies presented. These demonstrate that the measurement of atrophy is a powerful way in which to monitor clinically relevant disease progression. The results also indicate that the development of atrophy in MS is common.

The techniques are reviewed critically, compared to other current clinical and imaging measures of disease progression and shown to have high sensitivity to change and greater possible specificity to underlying pathology. The role of axonal loss in the development of atrophy and its relationship to inflammatory activity are discussed. It is concluded that atrophy may develop independently of inflammation. Finally improved techniques to further investigate the nature and significance of atrophy are suggested.

Contents

page no

Abstract	2
Acknowledgements	7

Chapter 1: Introduction

1.1: The personal and social cost of multiple sclerosis	9
1.2: Background	10
1.3: A hypothesis	12
1.4: Multiple Sclerosis	13
1.5: Previous MRI studies in multiple sclerosis	23
1.6: Pathophysiology of symptom production	33
1.7: Conclusions	35

Chapter 2: Common methodology

2.1: Introduction	36
2.2: Basic principles of magnetic resonance imaging	36
2.3: Quantification in MRI	49
2.4: Clinical measurement	54

Chapter 3: Spinal cord atrophy

3.1: Lessons from a serial study	59
3.2: Development of a new technique to measure spinal cord atrophy	70

3.3: Conclusions of the new study at C2	85
---	----

Chapter 4: Cerebral atrophy

4.1: Why measure cerebral atrophy	89
4.2: A new technique to measure cerebral atrophy	90
4.3: A serial clinical study of progressive cerebral atrophy	98
4.4: Discussion	107

Chapter 5: Conclusion

5.1: Practical uses of techniques to measure atrophy	114
5.2: Concluding remarks	115

Bibliography	120
---------------------	-----

Appendix	141
-----------------	-----

List of tables

Chapter 1: Introduction

1: Mean time spent in years at a given level of the DSS for patients who progress to the next level	57
---	----

Chapter 3: Spinal cord atrophy

2: Clinical characteristics	63
3: Cross sectional area measurements in healthy volunteers	64
4: Prevalence of atrophy at one or more levels	65
5: Mean cross sectional area in mm ² at 4 levels by patient group	65
6: Change in cord area in mm ² stratified by clinical progression	66
7: Intraobserver reproducibility measurements	79
8: Characteristics of patients and controls	81
9: Individual patient subgroups	84

Chapter 4: Cerebral atrophy

10: Clinical and MRI characteristics stratified by the development of atrophy	104
---	-----

List of figures***Chapter 2: Common methodology***

1: Precession of a single proton in the co-ordinate system	38
2: Free induction decay	41
3: Signal intensity from two tissues with differing TR's	42
4: Generation of a T2 curve	43
5: T2 curves for two different tissues	44

Chapter 3: Spinal cord atrophy

6: Gradient echo at C5	62
7: Scatter plot of cord area at baseline against change in cord area	67
8: A control scanned serially at the C5 level	69
9: Gradient echo at C2	70
10: Axial reformat from a volume acquired inversion prepared sequence	71
11: Benign and progressive MS	74
12: ROI “inner” and “outer”	76
13: Contrast adjusted phantom	78
14: Scatter chart of EDSS and cord area in all patients	82

Chapter 4: Cerebral atrophy

15: A brain extraction using eXKull	93
16: Consistency of gadolinium across time	94
17: Reproducibility assessed with weekly scanning	96
18: Serial measurement over 18 months	102
19: Development of atrophy	106

Acknowledgements

All work described in this thesis was carried out in the NMR Research Unit at The Institute of Neurology, Queen Square London. The NMR Research unit is supported by a generous grant from the Multiple Sclerosis Society of Great Britain and Northern Ireland. All patients who participated in studies described gave informed written consent to enter them and I am grateful for their willingness and time. All studies were approved by the ethical committee of the National Hospital for Neurology and Neurosurgery.

I am very grateful to my supervisor Dr Alan Thompson for his help, encouragement and ability to see the trees from the wood. I am also very grateful for the help and advice given to me by Professor David Miller, Professor Ian McDonald, Dr Paul Tofts, Dr Liqun Wang and Dr Carolyn Gabriel.

Many thanks are also due to David MacManus, Stephanie Webb, Helen Gallagher and Kim Birnie who carried out all the imaging and reformatting for all studies described in this thesis. Other help was obtained from Dr Jonathan O’Riordan who was the other observer in the calculation of reproducibility for the technique to measure spinal cord atrophy. Dr Paul Tofts built the phantom used to assess the accuracy of the new technique to measure spinal cord atrophy. Dr Gareth Barker performed the image manipulation on the spinal cord phantom. Dr Mary Gawne-Cain inspected the scans used in the cerebral atrophy study for correct positioning. Dr Ming Lai collected all the data from the anti-CD4 trial, performed the disability measures and calculated the lesion load and gadolinium volumes. Mr Done Yoo designed the eXKull software which I used to develop the new technique to measure cerebral atrophy. Dr Liqun Wang wrote several software programs which eased various aspects of quantitative data analysis. I performed all other work described in the thesis and all relevant analysis was carried out blind. My position was generously supported by the Brain Research Trust and funds available to Dr Alan Thompson.

The work described has resulted in the following publications:

Losseff, N.A., Webb, S.L., O Riordan, J.I., Page, R., Wang, L., Barker, G.J., Tofts, P.S., McDonald, W.I., Miller, D.H. and Thompson, A.J. (1996) Spinal cord atrophy and disability in multiple sclerosis: A new reproducible and sensitive MRI technique with potential to monitor disease progression. *Brain* **119**, 101-108.

Losseff, N.A., Wang, L., Lai, M., Yoo, D.S., Gawne-Cain, M.L., McDonald, W.I., Miller, D.H. and Thompson, A.J. (1996) Progressive cerebral atrophy in multiple sclerosis: A serial MRI study. *Brain* **119**, 2009-2019. See "news" in *The Lancet* 1997; **349**, 35.

The techniques that I describe later are now being put into use in international treatment trials. I was awarded the Queen Square Prize for Neurology, a Multiple Sclerosis Society Grant Holders meeting prize and a European Neurological Society prize for the work described herein.

Chapter 1: Introduction

1.1 The personal and social cost of multiple sclerosis

There are probably about 87 000 people in the U.K. with multiple sclerosis (MS) (Holmes et al. 1995) and community based studies suggest that approximately 50% will require assistance for mobility within 15 years of onset (Weinshenker et al. 1989a). In addition to physical disability around 40% of community based patients show evidence of cognitive impairment when comprehensively tested (Rao et al. 1991a). These disabilities summate resulting in social dysfunction and unemployment (Rao et al. 1991b). Depression unrelated to cognitive dysfunction is common (Schubert and Foliart, 1993) and an increased risk of suicide has been reported of between 1.4-7 times that of the general population (Sadovnick et al. 1992; Weinshenker, 1994). Life expectancy is only slightly reduced overall (by approximately 6-7 years (Sadovnick et al. 1992)) but those with very high levels of physical disability have a 4 fold increase in case fatality when compared to controls (Sadovnick et al. 1992). A recent study (Holmes et al. 1995) in the U.K. has estimated the total annual cost burden at almost £1.2 billion from a sample survey of 672 members of the Multiple Sclerosis Society, based on the assumption that there was an even distribution in the community of 3 broad disability categories: unaided unlimited ambulation, requiring unilateral support for ambulation and wheelchair dependence. Of this £1.2 billion, over half is accounted for by lost earnings and state benefits, £153 million for NHS costs, £148 million in lost tax revenue, £76 million for industry loss and £140 million for private expense.

1.2 Background

The cause or causes of the clinical picture we term multiple sclerosis remain unknown and hence basic observations on the evolution of the disease and the associated disability are very important. This thesis describes work using Magnetic Resonance Imaging (MRI) which attempts to characterise and quantify the underlying central nervous system (CNS) changes that are responsible for this disability. There are two important reasons for this: Firstly and most importantly, if changes relevant to disability could be characterised and quantified, then the analysis of the evolution of such changes and their relationship to other measures of disease activity or progression may yield important information on the pathophysiology of disease progression in multiple sclerosis. Secondly if such changes could be quantified with sufficient reproducibility and accuracy to allow a high level of sensitivity in detecting meaningful change (i.e. responsiveness), then this would be of considerable value in evaluating the efficacy of a putative treatment. This last point is of topical importance. There is considerable interest in the use of quantitative MRI outcome measures in treatment trials (Miller et al. 1996) in view of the protean problems associated with disability scales, in particular their poor responsiveness, poor reproducibility (Francis et al. 1991) and tendency to be affected by day to day fluctuation in function (Whitaker et al. 1995). However it is well recognised that most standard MRI techniques are poorly predictive of outcome with regard to the development of disability. In MS, treatment with beta-interferon results in a significant decrease in the frequency of episodes of blood brain barrier opening as evidenced by gadolinium enhancement. Beta interferon (IFN) retards significantly the progression of "lesion load", (Paty and Li, 1993, The IFNB Multiple Sclerosis Study Group and the University of British Columbia MS/MRI Analysis Group, 1995) but it has not been convincingly demonstrated to slow the evolution of disability. There is thus a need to include

in treatment trials outcome measures that clearly relate to the development of disability but are superior to current clinical assessment methods. This thesis describes experiments suggesting that measurement of atrophy of the brain and spinal cord may provide such indices.

MRI has undoubtedly increased our understanding of the pathophysiology of multiple sclerosis and is a rapidly advancing field. Most investigators have concentrated on characterisation of the obvious focal visible abnormalities and have termed these "lesions". Lesions correspond well to underlying areas of abnormality detected by pathological examination (Stewart et al. 1986; Ormerod et al. 1987; Newcombe et al. 1991). The use of conventional cranial MRI to detect lesions is useful both in diagnosis and in predicting those with clinically isolated syndromes suggestive of multiple sclerosis who will go on to develop definite disease (Morrisey et al. 1993), but the relationship of lesions (investigated both by MRI and pathology) to the development of disability is more complex and at best limited (Thompson et al. 1990; Kidd et al. 1993; Filippi et al. 1994; Filippi et al. 1995c). This may be due in part to the pathological heterogeneity of the lesion. Demyelination, inflammation, axonal loss and gliosis probably have distinct functional consequences but they cannot be differentiated by conventional MRI. More pathologically specific imaging techniques such as magnetisation transfer imaging (Gass et al. 1994) and spectroscopy (Arnold et al. 1994) have considerable potential in this regard but there still remains a fundamental problem with characterisation (by whatever technique) of focal abnormalities: If a lesion is surrounded by an area of normal brain and there is complete destruction of tissue within the lesion then either a hole will develop or the surrounding tissue (or some other tissue reaction) will fill the space. If it is surrounding tissue that fills the space, the characteristics (e.g. a metabolite concentration) of the focal area *may* not appear to change. The only detectable change may

be contraction of the edges of the whole structure in which the focal abnormality is contained. Observation suggests that the nervous system can respond in this plastic manner, for in addition to lesions there is another abnormality evolving which is detectable only at the borders of the brain and the spinal cord with the cerebrospinal fluid (CSF) spaces: diffuse and symmetrical atrophy (Noseworthy et al. 1984). It seems likely that atrophy represents complete loss of tissue, which from a functional point of view may be the greatest insult, yet the investigation of atrophy has been relatively neglected.

1.3 A hypothesis

If we assume that atrophy to a large extent does represent complete loss of tissue then an important and workable hypothesis can be formed: *That atrophy is a significant change associated with or responsible for disease progression and therefore disability in multiple sclerosis.* To investigate this hypothesis it has been necessary to develop new highly reproducible techniques to quantify volumes of two key CNS sites; the high cervical spinal cord and the cerebral white matter. Using these techniques cross sectional and serial clinical studies have been carried out exploring the relationship between atrophy, disability and other quantitative parameters.

1.4 Multiple Sclerosis

1.4 (a) Clinical background and definitions:

MS is classically described as a relapsing-remitting disorder that affects multiple white matter tracts within the CNS, with its usual onset in young adults. Relapses are defined as acute or subacute episodes of clinical dysfunction that usually reach a peak in days to weeks followed by a period of relatively little change, and finally remission to a variable extent. Isolated or mixed motor or sensory symptoms are the most frequent initial symptoms, with less frequent involvement of visual, cerebellar and brain stem structures. 85 % of patients begin with a relapsing-remitting course (Runmarker and Andersen, 1993).

After this initial relapsing-remitting course the majority of patients will enter a progressive phase of the disease (50% within 10 years) (Runmarker and Andersen, 1993) characterised by permanent and increasing disability. Patients that begin with a relapsing-remitting course that then evolve to a progressive course are termed *secondary progressive* and they may in addition to progression continue or cease to have relapses.

Some patients have an illness in which the course is progressive from onset without superadded relapses. This form of the disease is termed *primary progressive*, and probably accounts for approximately 10-15% of cases (Weinshenker et al. 1989a; Runmarker and Andersen, 1993). Patients with primary progressive disease tend to present at a later age and in most cases the condition manifests as a progressive paraparesis or more rarely as a progressive hemiparesis, cerebellar syndrome or optic neuropathy. A final somewhat arbitrary definition is that of *benign* MS, which for the purposes of this work refers to patients with a disease duration greater than or equal to 10 years who have not developed

significant disability (a score of not greater than 3 on Kurtzke's Expanded Disability Status Scale (Kurtzke, 1983)). As will be discussed later the development of disability associated with the progressive phase of the disease is difficult to predict and benign cases may enter the progressive phase even after 15 to 20 years.

1.4 (b) Diagnostic criteria:

The diagnosis of MS is traditionally based on clinical history and examination and there is much truth in Kurtzke's observation that "multiple sclerosis is what a good neurologist says multiple sclerosis is". However in conducting research it is necessary to improve the homogeneity of patient groups and the Schumacher committee (Schumacher et al. 1965) elaborated six items needed to diagnose clinically definite MS: objective CNS dysfunction, involvement of white matter structures, two or more sites of CNS involvement, relapsing remitting or chronic (more than 6 months) progressive course, age 10-50 yrs at onset and no better explanation of symptoms assessed by a competent neurologist. The Poser committee later modified these criteria (Poser et al. 1983), expanding the age of onset to 59 and incorporating data derived from laboratory studies (CSF analysis), evoked potentials and neuroimaging. In this classification, patients with definite MS fall into two categories: (a) clinically definite; in which they have suffered two attacks separated in time and have clinical evidence of two separate lesions, or two attacks and clinical evidence of one lesion with paraclinical evidence of another different lesion. (b) laboratory supported definite; in which there is clinical evidence of two lesions and oligoclonal bands in the CSF, or clinical evidence of one lesion and paraclinical evidence of another different lesion (e.g. from imaging), plus oligoclonal bands in the CSF. All patients described in this work have

clinically definite or in the case of primary progressive patients, laboratory supported definite MS as described by the Poser committee.

1.4 (c) Epidemiology:

Surveys consistently show that MS is more common in women than men and a meta-analysis from studies conducted before 1977 calculated that the risk for women was 1.4 times greater than that for men (Acheson, 1977). The peak age of onset is 25-30 years, and is slightly later in men than women. Onset may be as late as the seventh or eighth decade and is very rare before the age of 15. The pattern of age of onset is well established and age specific incidence curves do not alter in their shape with the underlying frequency of disease.

There are over 250 prevalence surveys for MS which serve as the basis for identification of high prevalence areas ($> 60/100\ 000$ population). These areas include northern and central Europe, southern Canada and the northern United States, New Zealand and southeastern Australia. In general prevalence falls off with latitude gradient but there remain some important exceptions to this. Japan is a low risk area whilst at the same latitude as western European countries and the white population of South Africa in which the prevalence is medium is surrounded by a black population in which MS is virtually unknown. Race may therefore be in part responsible for the observed distribution but data on migrant populations suggest those migrating from a high prevalence area after a certain critical age retain the risk of the original geographic region (Dean and Kurtzke, 1971) suggesting an environmental agent acting in early childhood as a possible aetiologic factor.

1.4 (d) Genetics:

MS occurs more commonly in Caucasians on a genetic background associated with specific major histocompatibility complex (MHC) haplotypes (DR15/DQ6), and possibly other loci (Compston et al. 1995). Increasing evidence for a genetic contribution to aetiology is emerging. The geographical distribution, high prevalence of MS in people of European origin living in countries where the native population has a low incidence such as New Zealand (Miller et al. 1992), family studies, concordance rates in twins and studies of conjugal MS all support this (Compston et al. 1995). In a recent study of twins in which zygosity was confirmed with genotype analysis the concordance rate for monozygotes was 25% compared with 3% for dizygotes (Mumford et al. 1994). Whilst it is commonly believed that the difference between mono and dizygotic twins is a measure of genetic influence it is much more an indication of the number of genes involved in susceptibility and the dizygotic concordance rates suggest strongly an oligogenic determination of susceptibility (Risch, 1990). This low risk (which is echoed by familial studies of sibs and first degree relatives) is entirely consistent with this hypothesis.

Genetic studies have also raised important questions regarding environmental influence. In the Canadian adoptee study (Ebers et al. 1995) it has been clearly demonstrated that the risk for the first degree nonbiological relatives of an index case (adoptive parents and sibs) is no greater than that in the general population, suggesting that if environmental influences are important then they are likely to be operating at a population level.

1.4 (e) Natural history:

Disability

Another aspect may be added to the clinical description of types of MS. This is a description of the impairment, disability or handicap produced by the disease. Clinical symptoms and signs may be quantified by the use of impairment scales, limitations in activities of daily living by disability scales and limitations of social interaction by handicap scales. The most commonly applied of these measures is Kurtzke's Expanded Disability Status Scale (EDSS) (Kurtzke, 1983). The EDSS is the 20 point (0, 0.5, 1, 1.5...10) successor of the 10 point (0,1,2,3...10) DSS (Disability Status Scale). In effect the degree of disability reflected by a given integer on the DSS is the same as on the EDSS. The EDSS scale mixes impairment and disability but to date remains the commonest scale used for primary outcome in treatment trials and natural history studies. The long term development of disability is the major concern of patients and physicians and permanent severe disability usually develops in the context of progressive MS. One previous study has shown that within 10 years of onset, 50% of an incidence cohort of 308 patients had developed progressive MS (Runmarker and Andersen, 1993). This cohort was followed for at least 25 years and 50% of patients had reached DSS 6 (requiring unilateral support for ambulation) by 15 years. Another study (Weinshenker et al. 1989a) found that 12% of 231 initially relapsing-remitting patients developed secondary progressive MS when followed for five years but this had risen to 41% of 179 patients followed from 6 to 10 years and 57% of 118 patients followed from 11-15 years. In this study, which is the largest community based study (1099 patients) to apply survival analysis to the quantification of disability, by 15 years after onset 80% were at or

beyond DSS 3 (minimal disability), 50% were at DSS 6, 10% were at DSS 8 (wheelchair dependant) and 2% were dead. Whether there is a distinct pathophysiological basis for transition from relapsing-remitting disease to progression is unknown.

Prognostic factors

The biological basis for differing outcome is poorly understood and the variables predicting poor outcome (with regard to disability) differ considerably from study to study. Many recent studies as described above have used a multivariate regression approach to develop models, such as the factors predicting time to reach DSS 6 (Weinshenker et al. 1989a; Weinshenker et al. 1991; Runmarker and Andersen, 1993). However the factors examined, such as age of onset, sex, initial clinical presentation, temporal course and disability status account for little of the variation in DSS scores amongst individuals. The largest of these studies (Weinshenker et al. 1991) found that the models refine the predicted time for a given individual to reach DSS 6 by only 30% over the median time for the population as a whole. Individual studies differ in their conclusions regarding individual predictive factors for the later development of disability, but in clinical practice patients with relapsing-remitting disease are at greatest risk if they suffer (in approximate order of decreasing importance): frequent exacerbations, motor, cerebellar and possibly brain stem disturbance, older age of onset and residual pyramidal or cerebellar deficits 6 months following an attack. The development of significant disability (DSS 3) within 5 years from onset is probably the best clinical predictor of later worsening disability (Kurtzke et al. 1977; Miller et al. 1992).

1.4 (g) Pathology:

The principal histological features of typical MS are CNS inflammation and demyelination with relative axon preservation (Charcot, 1868; Dawson, 1916). MS "plaques" are often grossly visible and are well demarcated areas of demyelination not confined to specific areas or anatomical tracts. Large areas of white matter are commonly involved although grey matter plaques are also numerous (Brownell and Hughes, 1962; Powell and Lampert, 1983). In areas devoid of myelin, inflammatory cell infiltrates may also be found, such as the retina and leptomeninges (Adams et al. 1985; Lightman et al. 1987). MS lesions are multifocal and their distribution varies amongst patients. It was initially thought that the variation in the clinical manifestations of the disease was due to differences in lesion location, but it has proved difficult to correlate both pathological and chronic imaging abnormalities with clinical deficits.

In European cases, the optic nerves (Ulrich and Groebke-Lorenz, 1976), periventricular white matter (Brownell and Hughes, 1962) and spinal cord (Oppenheimer, 1978) are most commonly involved. Atrophy is a common non-specific finding and the author is only aware of one study in which microscopic appearances have been correlated with the presence of atrophy. This study (Fontaine et al. 1994) demonstrated a relationship between atrophy of the corpus callosum and axonal loss. Although MS is classically described as a demyelinating disease with relative preservation of axons there are numerous pathological reports of axonal loss (Bielschowsky, 1903; Dawson, 1916; Greenfield and King, 1936; Adams and Kubik, 1952; Ozawa et al. 1994; Lassmann et al. 1994) and this may be extreme. Biopsies show that axonal loss may occur acutely (Ozawa et al. 1994). These studies may suggest that the factors that mediate injury to myelin may also damage axons.

In addition the oligodendrocyte and its myelin sheath may not be a simple passive insulation but also help to sustain the axon, hence oligodendrocyte death may result in secondary axonal loss . It has been found that selective myelin damage is more common in the early stages of MS but as the disease progresses the oligodendrocyte itself dies and different mechanisms may underpin this (Lassmann et al. 1994).

Evolution of multiple sclerosis plaques

At any given time plaques are variable in size, extent and stage of evolution. They probably evolve through multiple demyelinating and remyelinating episodes (Prineas et al. 1993a) the end result being a chronic plaque. Post mortem examination frequently shows a mixture of old inactive (non-inflammatory) and new active inflammatory demyelinating lesions. Histological examination of active plaques reveals evidence of a cellular immune response with perivascular infiltration of lymphocytes (predominantly T cells) and macrophages with occasional plasma cells. Perivascular and interstitial oedema is often prominent. Within the plaque myelin is disrupted and myelin debris may be found in clumps or within lipid rich "foamy" macrophages. A recent pathological study of primary progressive MS has shown significantly less inflammation than that found in secondary progressive disease (Revesz et al. 1994). The other important histological feature of plaques is astrogliosis. Acute MS plaques show astrocyte hypertrophy and in chronic lesions the extent of astrogliosis is considerable.

The earliest event in the development of a new plaque is not definitely known but in patients presenting with mass lesions who have undergone biopsy considerable demyelination is usually shown (Ozawa et al. 1994). However from pathological studies

(Powell and Lampert, 1983) and evidence from imaging (Kermode et al. 1990; Katz et al. 1993), the cellular immune response is believed by most to be the earliest identifiable event in the genesis of a new plaque. Whether this immune response is the primary pathology or a response to another pathological process within the brain is unknown, although most assume it to be a response to an underlying CNS antigen or multiple antigens of which myelin associated proteins (myelin basic protein being the most abundant) are the most likely candidates.

Immunopathology

In cellular immune reactions in the CNS, T cells, B cells and monocytes migrate from the circulation through the walls of small venules and capillaries into the perivascular space and parenchyma. The first barrier in the migration of these cells into the CNS is the endothelium and much research has been carried out elucidating the interactions that take place between endothelial cells and specific molecules that mediate leucocyte attachment and migration. Early in this migration endothelial cells develop a high endothelial venule like morphology and enhanced deposition of plasma proteins (such as fibronectin and fibrinogen) and members of the immunoglobulin gene and selectin adhesion molecule families are expressed on the luminal surface (Esiri and Morris, 1991; Lassmann et al. 1991). These proteins mediate leucocyte adhesion to the endothelium (Languino et al. 1993) as they are recognised by leucocyte cell surface molecules and leucocyte-endothelial cell adhesion is promoted. It is possible that the initiating event may be presentation of antigen to CD4+ T cells by endothelial cells, as class II MHC molecules have been found on CNS microvascular endothelial cells in the pre-inflammatory phase of experimental allergic encephalomyelitis

in guinea pigs. Human cerebral endothelial cells do express class II MHC if they are exposed to interferon-gamma in vitro (McCarron et al. 1991) but in MS it has been difficult to differentiate endothelial cells and perivascular microglia (another potential source of antigen presentation) by immunohistochemical staining.

The next barrier to CNS migration is the smooth muscle wall. Distinct immunological roles for smooth muscle cells have been demonstrated in animals and are proposed to also occur in the human CNS. These include antigen presentation and production of cytokines (Hart et al. 1992). In an acute lesion once perivascular leakage is established there may be complete destruction of the microvascular wall integrity (Shaw et al. 1987). This in turn may result in proteins and immunoglobulins entering the CNS parenchyma, which may in itself have a pathological effect such as activation of T cells.

Cellular immune responses are initiated by T cells that may recognise diverse epitopes. As T cells are activated through recognition of peptide antigens bound by MHC molecules the expression of MHC and other stimulatory molecules may be critical. There are many potential sources of T cell activation and these include resident microglia, astrocytes, mast cells, B cells and macrophages. However the source of activation is unknown and because most inflammatory cells are recruited to sites of immune reactions by non-antigen specific mechanisms, the T cells that initiate a lesion may be far outnumbered by a heterogenous population in the acute phase (Sobel and Kuchroo, 1992).

The mechanisms by which this cellular immune reaction produces damage is complex. Activated T cells may induce production of lymphokines or cytokines which may directly mediate toxicity to myelin and oligodendrocytes. Among the cytokines identified in MS tissues are interleukin (IL) 1, IL 2, IL 4, IFN α , IFN γ , tumour necrosis factor (TNF) α and lymphotoxin (Traugott and Lebon, 1988; Selmaj et al. 1991; Wucherpfennig et al. 1992;

Brandt et al. 1993). Additional toxic products such as neopterin and nitric oxide may also be generated by macrophages as a result of stimulation by T cell lymphokines.

B cells and immunoglobulin are also found in MS plaques. B cells may express class II MHC molecules and are therefore potential antigen presenting cells (Abbas, 1987) but the degree to which B cell antigen presentation occurs in non-lymphoid tissue is uncertain. To date no myelinotoxic antibody has been identified in MS although in experimental allergic encephalomyelitis antimyelin antibodies have been shown to enhance demyelination (Schluesener et al. 1987), suggesting that both cellular and humoral mechanisms may be important for full expression of immune injury.

Key questions remain: What is the initiating event in the development of the disease? Is the inflammatory reaction the most important cause of permanent damage? Does another distinct mechanism exist?

1.5 Previous MRI studies in multiple sclerosis

1.5 (a) Introduction

It was first shown in 1981 that patients with MS had consistent changes on T1 weighted MR images (Young et al. 1981) and it was quickly realised that MRI was far superior to CT in the identification of these white matter abnormalities. In patients with clinically definite MS, the incidence of brain lesions is 98 % (Stewart et al. 1986; Ormerod et al. 1987) and these lesions correspond well to areas of pathological involvement (Stewart et al. 1986; Ormerod et al. 1987; Newcombe et al. 1991). Whilst MR is highly sensitive it is not necessarily specific to a particular disease and very similar abnormalities to those seen in MS may be

found in a number of other white matter diseases including neurosarcoidosis (Miller et al. 1988a) and acute disseminated encephalomyelitis (Kesselring et al. 1990). In addition, over the age of 50 years vascular white matter abnormalities in the brain are very common (Fazekas et al. 1988) though they are very uncommon in the spinal cord (Thorpe et al. 1993) and useful criteria exist to distinguish these abnormalities from MS (Fazekas et al. 1988; Paty et al. 1988). It was also found early in the use of clinical MRI that most patients (about 60-70%) presenting with isolated syndromes suggestive of MS (e.g. optic neuritis) had white matter abnormalities typical of those seen in established multiple sclerosis (Ormerod et al. 1987; Miller et al. 1988b). 67% of these patients were followed up at 5 years of whom 72% of those with initially abnormal scans had developed clinically definite MS but only 6% of those with normal scans had experienced further clinical events (Morrisey et al. 1993). An ongoing 10 year follow up of these patients has to date confirmed progression to clinically definite MS in 83% of patients with an initial abnormal scan and 11% of those with an initial normal scan (O'Riordan et al. 1996).

Serial studies (Isaac et al. 1988; Willoughby et al. 1989; Thompson et al. 1992; Smith et al. 1993) demonstrated that these high signal abnormalities (or lesions as they became known) are not static in nature but fluctuate both in size and number over time. New lesions were found to be commonly asymptomatic and in one study they occurred 7 times more frequently than clinical events (Thompson et al. 1992). However with the occurrence of a clinical relapse the number of new lesions dramatically increases (Isaac et al. 1988; Willoughby et al. 1989; Thompson et al. 1992).

Whilst there is an excellent relationship between acute lesions in clinically eloquent sites of the CNS (such as the optic nerve (Youl et al. 1991)), the relationship of chronic changes to function is more complex. In a comparison of benign and primary progressive MS

(Thompson et al. 1990) it was found that the patients with benign disease had considerably more lesions than the more disabled progressive group. In addition, the lesions in the benign group were in a similar distribution to that found in patients with secondary progressive MS, although in the secondary progressive MS the lesions tended to be more confluent and periventricular. Later serial studies also showed different behaviour in the frequency of new lesions detected by serial gadolinium enhanced scanning in differing subgroups. In one serial study (Thompson et al. 1992) patients with benign MS developed fewer lesions than those with early relapsing remitting disease and this was confirmed subsequently (Kidd et al. 1994). In a further study (Thompson et al. 1991) it was found that patients with primary progressive disease developed very few lesions on serial monthly scanning for 6 months.

The lack of correlation between the volume of lesions seen on MRI and clinical deficit may in part be explained by the pathological heterogeneity of the lesion (i.e: inflammation, demyelination, gliosis and axonal loss may have distinct functional consequences but cannot be differentiated by conventional MRI). It is obvious that site is also important. In view of the predilection of the periventricular area for lesions investigators have examined the relationship between cognitive impairment and brain lesion extent finding a positive correlation (Rao et al. 1989). As disability assessed by the EDSS is strongly locomotor weighted, further insight into the functional consequences of lesions could be examined by studying the spinal cord. A large cross sectional study (Kidd et al. 1993) of 80 patients failed to reveal a correlation between the extent of spinal cord lesions and disability.

Whereas the cross sectional correlation in established MS between lesion extent (or "lesion load" as it is often known) and disability is poor (Thompson et al. 1990) there is evidence to suggest that change may be important and that baseline findings may predict later clinical deterioration. There is major interest in this issue as it has been found that beta-

interferon significantly retards the growth of lesion load (Paty and Li, 1993) and hence the relationship between changes and clinical status is of extreme importance. In clinically isolated syndromes suggestive of MS, both semi-quantitative assessment (Morrissey et al. 1993) and quantitative assessment (Filippi et al. 1994) of lesion load predict to a moderate extent disability measured five years later and 10 years later (O'Riordan et al. 1996). Serial activity (the frequency of new lesions detected by gadolinium enhanced T1 weighted scans and/or T2/proton density weighted scans) or lesion load measures may also be weakly predictive of future deterioration in established MS. In one study (Filippi et al. 1995c) two conventional T2 weighted MRI scans were obtained on 281 patients with MS separated by an interval of 24-36 months. There was a weak ($r=0.2$) but significant correlation between the number of new and enlarging lesions and change in disability. The North American beta-interferon-1b trial examined the relationship between lesion load and change in disability in a large cohort over several years. Although no correlation emerged over the first 2-3 years (Paty and Li, 1993) a significant correlation ($r=0.23$) was found in patients followed up for 4 years (The IFNB Multiple Sclerosis Study Group and the University of British Columbia MS/MRI Analysis Group, 1995). With regard to the prognostic value of activity measures Paty and colleagues (Paty et al. 1992) have shown a significant, albeit modest, relationship between T2 activity over 6 months and EDSS change after 4 years in a group of 24 patients with relapsing remitting MS ($p<0.05$). Another study (Losseff et al. 1996) found that activity was to some extent predictive of long term disability in a group of 12 secondary progressive patients ($p<0.05$) but the same was not true for primary progressive MS. Two shorter studies of relapsing remitting and secondary progressive MS (Smith et al. 1993; Khoury et al. 1994) have also shown a modest relationship between MRI activity and change in disability.

1.5 (b) The acute lesion

From work on experimental allergic encephalomyelitis (EAE) (Hawkins et al. 1991) and from the histopathology of a patient who had died 10 days following an MR examination with the paramagnetic contrast agent gadolinium (Katz et al. 1993), there is good evidence that the leakage of gadolinium into the brain and hence its appearance in the brain parenchyma occurs as a result of breakdown of the blood brain barrier. In the case with histopathological confirmation, enhancing areas on MRI showed intense perivascular inflammation, contrasting with the absence of inflammation in non-enhancing lesions. Using gadolinium it has been possible to define the sequence of events visible to imaging that take place in the development of a new lesion (Kermode et al. 1990). In relapsing-remitting and secondary progressive patients the earliest detectable event is focal gadolinium enhancement which, from the studies described above, is thought to represent the presence of inflammation. A change in signal abnormality then becomes apparent on non-enhanced images and reaches its peak at about 4 weeks, after which there is some diminution in size. Gadolinium enhancement (and hence probably blood-brain barrier breakdown) ceases at this point. Evidence from proton spectroscopy suggests that demyelination occurs in this inflammatory phase as evidenced by the presence of lipid peaks (Davie et al. 1993; Davie et al. 1994). The functional significance of these acute changes has been elegantly studied in the optic nerve (Youl et al. 1991) in 18 patients with acute optic neuritis. Leakage of gadolinium was a consistent feature in the acute lesion and was associated with abnormal acuity and a reduced amplitude of the P100 component of the visual evoked potential (providing evidence for conduction block). When the patients were studied 4 weeks later, in 9 of 11 cases leakage had ceased and acuity and the amplitude of the P100 had improved.

The latency of the visual evoked potential was prolonged throughout. Hence there is good evidence that inflammation (as evidenced by gadolinium leakage) plays an important role in the development of conduction block and clinical deficit and that its resolution is an important step in remission. The persistent delay in the visual evoked potential suggests that demyelination is still present and despite this good function was recovered in these patients, so whatever contribution demyelination may make to function in these patients, conduction block associated with inflammation is a critical element.

1.5 (c) The chronic lesion

Many questions remain unanswered about the events leading to irreversible deficit in MS and why the characteristic initial good recovery from symptomatic relapses ceases and permanent deficit either as a result of relapses or from chronic progression becomes prominent. The longstanding lesion has been studied using electron microscopy and MRI (Barnes et al. 1991). Both the MRI (by T2 magnetisation decay curve analysis¹) and ultrastructural analysis (from different patients) revealed heterogeneity in chronic lesions: some are "closed" with no detectable extracellular water, but most are "open" showing expansion of the extracellular space to as much as 87% of tissue area. Evidence of blood brain barrier damage was found in only 17% of lesions and was less severe than that seen in acute lesions. These findings suggest progressive axonal loss in lesions as they age.

1

T2 magnetisation decay analysis is a technique by which the process of transverse relaxation of hydrogen protons can be described. A multi-echo sequence is used from which a curve can be generated describing the relaxation. In homogeneous tissue transverse magnetisation decays as a mono-exponential function. However the presence of biexponential decay suggests an expanded extracellular space.

1.5 (d) Improving pathological specificity

The lack of strong correlation between conventional MRI and disability has led to a search for techniques that may have the potential to separate out the underlying pathological substrates of multiple sclerosis. In this regard the three most promising areas are magnetisation transfer imaging, spectroscopy and the measurement of atrophy.

Magnetisation transfer imaging

Contrast in conventional MRI mainly results from differences in the relaxation times and proton density of mobile protons. However there exists a pool of water protons that is tightly bound to macromolecules which because of their short relaxation times are MR invisible. By exploiting the difference in resonance between the bound and unbound pool it is possible to selectively saturate the bound pool. As the bound and unbound pools are in rapid equilibrium this has the effect of reducing the signal from the unbound pool. The magnitude of this effect is termed the magnetisation transfer ratio (MTR) and is an indirect measure of the amount of macromolecular structure present per unit volume (Wolff and Balaban, 1989).

MTR is reduced in MS lesions (Gass et al. 1994; Tomiak et al. 1994) and experimental models suggest that the lipid bilayer may be the major determinant of the MTR (Fralix et al. 1991). The MTR reduction in MS lesions may therefore represent demyelination. A clinical study of 43 patients with MS found a correlation between clinical disability and mean reduction of MTR in brain lesions (Gass et al. 1994). However in this study there was also a correlation, albeit weaker between lesion area and disability. This is important as the technique to measure MTR is dependent on the size of the region under

study: the larger the region, the lower the MTR will be for a given degree of pathological change. This methodological difficulty was overcome in a study of the optic nerve (Thorpe et al. 1995) in 20 patients with previous optic neuritis. A significant correlation was found between MTR reduction and the prolongation of the VEP latency. However the reduced MTR did not correlate with final visual acuity. In a study of acute gadolinium enhancing lesions (Lai et al. 1997) MTR was found to be reduced dramatically when the lesions showed gadolinium enhancement and then returned often to near normal. Animal models of EAE have shown that oedema and inflammatory infiltrates alone may only produce a slight reduction in MTR (Dousset et al. 1992). It is most likely that multiple factors may influence this measure and a relationship to demyelination alone may be an over simplification. The myelinated and unmyelinated nerves of the garfish produce similar steady state reductions in MTR (Beaulieu and Allen, 1994) and axonal loss has also been shown to reduce MTR (Lexa et al. 1994).

Hence the present situation is not clear with regard to the use of MTR as a marker of structural integrity or to investigate the underlying changes in MS that are responsible for fixed deficit.

Spectroscopy

Proton magnetic resonance spectroscopy evaluates a number of metabolites of which N-acetyl-aspartate (a neuronal marker) is of particular interest. Reduction of N-acetyl-aspartate (NAA) in MS lesions has been recognised by many investigators and when persistent in chronic lesions is probably a measure of axonal loss. Investigators have found encouraging correlations between the quantification of NAA and functional deficit in MS (Arnold et al. 1994; Davie et al. 1995) but it appears that NAA reduction may have a floor effect as relapsing-remitting patients scanned serially show a progressive reduction but secondary progressive patients do not (Arnold, 1996).

Atrophy

Atrophy is likely to represent tissue destruction and previous studies have shown encouraging correlations between atrophy and disability. Much of the motor disability that develops in MS is thought to be due to disease of the spinal cord, which is a common site of involvement and hence the spinal cord provides a good model to investigate the functional significance of atrophy. In one study patients with MS who had atrophy (defined as 2 SD less than controls) at one or more of four spinal levels (C5, T2, T7 and T11), had significantly higher scores on Kurtzke's EDSS than those who did not have atrophy (Kidd et al. 1993). Despite this relationship there was no significant difference in cord area between less disabled subgroups of patients (relapsing-remitting and benign) and more disabled (primary and secondary progressive). Another study concentrating on the C5 level has shown a significant difference in cord area between patients with benign and secondary progressive MS (Filippi et al.

1995a). A further longitudinal study of progressive patients (Kidd et al. 1996) showed a decrease in mean cord area over one year but no definite correlation with disease progression. In addition the changes seen in individual patients were within the 95% confidence limits for measurement variation.

Another area commonly involved in multiple sclerosis is the periventricular white matter and the significance of atrophic changes to this area has been in part addressed by studies of cerebral atrophy. The presence of cerebral atrophy in excess of what might be expected for age is well described in multiple sclerosis both with CT and MRI (Loizou et al. 1982; Noseworthy et al. 1984; Rao et al. 1985; Hageleit et al. 1987; Huber et al. 1987; Comi et al. 1993; Gross et al. 1993). However investigators have differed in their interpretation of the clinical significance of such changes. Most studies have specifically investigated the relationship between cerebral atrophy and dementia in a cross sectional design and of these some have found a positive correlation (Rao et al. 1985; Comi et al. 1993) and others a weak correlation or trend (Huber et al. 1987; Hageleit et al. 1987). More recently a CT study (Gross et al. 1993) has suggested that the development of brain atrophy early in the course of the disease is a poor prognostic sign in relation to the development of disability and identified a "malignant" subgroup with detectable atrophy on CT within a year of diagnosis. A further MRI study of the cerebellum (Davie et al. 1995) has demonstrated a strong relationship ($r=0.5$) between atrophy here and clinical deficit.

Monitoring treatment

Conventional MRI provides us with an objective and sensitive way of assessing some aspects of the pathological process in MS (e.g. blood brain barrier breakdown) and hence the effects of treatments on these processes. There are however several areas of difficulty, most notably the lack of strong correlation between chronic changes on conventional MRI and disability. The reasons for this have been discussed and in this regard the more pathologically specific imaging techniques have considerable potential. However it remains to be seen if these techniques are sufficiently practical for inclusion in treatment trials.

1.6 Pathophysiology of symptom production

How may the varying underlying pathologies result in symptom production? The mechanisms by which demyelination may affect conduction have been extensively investigated (McDonald, 1963; McDonald and Sears, 1970) and as has been discussed, in acute lesions, maximal functional impairment is associated with blood brain barrier breakdown. What factors associated with the inflammatory response may be responsible for this functional disturbance? Recently it has been shown that infusion of the humanized monoclonal antibody CAMPATH-1H (a putative treatment for MS that targets the CD52 antigen) results in transient exacerbation or re-awakening of previous symptoms (Moreau et al. 1996). This effect is acute, lasts several hours and correlates with increased serum levels of TNF- α , IFN- γ and IL-6. Pretreatment with intravenous methylprednisolone prevents this response. It seems likely that soluble immune mediators may be responsible for this transient deterioration and that they may directly affect conduction. In another study CSF from patients

with MS who were in acute relapse caused inactivation of neuronal sodium current in vitro (cultured embryonic rat cortical neurones) (Koller et al. 1996). This effect was reversible by washing and could be abolished by CSF heat inactivation. Similar inactivation could not be produced in the same model by IL-6 or TNF- α , so the nature of the blocking factor is still unknown.

In chronic lesions the situation may be more complicated. In addition to the dichotomy seen in MR studies (between function and visible abnormalities) there are a limited number of pathological studies illustrating a similar point which deserve discussion. A patient has been described who died of an overdose 5 years after the onset of MS. She had been examined 19 days before death and a number of her earlier symptoms could be explained by the location of various plaques found at autopsy, but there were many lesions without recognisable clinical counterpart. The posterior columns were completely demyelinated yet clinical modalities such as position sense and vibration sense were only minimally disturbed. The pyramidal tracts were involved at many levels and almost totally in the cervical region but no signs were attributable to this in the upper limbs (Namerow and Thompson, 1969). Other examples of normal or well preserved function in the face of demyelination also exist in clinically eloquent areas such as the optic nerve (Ulrich and Groebke-Lorenz, 1976; McDonald, 1976) and the spinal cord (Ghatak et al. 1974). One important reason may be that conduction in demyelinated lesions of multiple sclerosis may be restored by an increase in sodium channels (Moll et al. 1991). Hence the histopathological and imaging abnormalities remain in the face of restored function. A second important reason is the increasing evidence from imaging, spectroscopy and neurophysiology that axonal loss rather than demyelination may be a key factor in determining fixed deficit. However although there are numerous reports of pathological studies demonstrating axonal loss these are few

in comparison with those showing little if any axonal loss. One explanation for this may be that the extent of complete tissue destruction and axonal loss may be underestimated if the nervous system was to contract in response to this tissue loss: The extent of completely destroyed tissue (axon and myelin) may not be apparent within a focal lesion as the only finding to reflect this may be atrophy of the structure within which the focal lesion is contained. One area where this contraction or reorganisation does not occur is the fundus and extensive defects in the retinal nerve fibre layer have been observed in MS using red-free photography (MacFadyen et al. 1988; Frisen and Hoyt, 1974).

1.6 Conclusions

Multiple sclerosis is an unpredictable disease that commonly results in progressive disability. The changes responsible for this disability are unclear and as yet we have no practical and convincing way with which to characterise these changes that could then be applied to further investigate the mechanism of disease progression. There is some evidence that axonal loss contributes to permanent disability, but to characterise and quantify this possibly requires a technique that can monitor change outside of the lesion, as the nervous system may contract or reorganise in response to loss of tissue. Hence the measurement of atrophy may provide the key to disability. This can be investigated further by examining a site in which atrophy and fixed functional deficit can be readily assessed (the spinal cord) and a site in which longitudinal observations can be made on the relationship between the development of atrophy and other quantitative MR parameters (the periventricular white matter).

Chapter 2: Common methodology

2.1 Introduction

This chapter details methodology common to experiments described later. It discusses the basic physics behind MRI and the principles and difficulties of quantification in clinical medicine and imaging. Quantification methods specific to individual experiments described later are dealt with in the relevant chapters.

2.2 Basic principles of magnetic resonance imaging

2.2 (a) Introduction:

The first descriptions of nuclear magnetic resonance (NMR) in condensed matter were published over 50 years ago (Bloch et al. 1946; Purcell et al. 1946), and applications of the principle of NMR were initially confined to physics and chemistry. The first NMR images of an object were described 30 years later (Lauterbur, 1973) but for the production of satisfactory images from humans, large-bore magnets with homogeneous magnetic fields were required and an efficient method of spatial localization was needed. This was achieved in the early 1980s when the first whole-body imagers were built and two-dimensional Fourier transformation was used to constitute the images from the basic NMR signal (Eldenstien et al. 1980).

To produce an NMR signal an atomic nucleus must be mobile and contain an odd number of protons. Images are constructed from the NMR signals derived from such nuclei after the application of a radiofrequency excitation pulse. For conventional NMR images the ¹hydrogen nuclei which are present in abundance in water and fat are the source of this image.

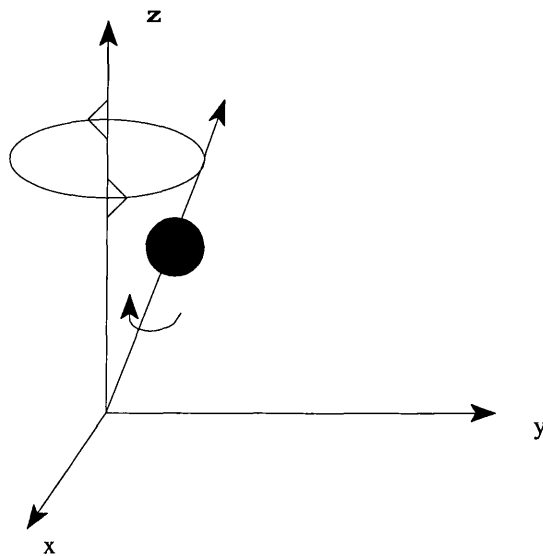
Protons present in hydrogen molecules have both electrical charge and motion. They therefore create an electrical current and a magnetic field. Protons are normally aligned at random but if they are subjected to the force of an external magnetic field they align themselves either parallel or antiparallel to this field. These two states, parallel or antiparallel, require different energy levels and more protons will align on the lower (parallel) energy level although the difference in absolute numbers is small. Aligned protons are not static, they precess around the axis of the external magnetic field with a motion analogous to a spinning top. The frequency of precession is not constant but depends on the strength of the external magnetic field. The frequency of precession can be precisely calculated by the Lamor equation:

$$\textit{precession frequency} = \textit{gyromagnetic ratio} \times \textit{external field strength}$$

The gyromagnetic ratio differs depending on the material under examination. In clinical practice magnets used for imaging usually have field strengths between 0.5 and 1.5 Tesla (the magnet on a refrigerator door is about 0.01Tesla).

To understand the basic principles of how these physical properties can be exploited for imaging it is necessary to introduce a coordinate system with a z axis in the direction of the magnetic field and an x and y axis perpendicular to the z axis (figure 1).

Figure 1: Precession of a single proton in the co-ordinate system



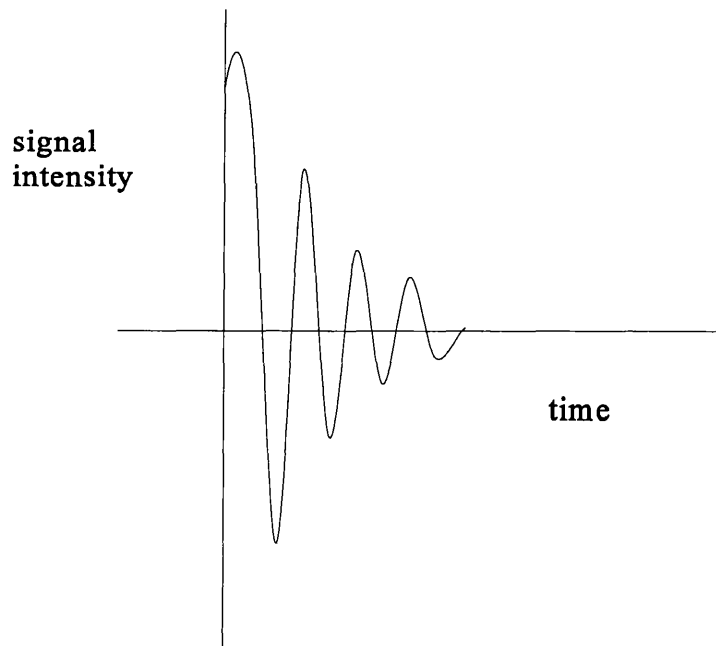
At any given point in time the protons will each be exerting a magnetic field with a given force and direction. In an external magnetic field all these magnetic forces cancel each other out save for those parallel to the field's axis. In view of the fact that more protons precess parallel, a net magnetic vector forms in this direction and is termed longitudinal magnetisation. It is not possible to directly measure this magnetisation as it is in the same direction as the external magnetic field. However if a radiofrequency (RF) pulse is applied which has the same frequency as the protons, energy would be exchanged between the two (a phenomenon termed resonance) and some protons would be lifted to a higher energy level (anti-parallel) thus decreasing longitudinal magnetisation. The RF pulse has another effect:

it causes the protons to precess in phase, and whereas before when random motion resulted in the cancellation of any net transverse magnetic force the protons now "point" in the same direction at the same time resulting in a net transversal magnetisation. This magnetic vector moves in phase with the precessing protons, circling perpendicular to the z direction and this can induce an electrical current in an antenna. As this transverse magnetic vector moves around with the precessing protons it comes towards the antenna (and goes away) with the precession frequency. This is the NMR signal.

If the RF pulse is now switched off the whole system returns to its original state (relaxation). The longitudinal magnetisation returns to its original size (longitudinal relaxation) and the transverse magnetisation decays to zero (transverse relaxation). In relaxation, energy is dispersed to the surroundings (termed the lattice). If time versus longitudinal magnetisation is plotted out a curve is formed describing the increase of longitudinal magnetisation with time. This is known as a T1 curve. T1 is in fact a time constant describing the rate of this process. In transverse relaxation the protons during application of the RF pulse have been precessing with different frequencies due to the inhomogeneity of the external magnetic field and each proton is in addition influenced by small magnetic fields from neighbouring nuclei. These internal magnetic fields are characteristic for a given tissue. Once the RF pulse is switched off the protons start to dephase and transverse magnetisation is lost and again this can be plotted against time giving a T2 curve.

It is difficult to pinpoint the exact time at which relaxation finishes and so T1 is defined as the time for 63% of the original longitudinal magnetisation to recover and T2 as the time when transverse magnetisation decreases by 37%. In biological tissues T1 is about 300-2000 milliseconds (ms) and T2 is about 30-150 ms with a good deal of overlap between

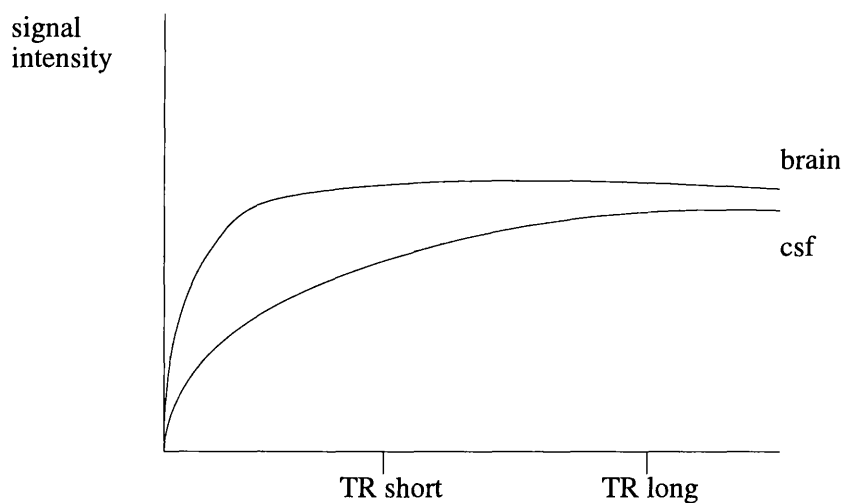
different tissues. In a lattice of high water content T1 is long as the protons exchange energy slowly, whereas the carbon bonds at the ends of fatty acids have frequencies close to the Larmor frequency resulting in effective energy transfer. Thus fat has a short T1. If there are no big differences in local magnetic inhomogeneities protons will dephase slower and hence T2 will be longer (as in areas of high water content, for example in CSF, T2 approaches that of T1) whereas in liquids containing large molecules the local magnetic fields are far more inhomogeneous thus protons can dephase faster with resultant short T2. In fact these processes (longitudinal and transverse relaxation) produce a net magnetic vector which performs a spiralling motion around the z axis and it is this vector which induces a signal in an antenna. This signal disappears with time and is greatest just after the RF pulse is switched off; however it has a constant frequency during relaxation. This type of signal is known as free induction decay and is illustrated in figure 2 overleaf.

Figure 2: Free induction decay**2.2 (b) A simple experiment:**

Let us consider two tissues with different longitudinal (T_1) relaxation properties, one short and one long. After a 90° RF pulse is applied, longitudinal relaxation occurs; if another 90° RF pulse is applied at a time when one tissue has completely recovered longitudinal magnetisation but the other has not, the resulting transverse magnetisation would be greater in the tissue that had started from its resting point (the one that had recovered full longitudinal magnetisation). This would translate into a greater net signal returned from this tissue after the 2nd RF pulse. If we waited until both tissues had completely recovered the signal would be the same. The time between RF pulses (time to repeat = TR) can thus be

manipulated to exploit physical differences between tissues that then translate into differing signal intensities. By using a short TR (< 500 ms) the resultant picture is T1 weighted. For example brain has a shorter longitudinal relaxation time than CSF; with a short TR the contrast in signal intensity between the brain and the CSF is greater than that obtained with a long TR (see figure 3).

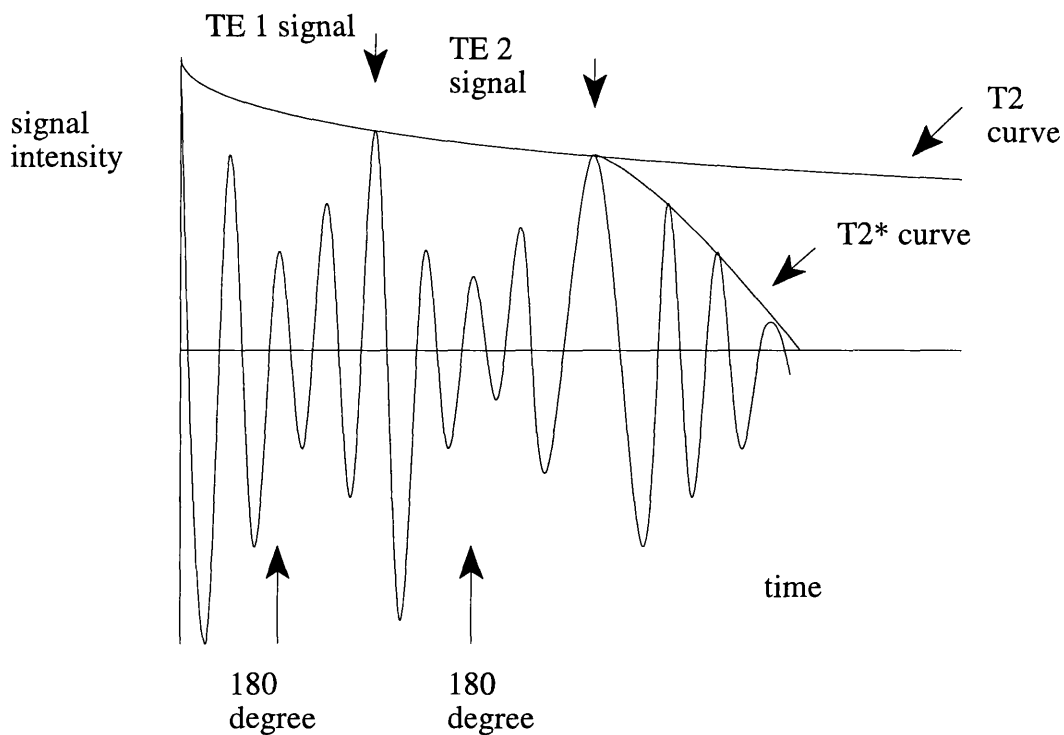
Figure 3: Signal intensity from two tissues with differing TR's



If the TR is very long, T1 no longer influences the tissue contrast but there may remain a difference in the absolute proton density between tissues which influences the signal, hence "proton density" (PD) weighted images can be formed. In this situation where PD predominates CSF will eventually give a higher signal than brain.

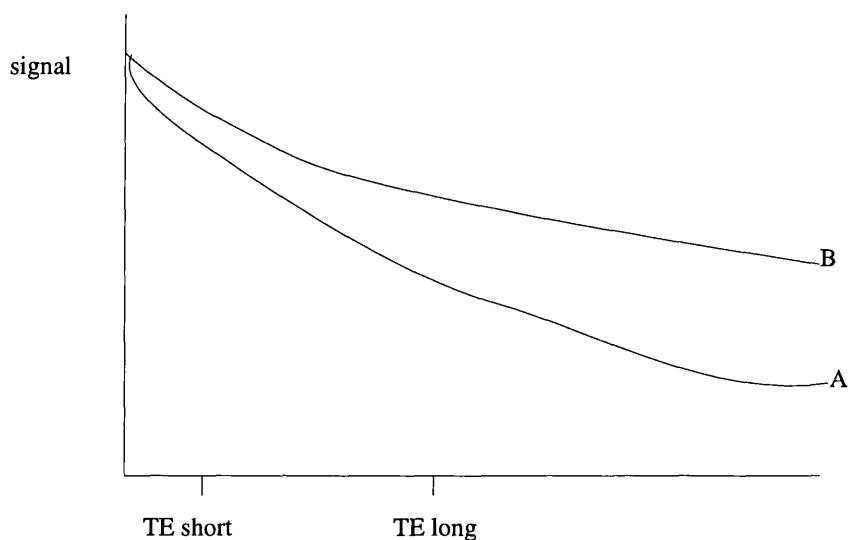
To generate a T2 weighted image requires a further RF pulse this time in a 180° direction, producing an echo. The timing of this is referred to as time to echo (TE). If this is applied whilst transverse magnetisation is decaying it will rephase the dephasing protons increasing the signal. This pulse can be repeated and a curve connecting the signal intensities (figure 4) is dependent on factors influencing transverse (spin-spin) relaxation; these are true T2 properties. T2* describes the decay which is due to inhomogeneities in the local magnetic field as well as true T2 (spin-spin) relaxation effects. If a refocusing pulse is not used, signal decay is more rapid because of these local field inhomogeneities, thus T2* is shorter than true T2. Such T2* sequences include gradient echo methods (see section 2.2(f)).

Figure 4: Generation of a T2 curve



As for T1 weighting, the properties of tissues that affect transverse relaxation can be exploited to give tissue contrast by altering the TE as illustrated in figure 5 for two tissues, tissue A with a shorter T2, thus losing transverse magnetisation faster than tissue B. With long TE's T2 properties are better distinguished.

Figure 5: T2 curves for two different tissues (assuming a long TR to minimise T1 effects)



2.2 (c) The spin echo sequence:

These principles underlie the most basic sequence used in MR, the spin echo sequence: a 90° RF pulse followed (after TE) by a 180° pulse followed (after TR) by 90° pulse, followed (after TE) by a 180° pulse. By manipulating the TR and TE we can change the sensitivity of

the sequence to T1 (short TR, short TE), T2 (long TR, long TE) or proton density weighting (long TR, short TE).

2.2 (d) Spatial information-slice selection

To obtain spatial information it is necessary to create inhomogeneity in the external magnetic field as this in turn produces differing precession frequencies which can be allied to a certain location. This inhomogeneity is produced by applying an additional field called a gradient field (in this case the slice select gradient). The gradient field can be applied in any direction which allows definition of varying imaging planes (see also section 2.2 (e)). The presence of this inhomogeneous field again means that protons within the structure under examination will exchange resonance with different frequency RF pulses. Hence if an RF pulse containing different frequencies (within a bandwidth) is applied it will exchange energy only within a certain spatial dimension. The larger the bandwidth the greater the volume of excitation. Hence both the position of a slice and its thickness can be determined by manipulating the frequency and bandwidth of the RF pulse and the external gradient field strength. In clinical practice the thickness of slices is 3-5 mm. Slices normally have an inter-slice gap which prevents cross talk between slices, and interleaving allows contiguous slices to be acquired.

2.2 (e) Spatial information within a given slice

Gradient fields are again used to define spatial information within a given slice in a similar way to slice selecting gradients. After an RF pulse is applied a gradient is generated, for example across the x direction (the frequency encoding gradient), this creates field

inhomogeneity and hence differing precession frequency in columns across the direction of the gradient. However, to map areas within different columns it is necessary to apply a further gradient (phase encoding gradient) across the column which results in the protons at different levels in the column to be spinning in different phases. At the end we have a mixture of different signals. These have different frequencies, and signals with the same frequency have different phases. By means of Fourier transformation these signals can be assigned to a certain location within a slice and an image can be constructed by converting these signals to a digital grey scale (in which the underlying image intensity is arbitrary). A typically *field of view* of each slice is in the order of 24 x 24 cm (for cranial images) which will contain basic subunits of 256 x 256 pixels. Thus in clinical practice the resolution of the images obtained is often about 1mm x 1mm in plane.

2.2 (f) Fast imaging:

Spin echo imaging takes some time and the TR is the most time consuming aspect. If the TR is shortened significantly it is not possible to apply a 180° spin echo and longitudinal magnetisation will have recovered less, so when the next RF pulse is applied the resulting signal is smaller. These problems can be solved by refocussing the dephasing spins by a further external magnetic field (gradient) then switching it off and on in the opposite direction (similar to the 180° pulse). This is termed a gradient echo. The other main aspect of fast imaging is to apply RF pulses with smaller angles than 90°. These "flip angles" are mostly in the range of 10-35° and hence do not totally abolish longitudinal magnetisation. Therefore the next pulse "tilts" the substantial amount of longitudinal magnetisation remaining even with a short TR. In addition if a 180° refocussing pulse is not used the signal

decays faster ($T2^*$ effect, see figure 4). Hence time can be saved in many aspects. A conventional dual echo sequence of the brain takes approximately 12 minutes to acquire; fast spin echo approximately halves this time.

2.2 (g) Contrast media:

Certain substances have small local magnetic fields which cause a shortening of relaxation time. A physiological example is deoxyhemoglobin. Gadolinium (Gd), a rare earth metal is another such substance and if it is chelated to DTPA it is rendered non-toxic. Normally Gd-DTPA is excluded from the brain parenchyma by the blood brain barrier. When there is an increase in permeability of the blood brain barrier during disease Gd-DTPA enters the brain parenchyma and shortens both the $T1$ and $T2$ locally; hence for a given TR there is more signal and for a given TE there is less signal. In practice, the $T1$ shortening effect predominates, thus leading to higher signal particularly on $T1$ weighted images.

2.2 (h) Flow:

Flow can produce signal void in an image. The detailed explanation of the phenomenon is complex, but at a simple level it can be explained as follows: When a 90° pulse is applied, all the protons excitable by its bandwidth will exchange energy. However the spatial location occupied by these resonant protons will soon be occupied by non resonant protons if there is sufficient movement (e.g. arteries, CSF spaces) and these will return no signal.

2.2 (i) Volume acquisition and inversion preparation:

Finally it is necessary to discuss these two further aspects as they are both relevant to the experiments later described. Volume imaging acquires data from an entire volume of tissue rather than individual slices. The excitation pulse is not slice selective and at the end of the acquisition the volume is divided into discrete locations or partitions by the slice select gradient. Many slices can be obtained, they are contiguous and can be set up so that the most basic units of the image (the pixel for 2D imaging and the voxel for volume imaging) are isotropic. After the image has been collected it can be reformatted in any plane or direction allowing precise anatomical coregistration on serial studies even when patient repositioning is imperfect.

Inversion recovery describes a sequence which first uses a 180° pulse. This pulse turns the longitudinal magnetisation in the opposite direction (hence all protons are now anti-parallel) and this is then followed by a 90° pulse. The time between these pulses is the inversion time "TI". This results in a heavily T1 weighted image.

2.2 (j) Coils

Coils are necessary to send and receive the NMR signal. All imagers contain volume coils which completely surround the part of the body to be examined. These volume coils are the transmitter for all types of examination. Receiver coils are usually modelled to the part of the body under examination, a helmet type head coil for example or surface coils which are placed directly over the area of interest (e.g. the spinal cord). Sometimes the same coil serves both the transmit and receive functions.

2.2 (k) MRI sequences in multiple sclerosis

The first clinical MR images in MS were acquired using a T1-weighted inversion recovery sequence, which showed normal white matter as high intensity and lesions as low intensity (Young et al. 1981). However, it was soon realised that proton density and T2 weighted spin echo sequences were more sensitive in detecting lesions in MS which were seen as high signal regions surrounded by lower signal in the normal appearing white matter (Ormerod et al. 1987). Proton density and T2 weighted spin echo are still widely used for routine diagnostic studies in MS but fast spin echo is becoming increasingly popular. In the spinal cord it is time consuming to detect intrinsic lesions due to MS using conventional surface coils and T2 weighted spin-echo pulse sequences. A significant and recent technical advance has been the application of multi-array coils (Thorpe et al. 1993) and fast-spin echo which allow a large field of view to be examined in a short time. In addition gradient echo sequences have been shown to be useful in delineating the border between the spinal cord and the cerebrospinal fluid (Thorpe et al. 1993).

2.3 Quantification in MRI

2.3 (a) Principles of measurement

Once images have been acquired qualitative and quantitative changes may be assessed. MRI has entered a phase in which quantification has become increasingly important. Quantification may relate to the area or volume of an abnormality (e.g. a lesion) or normal appearing tissue compartments (e.g. the cross sectional area of the spinal cord at a given

level) or the absolute T1 or T2 of a given region. Therefore techniques have been developed which distinguish one region from another and this can then be expressed as a volume, area or intrinsic property (e.g. an absolute T1 value). These techniques need to be evaluated for their measurement properties (psychometric properties) (Hobart et al. 1996). Firstly is the measurement reliable, that is to say is it accurate, stable over time and reproducible? Secondly is it valid, i.e. does the method measure what it purports to do? Thirdly is the measure responsive and sensitive enough to detect relevant change if it is applied serially.

In assessing reliability of imaging techniques accuracy may be hard to define as is well illustrated by the measurement of lesion load in which the traditionally accepted method (the manual tracing of observer identified areas of pathology) to which others are compared is itself a surrogate of the real abnormality. Hence the accuracy of a different method of quantification (e.g. a computerised automatic tracing of lesions) is expressed as a deviation from this surrogate, whereas it may in fact be biologically more accurate.

Reproducibility is most commonly expressed in imaging studies as rater reliability (the differences in measurements between or within raters), but many MRI studies that purport to measure reproducibility have only estimated the reproducibility of a part of the experiment, such as the repeatability of an area measurement in tracing around a predefined region of interest. To establish the true reproducibility the whole experiment should be repeated, ideally over time.

Validity is harder to determine in imaging studies but should be tested by comparing evidence from multiple sources. Validity in one setting (e.g. the measurement of spinal cord atrophy in multiple sclerosis) does not necessarily imply validity in another situation.

The ability of a measure to detect biologically relevant change is the final essential quality of a quantitative measure. It can be assessed by comparing the measure against other criteria of change and comparison with other measures of the same concept.

Unfortunately not all aspects of measurement can be readily assessed (especially accuracy and validity) as one of the main advantages of MRI is its non-invasive in-vivo nature. However as many of the psychometric properties of a measurement as possible should be explored as this will help interpretation of the results. The weight that quantitative results carry is well illustrated by the licensing of interferon-beta-1b for the treatment of relapsing-remitting MS. Part of the evidence considered by the Food and Drug administration of the United States was the observation that the interferon retarded the progression of lesion load in treated patients.

2.3 (b) Quantification methods in imaging

The final image as displayed on a computer or hard copy is the summary of the MR examination and has a field of view determined by the imager (e.g. 24 cm²). Within the field of view there is a given matrix (e.g. 256 x 256 pixels). As the field of view is known real dimension it is simple to physically express the volume of a given number of voxels, if the assumption is made that the field of view (which depends on the physical properties of certain gradients) is stable and accurate. The accuracy and reproducibility of the field of view in current MRI systems is excellent and measured variations may principally reflect the variability of the measurement technique from which the field of view is checked (Dr G J Barker and Miss S W Webb personal communication). However the contribution of these

changes may become important if the quantification of small % changes in a given area of interest are important.

The type of sequence used is also important and the volume of a given abnormality may be measured differently even if very similar looking images are quantified: In one comparison of measured lesion load volume, conventional spin echo resulted in higher measured load than fast spin echo although this was not statistically significant (Gawne-Cain et al. 1996a). Part of this difference may relate to the apparent size of individual lesions on the image or a bias towards detecting greater numbers because of a particular sensitivity to anatomical areas (Gawne-Cain et al. 1996b).

The most basic method of quantification in imaging is a simple count of the number of a particular abnormality present (e.g. lesions) and if desired a visual estimate of the size of each abnormality can be performed from which an ordinal score can be derived (Thompson et al. 1990). Further sophistication is obtained by an observer manually tracing (using a mouse or tracker ball) around a structure or region of interest from which an area or volume is computed (Isaac et al. 1988). This technique relies on a human decision to delineate the boundary of an abnormality. This is not without difficulty as surrounding any abnormality is an area of "partial volume" (where given pixels are occupied partly by two distinct compartments of tissue) and hence the edges may be indistinct.

A further improvement on manual outlining are edge detection techniques such as the contouring technique (Grimaud et al. 1996). Here the operator selects a pixel within the image which he/she considers to lie at the border of the region of interest. A computer algorithm then searches within 2 neighbouring pixels for a pixel of image intensity most removed from the selected pixel. A line is then formed between these 2 pixels which represents the steepest edge gradient present in the area selected. The mean of this gradient

is then used as a seed point and a line is generated by searching for pixels with identical or most similar intensities. Another technique is based on applying a universal threshold to segment the image followed by manual editing (Wicks et al. 1992). Here the operator applies a universal threshold to the image and makes a decision based on visual inspection as to what threshold most accurately segments areas of abnormality from normal appearing areas. The reproducibility of these techniques has been extensively studied and the best intraobserver co-efficient of variation in comprehensive studies for manual outlining is 6.5%, 2.9% for contouring and 1.6% for thresholding (Filippi et al. 1995b). However none of these studies take into account a repeat of the whole experiment and are in fact measures of the tracing error of the technique. Many other factors may affect reproducibility in scan-rescan including lesion selection, repositioning (Gawne-Cain et al. 1996c), random or systematic gradient drift and motion artefacts. These factors have not been systematically studied.

Accuracy is much harder to define for in-vivo imaging studies for obvious reasons. However, recent studies have been conducted to define accuracy of imaging measures from the use of phantoms. In one (Tofts et al. 1996), an oblique cylinder contrast adjusted phantom was imaged following which volume measurements were made using manual and contouring techniques. It was found that marked variation occurred particularly at small volumes, with the total volume estimate being inaccurate by as much as 30%.

Accuracy and reproducibility per-se are important mainly for determining the power of a technique to detect useful change and to quantify to some degree the "noise" inherent in a technique which may be useful in interpreting the results of studies. A co-efficient of variation of < 1% and accuracy of 99% sound very attractive but are of little use in serial evaluation if the changes expected are < 0.5%. In addition, poor reproducibility may be overcome by expanding the numbers under study.

2.4 Clinical measurement

2.4 (a) Impairment and disability

Impairment (clinical signs and symptoms produced by damage to the nervous system) is but one of three categories of dysfunction proposed by the World Health Organisation (WHO) in 1980 (World Health Organisation, 1990). The other two; disability (the personal limitations imposed upon activities of daily living by the impairment and handicap (the social and environmental effects of the disability), whilst of considerable importance to patients, may be less useful for the physician involved in assessing the progression of a disease as they are readily influenced by environmental interventions.

One of the most important methodologies used in this work is the clinical assessment of neurological impairment. Scales which measure impairment have been formulated principally for use in treatment trials and although they have many problems, which will be discussed later, clinical endpoints have remained the most important outcome measures. Other methodologies such as MRI which purport to assess impairment must be validated against these clinical measures. There is thus a possibility of a circular argument: We wish to use MRI instead of clinical assessment as it may be a more objective/sensitive/reproducible measure of disease activity/ progression, yet to validate MRI it must show a close relationship with the clinical state.

There are now a number of scales in use to quantify impairment in multiple sclerosis. Experiments described in this thesis have used the EDSS in the evaluation of all patients. The

EDSS is distinguished from other scales by virtue of its widespread use including extensive natural history studies of MS and common awareness of its advantages and disadvantages.

2.4 (b) The Expanded Disability Status Scale:

In 1955 Kurtzke (Kurtzke, 1955) introduced a 10 step Disability Status Scale (DSS) for following progress of patients and disease over time: it was in fact developed to test Isoniazid as a potential treatment for MS (Kurtzke and Berlin, 1954). In 1961 it was expanded by the inclusion of a complementary set of scales for eight "functional groups" later called functional systems. A further major change was made in 1983 (after criticism of the DSS insensitivity) with the introduction of the EDSS which divided in two each of the former 10 steps. The functional systems (FS) rate from a scale of 0 (normal) to 5 or 6 (maximal impairment) objectively verifiable deficits due to multiple sclerosis. Kurtzke instructs that symptoms should be discarded and this is practical except in the rating of sphincter function. The eight functional system scores are based upon examination of pyramidal, cerebellar, brain stem, sensory, sphincter, visual, cerebral (cognitive) and "other " e.g. the presence of spasticity. Kurtzke claims that each FS is independent of the other and whilst this is true in a pure sense, a single lesion depending on its site will have very different consequences on the FS scores (and hence in some cases the EDSS).

The EDSS score itself is derived at its lower end (0-4) from the pattern of scores of the functional systems and therefore measures impairment. The higher values are more reliant upon assessment of the patients *disability*. The full scale is listed in the appendix.

As with any measure an impairment scale should be accurate, sensitive, reproducible and objective. It is not possible to assess the true accuracy of this scale as we have only other

scales to compare it against and measures such as obtained from MRI. Whilst MRI measures such as lesion load analysis may reflect one or a number of components of biological abnormality, we do not know the true relationship of these to impairment and discrepancies between abnormal signal in a clinically eloquent structure and impairment are not uncommon. We can however observe the linearity of the scale and see how one step relates to another.

Kurtzke found the DSS to be linear in his hands with a Gaussian distribution but despite this he reminds us that for analytical purposes it should be used as a rank order ordinal scale. Others have not found the DSS or EDSS to be linear (Noseworthy et al. 1990, Weinshenker et al. 1991). These studies found both scales to be bi-modal in distribution with peaks at EDSS 1 and 6. The peak at 6 is probably explained by the automatic inclusion in this category of those who need unilateral support; patients may use support for many reasons. Although these biases should be overcome by a disciplined assessment they are frequently not by some observers and explain part of this concentration at grade 6. In addition to the bimodality, there is data detailing the average time that a patient will spend at a given level of the DSS for those who progress to the next level (Weinshenker et al. 1991) (table 1). This illustrates the marked variability in time for patients to progress through different levels of the scale and implies that it is an ordinal scale and should be treated as such.

Table 1: Mean time spent in years at a given level of the DSS for patients who progress to the next level.

	DSS 1	DSS 2	DSS 3	DSS 4	DSS 5	DSS 6	DSS 7	DSS 8	DSS 9
Mean time spent in years	4.09	2.8	1.95	1.22	1.25	3.06	3.77	2.41	2.51

from Weinshenker B. G. et al. (1991). The natural history of multiple sclerosis: a geographically based study. 3. Multivariate analysis of predictive factors and models of outcome. *Brain* 114: 1045-1056.

The next problem is one of sensitivity and it was criticisms of the insensitivity of the DSS that led to the formulation of the EDSS. The question of sensitivity is currently being addressed in the Mayo Clinic-Canadian Sulfasalazine study where at each quarterly visit the evaluating neurologist is asked to record whether there has been objectively verifiable clinical worsening. For that purpose relapse or progression has been defined using a combination of step changes on the FS and EDSS scales and the examiner is asked for a "global opinion" as to whether the disease has been active in those who do not meet these definitions. Of 139 follow up visits, 14% of the visits judged to be inactive by definition using the FS and EDSS were felt to show clinical worsening when using the "global opinion"

(Noseworthy et al. 1994) raising concerns about the sensitivity of this scale for use in clinical trials.

Reproducibility of the EDSS has been extensively studied and there are now at least eight studies looking at the intra and inter-rater reliability. To a large degree most of these investigators have identified a similar degree of inter-rater agreement (Noseworthy, 1994). Perfect agreement occurs in 50-66% for the major divisions of the functional systems and for the EDSS perfect agreement is greater for the higher rather than lower end of the scale. Reproducibility over time is harder to examine but one study (Myers et al. 1993) has reported intra-rater reproducibility on the DSS in the range of 72-78% for some 1300 visits of patients seen within 90 days who were thought to be clinically static.

Another problem in applying clinical scales to quantify progression of disability is the effect of short term changes (e.g. diurnal variation) in patient performance. Changes in disability may be recorded which do not reflect genuine deterioration due to fixed tissue damage but that occur as a result of physiological variables such as temperature.

The current accepted but imperfect solution to these problems of non-linearity, insensitivity, poor reproducibility and tendency for patients to show diurnal fluctuation in clinical trials is to define an endpoint that is likely to reflect real change and that can be achieved in a large proportion of a trial's placebo group (thus not compromising power) over a given time. This is currently accepted as a change in EDSS of greater or equal to 1 point for patients entering with a score below EDSS 5.5, or greater or equal to 0.5 points for patients entering with a score greater or equal to EDSS 5.5 (Goodkin, 1991). Any change should be sustained and hence seen on two consecutive visits at least 3 months apart.

Chapter 3: Spinal cord atrophy

3.1 Lessons from a serial study

3.1 (a) Introduction

The importance of studying imaging abnormalities of the spinal cord has been discussed earlier. It is likely that spinal cord dysfunction is responsible for much of the motor disability that occurs in MS, and as this disability can be quantified in an ordinal manner using the EDSS, the spinal cord can be used as a model with which to investigate the clinical relevance of imaging abnormalities.

Three important studies of spinal cord atrophy have already been performed by previous investigators. The first was a cross sectional study (Kidd et al. 1993; Thorpe et al. 1993) in which 80 patients with clinically definite MS and 45 controls underwent spinal cord MRI. Axial sections of the spinal cord at 4 vertebral levels (C5, T2, T7 and T11) were acquired using multi-array coils and a gradient echo sequence. Following image acquisition the circumference of the cord was manually traced at each level using a mouse and from this the cross sectional area derived. Spinal cord atrophy was considered to be present when the measured area was more than 2 Standard Deviations (SD) below that obtained in the control population. The cord was found to be atrophic at one or more levels in 32 patients (40%) and disability was significantly greater in those with atrophy at one or more levels (mean EDSS = 6.0) than in those without atrophy (mean EDSS = 4.5) $p = 0.006$. Cord area did not correlate with patient age or disease duration. Despite the relationship of cord atrophy to

disability, individual patient subgroups with differing levels of disability did not have significantly different cord areas. The relapsing-remitting group with a mean EDSS of 4 had virtually identical cord areas to the more disabled secondary progressive group, mean EDSS = 6 (The respective cord areas \pm 1 SD at the C5 level were $97 \pm 16 \text{ mm}^2$ and $97 \pm 13 \text{ mm}^2$). A further serial study of 20 patients with secondary and primary progressive MS (Kidd et al. 1996) using the same technique over a 1 year period demonstrated a significant decrease in cord area at the C5 level from a mean of 100.7 mm^2 at entry to a mean of 96.73 mm^2 at one year ($p < 0.05$) but no significant change at any of the other 3 vertebral levels. No definite relationship of progressive atrophy to worsening disability was demonstrated but this may have been related to the short period of the study and the lack of sensitivity of the EDSS. Mean intraobserver coefficient of variation for cord measurement was 2%. In addition a further study of 10 relapsing-remitting patients over a one year period (Thorpe et al. 1996) using the same technique did not demonstrate progressive atrophy. Mean intraobserver coefficient of variation for cord measurement was 4.8%. Mean cord area at C5 was 88.8 mm^2 at entry and 86.4 mm^2 at one year.

The observation of worsening cord atrophy in patients with progressive disease concurs with findings of the initial cross sectional study, in that atrophy was greater in those with worse disability. The absence of progressive atrophy in relapsing-remitting patients is also in keeping with this group's characteristic good recovery from relapse. However the observation of greater disability in those with atrophy in the absence of a significant difference or even trend towards differing cord areas in sub-populations with marked difference in disability is contradictory, unless atrophy (as defined) is present only in extreme examples and this is not being reflected in the mean cord areas. In addition, the observations on serial change were undertaken by two independent observers who

presumably measured cord areas quite differently in view of the clear but unexpected finding that at the beginning of these serial studies the relapsing-remitting group had smaller cord areas than the progressive group. To clarify the situation a longer serial study involving greater numbers of patients was undertaken in which all observations would be made by one observer.

3.1 (b) Methods

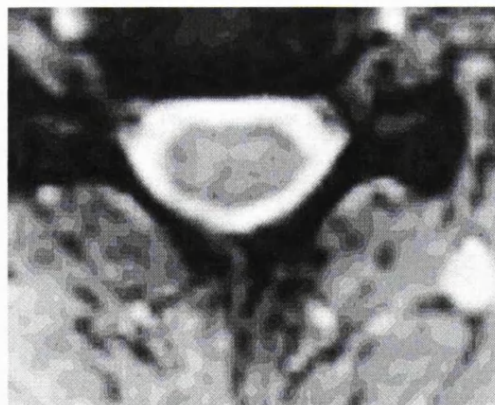
Of the original 80 patients in the cross-sectional study (Kidd et al. 1993) 60 were reviewed after a period of two years \pm 3 months. 19 were uncontactable or unwilling to participate in the study and one patient in a state of acute relapse was excluded from the study. Of the 60 patients, approximately one quarter (see table 2 for exact numbers) were in each of four clinical subgroups (relapsing-remitting, benign, primary and secondary progressive as previously defined). All patients were questioned and underwent a full neurological examination and evaluation of the EDSS score by one observer. Following this, MRI of the spinal cord was performed. Control subjects previously studied had answered a simple questionnaire regarding their general health and were excluded if any significant past or present illness was identified.

3.1 (c) MRI protocol and image post processing

All imaging was carried out on a Signa 1.5T superconducting system (General Electric, Milwaukee, WI) using phased array coils (Thorpe et al. 1993). Single axial 5 mm slices were acquired at 4 vertebral levels (C5, T2, T7, T11) using a gradient echo sequence (TR 300

ms,TE 15 ms, flip angle 15° , matrix 256 x 256, field of view 20 cm). Images were then transferred to a Sun workstation and displayed using the image analysis software Dispunc (D.L. Plummer, School of Physics University College London). All images from the patients (Baseline and 2 year follow up) and from 45 controls (45 scanned at baseline and 5 scanned in addition at 2 year follow up) were blinded and then analysed by one observer using a systematic manual technique to outline the spinal cord. This involved a constant enlargement and windowing against a reference image to ensure a similar level of image intensity and contrast between the CSF and spinal cord. With image interpolation the cord edge appears as a series of contours through the middle of which a border was manually traced (figure 6).

Figure 6: Gradient echo at C5



Two measurements were made of each image at different times (at least one week apart) and their values averaged. Atrophy was defined as being present when the cord area was 2 SD's less than controls.

3.1 (d) Results

Clinical characteristics:

The clinical characteristics of the patients are detailed in table 2 below. There had been a significant deterioration in EDSS score for the primary and secondary progressive group (Wilcoxon Signed Rank Test $p < 0.01$ and 0.05 respectively); 11 of the primary progressive subgroup, 4 of the secondary progressive, 3 of the benign and 3 of the relapsing-remitting subgroup had deteriorated significantly². Two of the relapsing-remitting group had entered the progressive phase.

Table 2: Clinical characteristics:

Group	Mean (range) of			
	Age at entry	Disease duration	EDSS (baseline)	EDSS (at year 2)
PP (n =17)	45 (35-62)	11 (5-20)	4.8 (3-7)	6(3-8)
SP (n=14)	45 (30-63)	14 (7-36)	6.3 (4-8.5)	6.8 (3.5-8)
BENIGN (n=15)	48 (35-62)	21 (15-30)	2.7 (1.5-3)	2.9 (1.5-4)
RR (n=14)	34 (27-48)	6.3 (3-12)	3.2 (1.5-8)	3.4 (0-8)

PP= primary progressive, SP= secondary progressive, RR=relapsing-remitting.

² A change in EDSS of greater or equal to 1 point for patients entering with a score below EDSS 5.5, or greater or equal to 0.5 pts for patients entering with a score greater or equal to EDSS 5.5.

Cross sectional area measurements:

There were 45 healthy volunteers (23 men and 22 women) aged 18-72 (mean 42.9 years) whose cord area was remeasured by a single observer with very similar results to the original cross sectional study (table 3).

Table 3: Control cross sectional area measurements in healthy volunteers

Cord area in mm² ± 1 S.D.

	Repeat measure by new observer	Original measurements (Kidd et al. 1993)
C5	104 ± 8	106 ± 9
T2	65 ± 5	68 ± 8
T7	56 ± 7	56 ± 7
T11	72 ± 9	72 ± 12

In the patients atrophy had not changed significantly in prevalence (table 4) for the original baseline information when re-measured by the new observer and there was no significant change in it's prevalence at 2 year follow up.

Table 4: Prevalence of atrophy (numbers of patients) at one or more levels

	Baseline	2 year follow up
PP	5	5
SP	8	6
Benign	5	4
RR	6	6

The mean cord cross sectional area in mm² for the individual patient groups at each of the 4 levels are listed in table 5 below for baseline and 2 year follow up

Table 5: Mean cross sectional area in mm² at 4 levels by patient group.

baseline/2 year follow up

	PP	SP	BENIGN	RR
C5	95 / 95	89 / 90	94 / 94	98 / 93
T2	60 / 58	60 / 59	60 / 60	66 / 61
T7	52 / 50	51 / 51	51 / 52	55 / 53
T11	64 / 67	63 / 71	65 / 67	73 / 71

There was a significant decrease in cord area only for the relapsing-remitting group (which had a substantially shorter disease duration) at the C5 and T2 levels ($p < 0.01$ and 0.007 ,

Wilcoxon Signed Rank Test) and for the whole patient group there was a significant change in cord area at the T2 level ($p < 0.01$ Wilcoxon Signed Rank Test). However there was no clear relationship between change in cord area and clinical progression (table 6).

Table 6: Change in cord area in mm² stratified by clinical progression.

	WORSE	STABLE
C5	-0.65	-1.12
T2	-1.8	-1.7
T7	-0.06	-0.5
T11	+1.28	+2.53

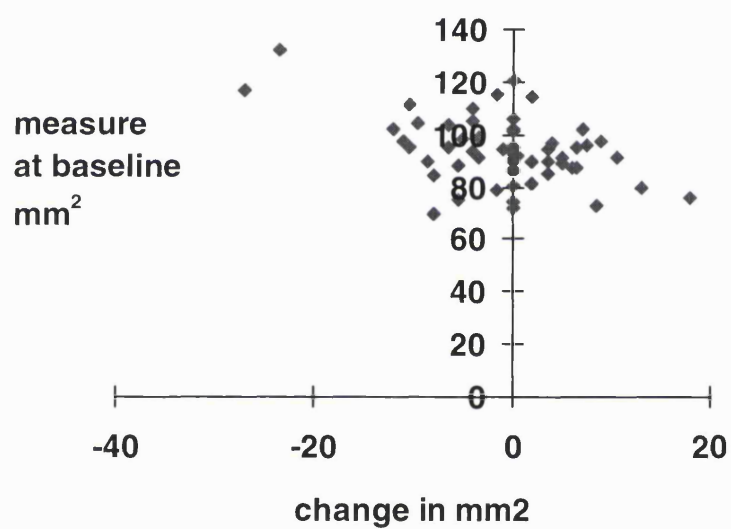
No significant correlation was found between cord size, age, duration or EDSS score. However for the 2 year follow up cord area measurements disability was significantly higher for those with atrophy at the T7 level ($p < 0.04$, Mann Whitney Test).

Reproducibility

The intraobserver coefficient of variation (Goodkin et al. 1992) for repeat measurements on the same scan was 4.1%. However for scan-rescan which had been performed on 5 subjects this increased to 7.4%. There was a significant correlation between the size of the cord at baseline and change (figure 7) illustrating a tendency for regression to the mean of the

measurement: cords that were originally measured small were subsequently measured larger and vice-versa.

Figure 7: Scatter plot of cord area at baseline against change in cord area ($r=-0.37$, $p<0.05$)

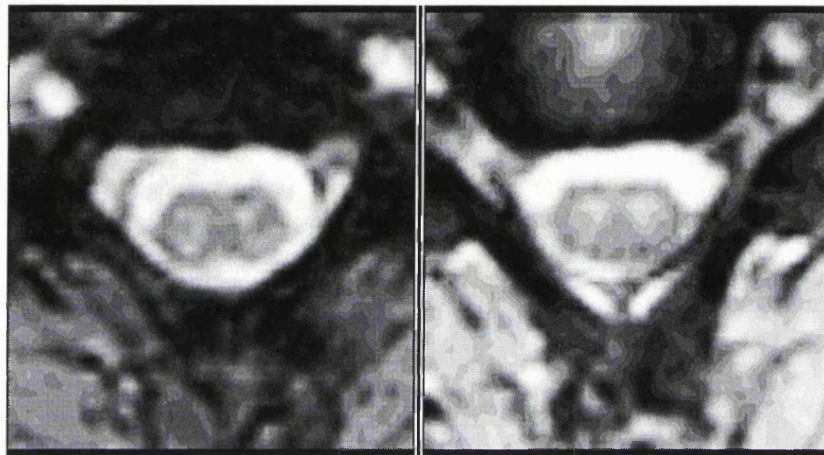


3.1 (e) Discussion

This study failed to demonstrate a relationship between clinical progression and worsening atrophy of the spinal cord. Findings were similar to the original cross-sectional study in that all the patient groups had significantly smaller cord areas than controls and that there was

some relationship between atrophy and disability. However this was not a graded relationship. The findings contradict the previous serial studies in that worsening atrophy was demonstrated in the relapsing-remitting but not progressive subgroups. However it may be possible to explain some of these results on the basis of measurement error. It is impossible to define the accuracy of this technique but certainly the technique is poorly reproducible. For scan-rescan one standard deviation of measurement variation (British Standards Institution, 1979) expressed as the coefficient of variation (Goodkin et al. 1992) is 7.4%. Given that the mean decrease in cord area of the most disabled subgroup is 13% this creates considerable concern over the validity of individual and serial measurements. The poor reproducibility was less apparent from repeated measures on the same image and the magnitude of the problem became apparent once scan-rescan reproducibility was calculated. This illustrates the considerable importance of assessing scan-rescan reproducibility for techniques that will be used to monitor change over time. Several factors may contribute to the poor reproducibility of the technique: Firstly imaging areas of the cord with marked local anatomical variability and therefore cross sectional area measurement demands precise repositioning for reliable results. This problem is most marked at the C5 level due to the cervical enlargement (Barson and Sands, 1977) and expansion of the cord associated with root outlets. This is illustrated overleaf in figure 8 which shows a control who has been scanned serially: there has been a slight change in positioning (visible by the appearance of CSF in the root outlets) leading to a larger area of the cord being imaged .

Figure 8: A control scanned serially at the C5 level. (Left image obtained in 1992, right in 1994) There has been a slight change in positioning (evidenced by the appearance of CSF in nerve roots), with resulting enlargement of the cord. A signal void (probably due to flow) is evident near the bottom right hand area of the cord (1994 image).

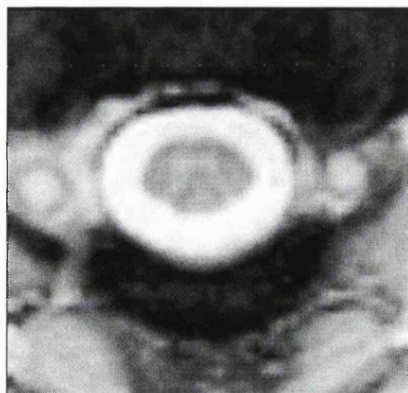


In addition, at C5 the CSF space is small leading to turbulent flow and signal void and as in the thoracic region, the cord commonly abuts the bony canal. Both these factors obscure the cord boundaries and lower the image contrast between the CSF and the cord. As a consequence most images acquired at these levels with this sequence can only be measured using a manual outlining technique as they lack sufficient contrast for automated or threshold calculated contouring to work properly. This further decreases reproducibility.

3.2 Development of a new technique to measure spinal cord atrophy

In view of the inadequacies identified in the technique it is possible that the strength of the biological relationship between atrophy and disability was being obscured. There was consistent evidence from all studies performed so far that some relationship of atrophy to disability was present and it seemed possible that a graded relationship might be hidden by "noise" in the measurement technique. It was therefore necessary to develop a new technique to measure spinal cord cross-sectional area with refinements based on the previously identified problems. The first improvement was to study an area of the cord without marked local anatomical variability and with a capacious CSF space. The cord segment opposite the C2 vertebral body has these characteristics and is illustrated in figure 9 below.

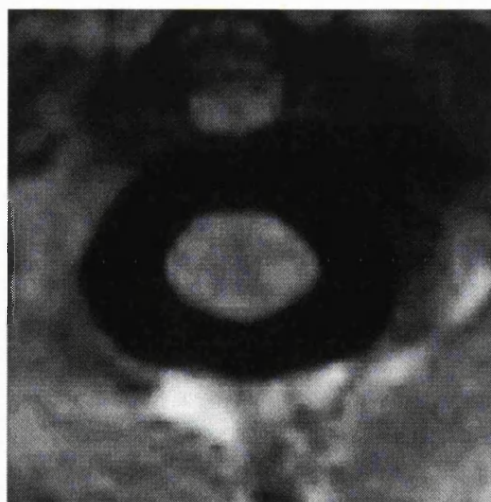
Figure 9: Gradient echo at C2. By simply changing the anatomical segment imaged, contrast between the CSF and the cord is increased from 1.5:1 to approximately 2.5:1.



This simple change in anatomical level also means that the CSF flow is less turbulent (as the CSF space is larger) and hence the image contrast between the cord and the CSF is increased. The image contrast can be further improved by use of a volume acquired inversion prepared sequence. Volume acquisition allows precise reformatting therefore improving reproducibility by virtue of accurate repositioning. If volume acquisition is coupled with inversion preparation, marked CSF suppression results which raises the cord/CSF contrast even further (figure 10). Finally C2 is an uncommon site for disk protrusion or spondylitic changes (Thorpe et al. 1993).

Figure 10 : C2 axial reformat from a volume acquired inversion prepared sequence.

With this heavily T1 weighted volume acquired sequence contrast is further increased to approximately 3.5:1.



It was found that by positioning subjects with the neck straight rather than in flexion or extension the cord would lie centrally within the CSF pool thus allowing a more objective measurement to be performed. The image under analysis now is characterised by a relatively

homogeneous area (the cord) placed in the middle of another relatively homogeneous compartment (the CSF), hence the theoretical border between these two compartments should lie at an image intensity halfway between that of the cord and CSF. Using these advances the relationship of spinal cord atrophy to disability in MS was re-investigated.

3.2 (a):Patients and methods

Sixty patients and thirty controls were recruited. All the controls were healthy volunteers. Of the 60 patients there were 15 in each of four clinical subgroups (relapsing-remitting, benign, primary and secondary progressive as previously defined). All patients were randomly selected within the four subgroups and this is reflected in the distribution of EDSS scores. Patients in a state of acute relapse were excluded from the study. Control subjects were selected to represent a wide range of age, height, weight and an equal sex distribution.

All patients were questioned and underwent a full neurological examination and evaluation of the Kurtzke EDSS score by one observer. Following this, MRI of the spinal cord was performed. Control subjects answered a simple questionnaire regarding their general health and were excluded if any significant past or present illness was identified.

MRI Protocol

All imaging was carried out on a Signa 1.5T superconducting system (General Electric, Milwaukee, WI) using phased array coils (Thorpe et al. 1993). A volume acquired inversion prepared fast spoiled gradient echo acquisition (SPGR) was performed. Sixty 1mm thick sagittal slices were acquired in a 3D volume centred on the cervical spine, with the following

parameters: (TI = 450ms, TE = 4.2ms, TR = 17.8ms, flip angle= 20° s, 256 phase encodings in the z direction, 1 average, field of view 25cm for both the z and y direction, matrix 256 x 256, read gradient superior inferior). The imaging time was seven minutes.

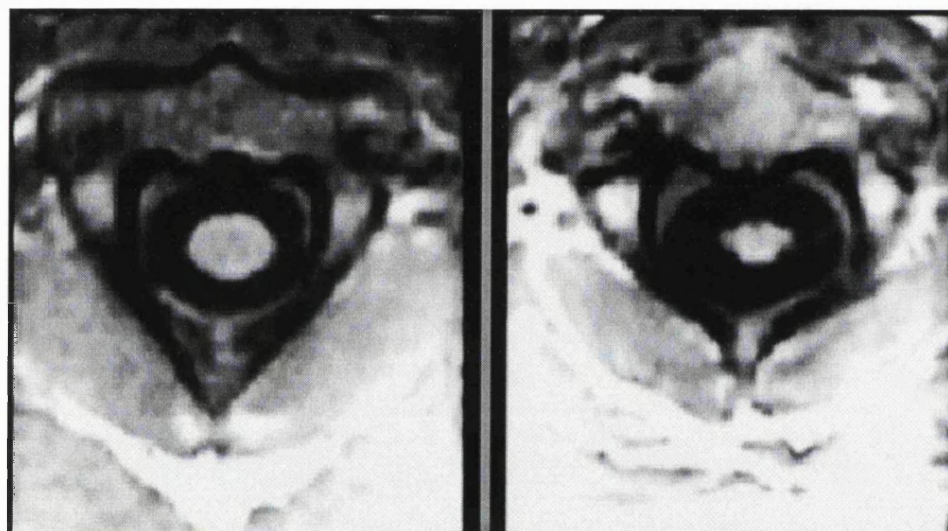
Image post processing

From the volume data set a series of five contiguous 3 mm pseudo axial slices were reformatted on the Signa using the centre of the C2/C3 intervertebral disc as a caudal landmark, with the slices perpendicular to the spinal cord.

Cross sectional area measurement

The resulting images are illustrated overleaf in figure 11 showing two patients, one with benign and one with progressive MS.

Figure 11: Benign and progressive MS. Inversion prepared fast spoiled gradient echo acquisition at C2 in benign (left) and progressive (right) multiple sclerosis. *Left*, female, age 46 years, disease duration 15 years, EDSS = 3, cord area = 85mm². *Right*, female, age 31 years, disease duration 10 years, EDSS = 8, cord area = 55mm². Patients are height and weight matched.



In view of the cord position and the strong signal intensity gradient between the cord (bright) and the surrounding CSF (dark) it was possible to apply a semi-automated measurement of the cord area as follows:

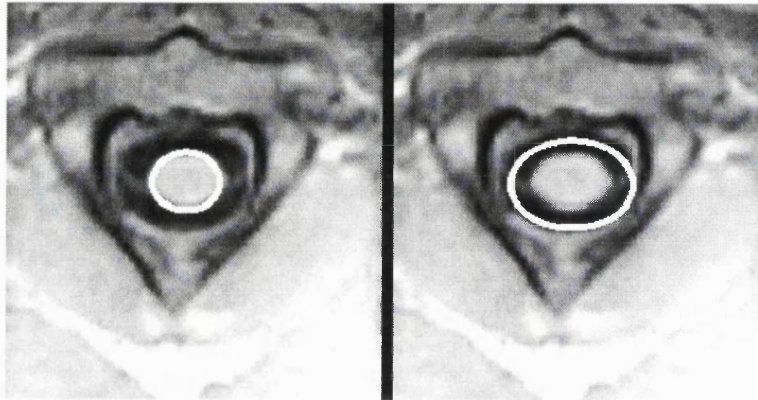
The partial volume effect blurs the appearance of the boundary between the cord and CSF. If the cord and CSF were uniform in their composition then a contour drawn in the image at a signal intensity (SI) half way between the SIs of the cord and CSF would be at exactly the true position of the boundary. This was the basis of the method for locating the cord boundary, thus it was necessary to determine the mean SI of the cord and CSF. Images were transferred to a Sun Workstation and uniformity corrected according to a previously

described method (Tofts et al. 1994). Following this the images were blinded so that the observer was unaware of their identity and then displayed using the image display programme Dispunc. Windowing was standardised visually for all images against a single control image which was displayed at the same time. A region of interest (ROI) was then drawn carefully around the cord in the top slice (ROI "inner") , followed by a ROI around the cord and CSF space (ROI "outer", figure 12). From these two regions the mean CSF and cord intensities were calculated. The mean cord SI is the direct value from the first ROI. The mean CSF SI is calculated by knowing the areas of the two ROI's and their mean signal intensities. This is derived from the formula:

$$\text{mean CSF intensity} = \frac{(\text{mean SI outer} \times \text{area outer}) - (\text{mean SI inner} \times \text{area inner})}{(\text{area outer}) - (\text{area inner})}$$

The boundary SI is the mean of the cord and CSF SIs. Following its calculation an automated border was then drawn around the spinal cord in all five axial slices at the boundary SI previously calculated, with resultant cross-sectional area measurement. The top slice was chosen to calculate the boundary SI, as this in most cases has the largest CSF space: This helps to minimize inaccuracies that are inevitably present due to placement of the cord outline, which will affect the values in both ROIs.

Figure 12: ROI "inner" and "outer". *Left*, region of interest "inner". *Right*, region of interest "outer".



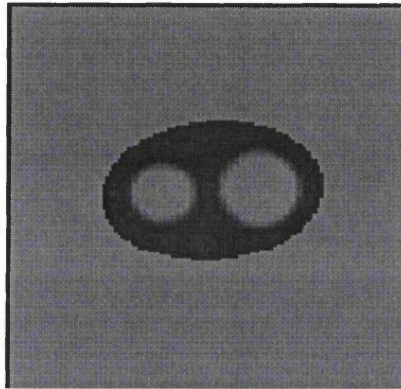
Reproducibility

Reproducibility was assessed for both the post acquisition measurement technique (i.e.: calculating the cord area twice on the same image) and for scan-rescan (i.e.: imaging the subject twice and then calculating the cord area from separate acquisitions), which is the realistic situation in a serial study. A series of 15 subjects (patients and controls) were selected to represent a range of spinal cord size. Each subject was scanned, removed from the magnet, repositioned and then rescanned. The images were then post processed. The boundary SI calculations and area measurements were then made by two investigators, one experienced with the technique (having developed it) and one not (a brief instruction on 5 data sets beforehand).

Accuracy

It was not possible to fully assess the accuracy of the 2D gradient echo technique using an in-vitro model as in-vivo imaging resulted in signal voids which could not be reproduced. However for the new technique a reasonable in-vitro model (a "phantom") could be constructed. This consisted of three acrylic resin plastic rods of known dimensions which were fixed in a water bath kept at room temperature. The rods were of uniform diameter to which the investigator was blind. These were imaged as above and five contiguous 3 mm slices were reformatted from the centre of the phantom. Uniformity correction was applied and following this contrast manipulation was performed to make the rods and surrounding water look as much like CSF and cord as possible. To achieve this the signal intensity of the two compartments (CSF and cord) of the control image (from which all windowing was adjusted) was measured and the two ends of the window (maximum and minimum) were noted. In arbitrary units the mean cord intensity = 21, mean CSF = 3, minimum window = 0 and maximum window = 40. From these figures the relative and absolute brightness of the phantom was adjusted to appear as nearly identical to the control image as possible (figure 13). This was achieved by inverting the signal intensities, shifting and scaling to give realistic values of CSF/cord contrast and then adding gaussian noise to give realistic signal to noise ratios. Following this, measurement was made as above.

Figure 13: Contrast adjusted phantom, showing 2 perspex rods. Two perspex rods are shown, following shifting and scaling of image intensities and addition of noise.



Statistics

Correlations between cord area and the EDSS were calculated using Spearman's Rank Correlation Coefficient (SRCC) and the Student's t test was used to evaluate the difference in cord areas between subgroups. Reproducibility was expressed as both the standard deviation of measurement variation (British Standards Institution, 1979) and the coefficient of variation (Goodkin et al. 1992).

3.2(b): Results

Reproducibility

The mean cord area of the 15 subjects was 85 mm² with a range of 45 mm² to 101 mm². The intraobserver standard deviation of measurement variation and coefficients of variation for the same scan and scan-rescan analysis are presented in table 7.

Table 7: Intraobserver reproducibility measurements

mean (range)

	Same image	Scan/rescan
Experienced	s=0.58 (0-1.9)	s=0.63 (0.14-1.9)
	cv=0.73% (0-2.4)	cv=0.79% (0.2-2.5)
Inexperienced	s=0.83 (0-2.7)	s=1.29 (0.1-5.6)
	cv= 1.03% (0-3.4)	cv= 1.61% (0.2-7%)

s= standard deviation of measurement variation in mm²

cv= coefficient of variation

With an experienced observer the coefficient of variation for scan-rescan was 0.79%, standard deviation of measurement variation = 0.63 mm². Hence changes as little as 1.2 mm² (1.96 standard deviations) in cord area would be beyond the 95% confidence limits for a change that may have occurred simply because of measurement variation. There was no significant correlation between cord size and the individual coefficients. The interobserver variability was also low with coefficients of variation for the same image and scan-rescan analysis of 0.83 and 1.7% respectively.

Accuracy

The known cross sectional areas of the 3 acrylic resin plastic rods were 131.7 mm², 77 mm² and 49.6 mm² (mechanical measurement with a maximum uncertainty of 1%). The imaging measurements were larger by 4.5%, 4.3% and 10.8% respectively (measured values 137.7 mm², 80.4 mm² and 55 mm²).

Controls

There were thirty controls whose characteristics are detailed in table 8. There was striking variation in cord size and no one factor was predictive. No significant correlation was seen between cord area and height, weight, body mass index or age. There were weak trends for increasing height and weight to correlate with increasing cord area: $r = 0.36$ and 0.28 respectively (SRCC). There was no relationship between age and cord area $r = -0.12$ (SRCC). Female subjects had a smaller mean cord area than males (82.05 and 87.24 mm² respectively) but this difference was not significant ($p = 0.11$).

Table 8: Characteristics of patients and controls

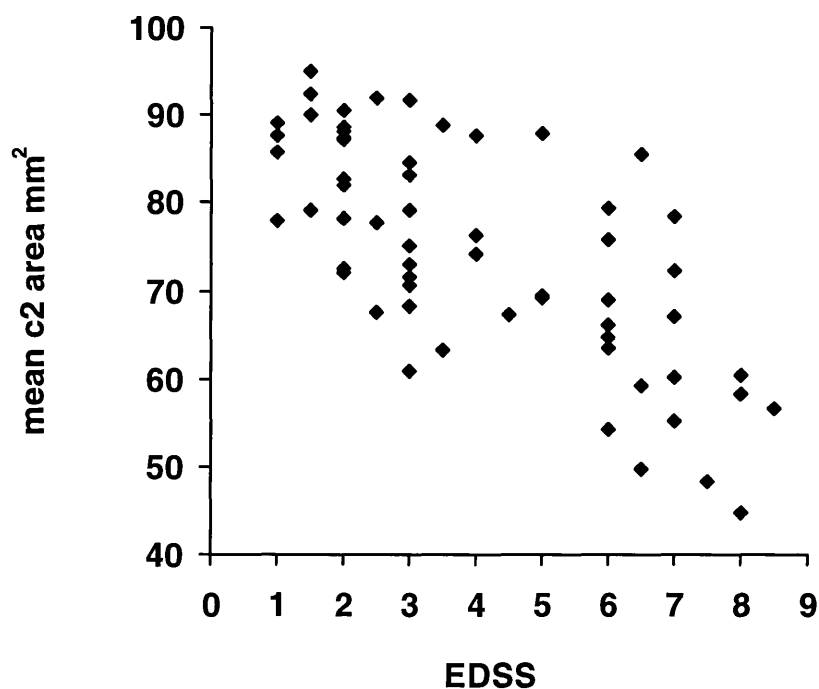
	Controls	All patients
numbers	30	60
mean age [years]	38	41
(range)	(26-57)	(21-63)
male:female ratio	15:15	26:34
mean height [m]	1.7	1.68
(range)	(1.4-1.95)	(1.48-2.15)
mean weight [kg]	65.6	65.7
(range)	(46-86)	(44-97)
cord area [mm²]	84.7	74.3*
(range)	(67-101)	(40-91)

* p < 0.001 for the difference in cord area between controls and patients

Patients

There were 60 patients whose characteristics are detailed in tables 8 and 9. There was a strong correlation between EDSS and cord area (See figure 14 overleaf) $r = -0.7$, $p < 0.001$ (SRCC). Significant correlations were also found when patients with high levels of disability were excluded: For the group EDSS 0-6, $n = 40$, $r = -0.6$, $p < 0.001$ (SRCC) and for the group EDSS 0-3, $n = 33$, $r = -0.4$, $p < 0.005$ (SRCC). There was a significant correlation between disease duration and cord area, $r = -0.5$, $p < 0.01$ (SRCC). At EDSS 3 the mean reduction in cord area compared to controls was 12% ($n = 10$), at EDSS 6 ($n = 7$) it was 21% and at EDSS 8 it was 35% ($n = 3$).

Figure 14: Scatter chart of EDSS and cord area in all patients



Significant correlation was also found between the functional system (FS) subscores of the EDSS, the EDSS itself and cord area reflecting the tendency in most patients for subscores to increase as the disease progresses. The most significant correlations were between the FS pyramidal and sphincter scores and cord area = -0.6 and -0.66 respectively $p < 0.001$, SRCC)

There were significant differences in cord area between the whole patient group and controls ($p < 0.001$) and the individual subgroups of benign, primary progressive, secondary progressive when compared with controls $p < 0.05$, < 0.05 and < 0.001 respectively. There was no difference between controls and the early relapsing remitting group most of whom had little disability. All patient groups were significantly different from each other ($p < 0.05$ - $p < 0.01$) with the exception of benign vs primary progressive. Within the patient group the largest difference was seen between the early relapsing remitting group and the secondary progressive group with mean cord areas of 85.63 mm^2 and 61.2 mm^2 respectively ($p < 0.01$).

Table 9: Individual patient subgroups

for all n=15

	Primary progressive	Secondary progressive	Relapsing Remitting	Benign
mean age [years] (range)	48.8 (38-63)	43.7 (31-57)	31 (21-50)	42.7 (30-58)
mean disease duration [years] (range)	10.4 (2.5-24)	15.9 (4-30)	4.1 (1-10)	14 (10-20)
median EDSS (range)	4 (2-7.5)	7 (4.5-8.5)	2.5 (1-6)	2 (1-3)
mean cord area at c2 [mm²] (range)	73.1 (48.3-88.8)	61.2 (44.8-72.2)	85.6 (74.1-95)	78.2 (60.8-92.3)
p = from controls	p<0.05	p<0.001	p=0.8	p<0.05

3.3 Conclusions to the new study at C2

This study showed a strong graded correlation between a clinical measure of neurological impairment/disability (the EDSS) and spinal cord atrophy. This relationship was present across all levels of disability suggesting a causal relationship. More importantly the magnitude of change observed in the patients and the reproducibility of the measurement suggest that this technique (to measure spinal cord atrophy) may prove more sensitive in monitoring progressive neurological impairment/disability than other currently used imaging parameters. There are several potential reasons why this study has shown a strong relationship between atrophy and disability and these relate to technical factors, the importance of the spinal cord and the nature of atrophy.

1. *Technical factors*: The high reproducibility of the newly developed technique relates to anatomical and imaging factors as discussed earlier. In addition, a semi-automated measurement technique was used to delineate the cord boundary which removes some of the imprecision that manual outlining and automated contouring have in delineating boundaries. In calculating the CSF image intensity by the method of one region (inner) within another (outer), errors of placement of the border that delineates the cord area and image intensity are counteracted: an overgenerous "inner" cord boundary will lower the calculated cord SI but raise the calculated CSF SI and in contrast a small "inner" cord boundary will increase the calculated cord SI and lower the calculated CSF SI. Thus within a certain range the technique produces a natural regression to the mean.

Our phantom experiments show that for normal size cords we probably overmeasure by approximately 4.5%. However the result from the smallest phantom shows over-

measurement by 10%. It is not surprising that over-measurement increases as the structure gets smaller and this has been our visual impression of the in-vivo situation. The greatest contribution to this inaccuracy is likely to be partial volume effects. As a structure gets smaller, the relative amount of partial volume that would be included in the first "inner" region of interest increases, reducing the calculated mean signal intensity of the cord and therefore lowering the calculated signal intensity at which the border lies with consequent enlargement of the area. However even with this bias which works against the detection of smaller structures a 35% reduction in cord area by EDSS 8 was shown. If this inaccuracy could be adjusted in some way (which should be possible with further phantom work) this measure of tissue destruction may become even more sensitive.

2. *The spinal cord and disability:* The EDSS is strongly weighted towards locomotion and hence more likely to correlate with destructive changes in the spinal cord than changes in the brain. The cervical cord is a common site for pathology in MS (Oppenheimer, 1978). However previous studies of the cord in which the visible abnormality has been quantitated (areas of high signal on T2 weighted scans) (Kidd et al. 1993) have shown no relationship between these areas of high signal and clinical disability. This is likely to have been due to the non specific nature of signal change detected by T2 weighted conventional or fast spin echo and possibly failure to detect small lesions.

3. *The significance of atrophy?* The contribution of demyelination to atrophy is uncertain as reactive gliosis may, at least to some extent, fill the space previously occupied by myelin. However Prineas (Prineas and Connell, 1978) has observed a reduction in axonal diameter associated with demyelination. Axonal loss is of course a potent cause of atrophy of the cord

as studies of trauma show (Guttman, 1973), is seen in many lesions in MS and may be extreme (Charcot, 1868; Bielschowsky, 1903; Dawson, 1916; Greenfield and King, 1936; Adams and Kubik, 1952; Ozawa et al. 1994). Biopsies show that axonal loss may occur acutely (Ozawa et al. 1994), and it may be detected by ophthalmoscopy as slits in the retinal nerve fibre layer early in the course of MS (Frisen and Hoyt, 1974) and even after a single episode of optic neuritis (personal observation). There is indirect in-vivo MRI evidence of axonal loss in chronic lesions derived from transverse magnetisation decay curve analysis (Barnes et al. 1991) and proton spectroscopy (Arnold et al. 1992; Davie et al. 1995). It is therefore likely that axonal loss makes a significant contribution to the atrophy we have observed, particularly when it is severe.

Three important issues remain to be addressed: One is the question of when detectable degrees of atrophy start to occur. In this study a significant difference between the cohort of patients with early relapsing-remitting MS and controls was not demonstrated. This cohort were characterised by a short disease duration (mean = 4.2 years) and it is noteworthy that the benign group with a similar level of disability but a much longer disease duration had a significant decrease in cord area. This implies that atrophy may be both a feature of disease duration and progressive deterioration. Whether this measure will be of predictive value in early MS for future disability will require serial evaluation. Secondly while there is a striking correlation between spinal cord atrophy and disability, marked scatter at most levels of the EDSS was observed. Whilst this may in part be due to natural biological variability, there remained some patients with marked disability (eg: due to ataxia or involvement of the internal capsule) who did not have obvious spinal cord atrophy. It would be of considerable interest to study these patients with other regional volume measurements. Thirdly can

features be identified that are associated with the atrophic process: for example, is MR activity (the appearance of new lesions) a predisposing factor?

Chapter 4: Cerebral atrophy

4.1 Why measure cerebral atrophy

A number of questions have been raised following the cross-sectional study of spinal cord atrophy. Does atrophy of other sites also relate to disability? Can atrophy of the CNS be detected early in the course of the disease? Can other features be identified that predict or are associated with the development of atrophy?

Another area commonly involved in multiple sclerosis is the cerebral white matter (Cruveilhier, 1829; Brownell and Hughes, 1962) and the significance of atrophic changes to this area has been in part already been addressed by studies of cerebral atrophy. These studies (performed with a number of imaging modalities) have given conflicting results as to the clinical significance of cerebral atrophy (Loizou et al. 1982; Rao et al. 1985; Hageleit et al. 1987; Huber et al. 1987; Comi et al. 1993; Gross et al. 1993), possibly because of their cross-sectional design, and the large intersubject variations in normal brain size (Blatter et al. 1995). To date there has been no definitive serial study of the measurement and significance of progressive cerebral atrophy in multiple sclerosis and the relationship of the development of atrophy to either clinical progression in disability or MRI markers of disease activity (change in number and volume of lesions and volume of gadolinium enhancing lesions). These questions could be most easily answered by serial evaluation of the cerebral white matter, in view of the predilection for pathological activity at this site and its accessibility to high definition MRI.

A new technique to quantify the volume of a region of the cerebral hemispheres was therefore developed and applied to a group of 29 patients with multiple sclerosis participating in an 18 month treatment trial with a monoclonal antibody against CD4 positive (CD4⁺) T lymphocytes. This was a multicentre, phase II, double blind, placebo controlled study set up to evaluate the effect of sustained suppression of CD4⁺ T lymphocytes with the chimeric monoclonal anti-CD4 antibody cMT412 (Centocor) on MRI measured disease activity (cranial MRI with gadolinium enhancement as the primary outcome) in multiple sclerosis. No reduction in MRI activity was seen (Barkhof et al. 1996).

The data collected at the NMR Research Unit during this trial was used to ascertain if progressive atrophy could be detected in individual patients outside the 95% confidence limits for measurement variation and if so what the relationship was to change in disability. The relationship of atrophy to lesion load, change in lesion load and volume of gadolinium enhancement detected during this serial study was also explored.

4.2 A new technique to measure cerebral atrophy

4.2 (a) Introduction

Numerous techniques for the measurement of brain and cerebral volume have been described and applied in cross sectional studies but at the time of performing this study it seemed unlikely that any existing techniques could be employed for serial evaluation (for exactly the same methodological reasons discussed in the preceding chapter on spinal cord atrophy). Atrophic changes are likely to be small over limited time periods and the significance of any change could be easily obscured by measurement errors. Ideally, it would be necessary to

define changes in *individual* subjects with a known degree of confidence as to whether they could be explained by chance.

The data from the CD4 trial provided an ideal opportunity to evaluate the significance of cerebral atrophy. Firstly, the patients selected formed a model treatment trial group with clinically aggressive disease and hence if any change was likely to be seen it should be detectable in this group. Secondly, the radiography (and therefore repositioning) was carefully performed according to trial criteria. Thirdly, disability ratings and quantitative MR measures (e.g. lesion load) were carefully evaluated and had been performed by one observer. Fourthly, the MRI data from this trial was in identical format to ongoing treatment trials and hence if a technique to measure atrophy on these scans could be developed it would serve as a useful technique for future analysis.

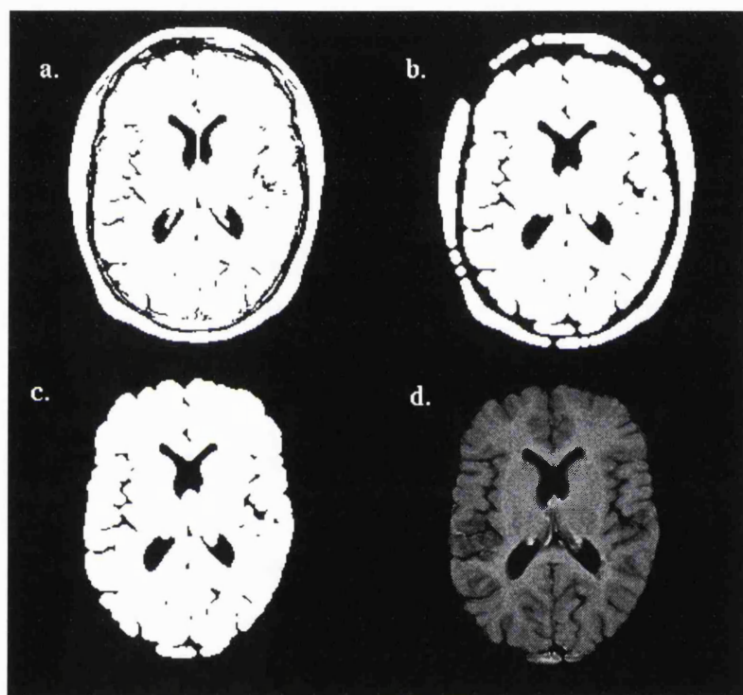
4.2 (b) A new technique

The basis of the new method to measure cerebral volume was to extract the brain from the skull and surrounding tissues, then simply count the number of pixels it occupies (each of which has a known size). This was achieved using an algorithm integrated in an image analysis package (eXKull copyright D.S. Yoo, Department of Medical Physics and Bio-Engineering, University College London) developed for work on skull segmentation (Yoo et al. 1995).

The method combines histogram-based automatic thresholding with sequences of morphological operations that distinguish the brain from surrounding tissues as illustrated in figure 15. The following procedure is performed when extracting the brain:

1. Automatic thresholding by discriminant analysis of the histogram: A histogram of image intensities represented in a complete slice is formed. It is then assumed that all pixels in the given slice belong to one of two classes, background or brain. Discriminant analysis searches for the optimal grey level that best separates these two classes by variance optimisation. Once the optimal threshold has been found, this is applied to classify the pixels into one of two classes: background or brain and a binary image (figure 15a) is thus created for the next step.
2. Morphological opening operation: The opening (dilation after erosion) is used to correct imperfections in the thresholded binary image by separating the brain from the undesired components in the head (e.g., bone, muscle and scalp) with a circular structuring element. The size of the structuring element is fixed through the whole process. (figure 15b).
3. Connected component analysis: This consists of three main operations: (1) connection of components with non-zero pixels, (2) labelling and counting the connected components and (3) selecting the largest connected component as the brain (figure 15c).
4. Masking operation: The resulting binary image of the brain is masked to the original grey image and finally the brain is extracted from the head (figure 15d).

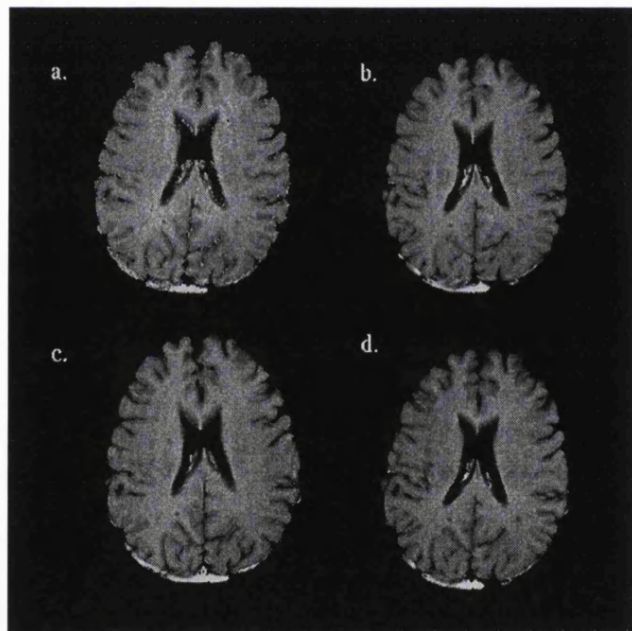
Figure 15: A brain extraction using eXKull. Following automatic thresholding, a binary image is produced (a), and the morphological opening separates the brain from the scalp and skull (b). The brain is determined as the largest component by connected component analysis (c), and finally the cerebral tissue is extracted by masking the binary brain image to the original grey image (d).



If T1 weighted images are used the CSF has grey levels close to background and is thus thresholded out. Hence progressive enlargement of the ventricles and CSF spaces could be sensitively detected. In approximately 2% of all slices the process fails, resulting in small islands of skull being left. These undesired regions can be removed manually by an operator. The process also commonly leaves undesired tissue such as choroid plexus and small areas

of sagittal or straight sinus enhancement (if post gadolinium-DTPA scans are analysed). These appeared consistent in any given patient across time (figure 16).

Figure 16: Consistency of gadolinium across time. A single patient scanned at 0, 6, 12 and 18 months (labelled a, b, c and d). There is consistency of the volume of undesired tissue, both intraventricular and sinus enhancement.



All these undesired regions could be eliminated by iterating the process with either a higher thresholding value or a larger structuring element size. However this would result in the introduction of arbitrary variables and was therefore not included in the methodology.

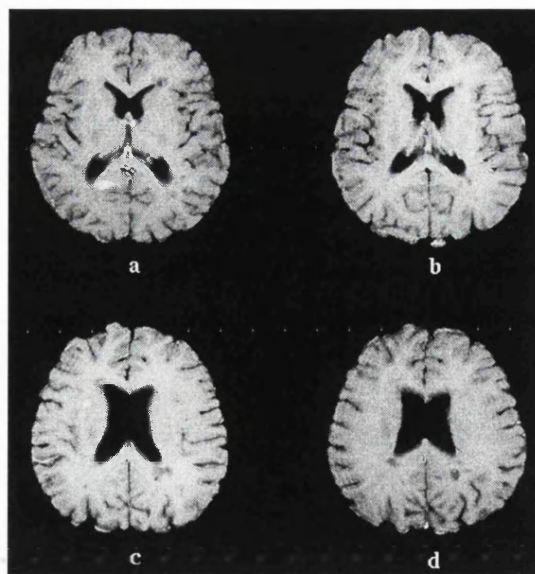
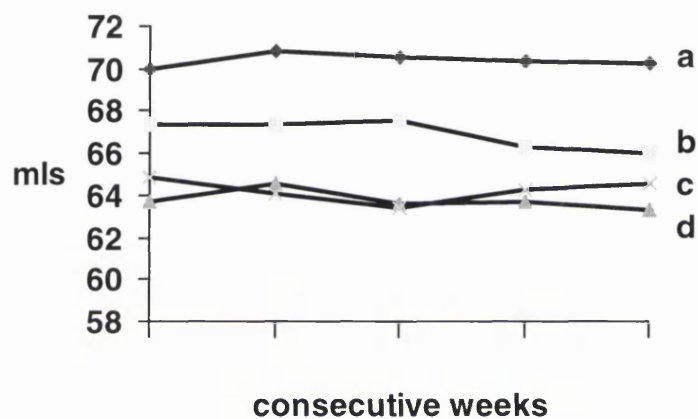
Following extraction and any editing the volume represented in an extracted slice can be calculated using software (Calc-Vol, L Wang, Institute of Neurology) which simply counts

the number of non zero pixels remaining and multiplies them by their size. This can then be expressed in mls. The method described would be susceptible to changes in the size of the image field of view produced by gradient fluctuations but examination of phantom data collected during the time period of the anti-CD4 treatment trial show that these are small (<1%), predominantly in the z direction and random. No systematic drift was observed.

4.2 (c) Reproducibility

Having established a technique which could segment brain tissue from other undesirable elements in an image it was necessary to apply this in a way that covered an appropriate region of interest in a reproducible manner. To establish this the technique was applied to different slice prescriptions from 5 patients with clinically definite multiple sclerosis scanned weekly for 5 weeks with an identical MRI protocol to those patients in the anti-CD4 trial. These patients were participating in a separate study set up to ascertain if weekly scanning detects significantly more enhancing lesions than monthly scanning. Scan-rescan reproducibility was assessed by comparing week 2 to week 1, week 3 to week 2 etc in each patient which gave a total of 20 scan-rescan observations. The assumption was that real changes in brain volume over a period of one week would be very small compared with apparent changes produced by measurement variation. From these patients it was ascertained that the best reproducibility containing the region of interest was obtained using 4 contiguous slices with the most caudal at the level of the velum interpositum cerebri, thus encompassing the lateral ventricles and associated white matter. An example of the volume of the 4 individual slices is illustrated in figure 17 for a single patient over 5 weeks.

Figure 17: Reproducibility assessed with weekly scanning. The volume of 4 individual slices is illustrated in a subject scanned weekly, labelled a, b, c and d with the extracted images shown below. Slice “a” caudal at the level of the velum interpositum cerebri and slice “d” rostral near the roof of the lateral ventricles.



Mean cerebral volume of the 4 slices for the 5 patients studied weekly was 299 mls (range 265-319). For any given series of slices the volume calculated from repeated brain extraction and non-zero pixel counting was identical. For scan-rescan analysis, which takes into account repositioning, the mean co-efficient of variation was 0.56% (range 0.15-1.5) with a mean standard deviation of measurement variation of 1.67 mls (range 0.4-4.5). Hence changes as little as 1.1% would be outside the 95% confidence limit for that occurring by chance due to measurement variation.

4.3 A serial clinical study of progressive cerebral atrophy

4.3 (a) Methods

Patients

Twenty nine patients were included in the London arm of the anti-CD4 trial of which 27 completed the trial. One patient dropped out at month 9 and one at month 12, both because of increasing disability. The inclusion criteria were as follows:

1. Clinically definite multiple sclerosis which followed a relapsing-remitting or secondary progressive course.
2. Evidence of clinically active disease: either 2 relapses within the 12 months prior to inclusion, one of which was in the preceding 6 months, or deterioration of at least one point on the EDSS within the preceding 18 months.
3. Current EDSS 3-7.

Exclusion criteria included primary progressive multiple sclerosis, significant cognitive impairment and treatment with corticosteroids within the last month.

MRI protocol

All imaging was performed on a Signa 1.5T machine (General Electric, Milwaukee WI) using a standard quadrature head coil. Patients were imaged monthly from month minus 1 to month 9 and then at 12 months and 18 months with the following sequences:

1. Dual echo T2 weighted, (TR = 3000 ms, TE = 30 and 80 ms.)

2. T1 weighted (TR = 600 ms, TE = 20 ms) 10 minutes post injection with gadolinium DTPA 0.1mmol/kg.

All sequences were acquired as axial contiguous 5 mm slices, 256^2 image matrix, 24 cm field of view. Repositioning was ensured by 4 oblique pilots.

Clinical

At each of the above timepoints the patients underwent a full neurological and general examination by one observer who scored them on the EDSS . A definite change in EDSS was defined as progression of greater or equal to 1 point for patients entering with a score below EDSS 5.5, or greater or equal to 0.5 points for patients entering with a score greater or equal to EDSS 5.5 (Goodkin, 1991). Any change had to be sustained for three months or more.

Image analysis

Lesion load and gadolinium volumes

The total lesion load on the mildly T2 weighted image (SE 3000/30) was calculated at baseline and 18 months. The volume of new gadolinium enhancement was calculated on each monthly scan for the period from month 0 to 9. These calculations were all performed by one observer who was blind to the scan identity and using the image display programme Dispunc with a contouring technique (Grimaud et al. 1996).

Measurement of cerebral volume

Brain extraction was performed as previously described on the gadolinium enhanced T1 weighted images for months 0, 6, 12 and 18 (for the two patients who dropped out images were analysed for months 0, 3, 6 and 9 and 1, 4, 8 and 12 respectively). Before brain extraction the scans were examined by an experienced radiologist blind to the clinical details and identity of the localising slice, to ensure that repositioning was satisfactory by using current accepted treatment trial criteria (Polman et al. 1995). This inspection was important as progressive atrophy of areas of the brain used as landmarks for repositioning (e.g. the corpus callosum) may result in spurious movement of numbered slices. Following this the radiologist selected 4 contiguous slices from each scan with the most caudal at the level of the velum interpositum. Of the 116 scans examined, 5 were excluded from analysis as repositioning was considered unsatisfactory. No patients had fewer than 3 timepoints for analysis after rejection of unsatisfactory images. Three patients were not represented at month 18 as two had dropped out and in one other the scans were rejected as repositioning was unsatisfactory.

4.3 (b) Results

Baseline characteristics (month 0)

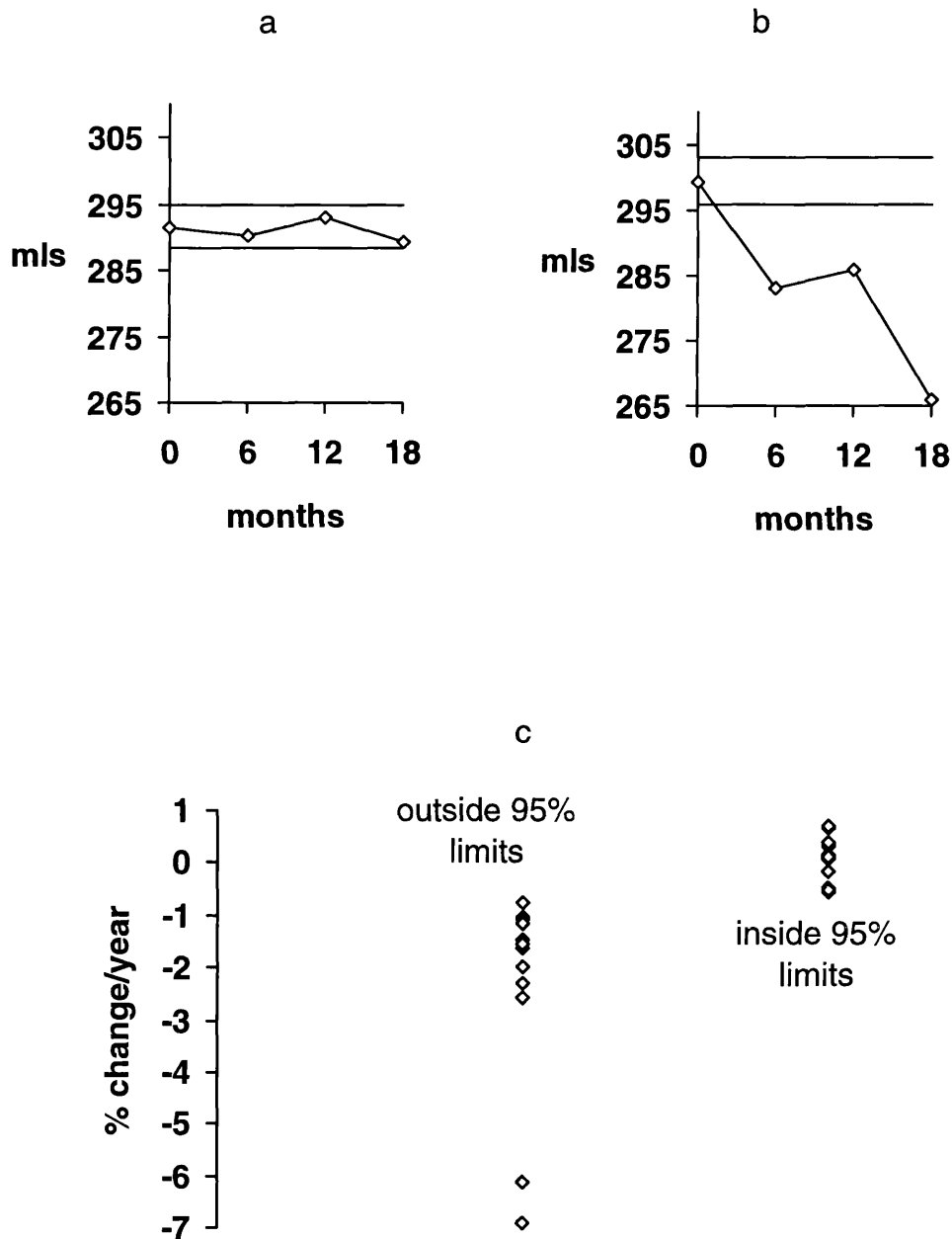
There were 29 patients, mean age 38 years (range 26-53), 13 male and 16 female, 13 had relapsing-remitting multiple sclerosis while in 16 it was secondary progressive. Mean disease duration was 8.8 years (range 1-29). Mean EDSS at entry was 5 (range 2-8) . Mean cerebral volume in the 4 slices was 302 mls (range 270-346 mls). Males had significantly larger cerebral volumes than females (mean 316 mls compared with 291 mls, $p < 0.01$). There was no significant difference between the cerebral volume of the relapsing-remitting group and the secondary progressive group though the latter group contained a higher proportion of men. There was no cross sectional correlation between cerebral volume at baseline and the EDSS or its functional system subscores.

Serial results

Mean EDSS at exit for all patients was 5.9 (range 1-8.5). The mean rate of brain volume change by the end of the study for all patients was -3.4 mls/year ($p < 0.001$ comparing month 0 with exit).

In each patient graphs were constructed illustrating the measured cerebral volume at the 4 time points. Examples of which are given in figure 18 showing change inside and outside the 95% confidence limits for measurement variation. Also shown is the rate of atrophy per year for the 2 groups: those who fell outside or inside the 95% confidence limits for measurement variation by the end of the study.

Figure 18: Serial measurement over 18 months. Two patterns are illustrated, showing no significant (a) and significant change (b) of cerebral volume in two patients over 18 months. The straight lines mark the 95% confidence limits for measurement variation. The bottom graph (c) illustrates change per year in all patients for two groups, those who exceeded the 95% confidence limits for measurement variation at month 18 and those who did not.



Four individuals had developed a significant reduction in brain volume by 6 months, eight by 12 months and 16 by 18 months. Both of the patients who dropped out had a significant reduction in brain volume by 3 and 4 months respectively. The remaining 13 patients did not show individual change outside of the measurement variation at 18 months.

There were five occasions out of a total of 109 separate timepoints in which the upper limit for measurement variation was exceeded (none at 18 months) compared with 44 separate occasions in which the lower limit was exceeded. Patients were stratified into two groups: those who did ($n = 16$) or did not ($n = 13$) develop change outside of the 95% confidence limits for measurement variation by the end of the study. The change in cerebral volume in % is illustrated for these two groups in figure 18 and their full clinical and MRI characteristics are described in table 10 overleaf.

Table 10: Clinical and MRI characteristics stratified by the development of progressive atrophy

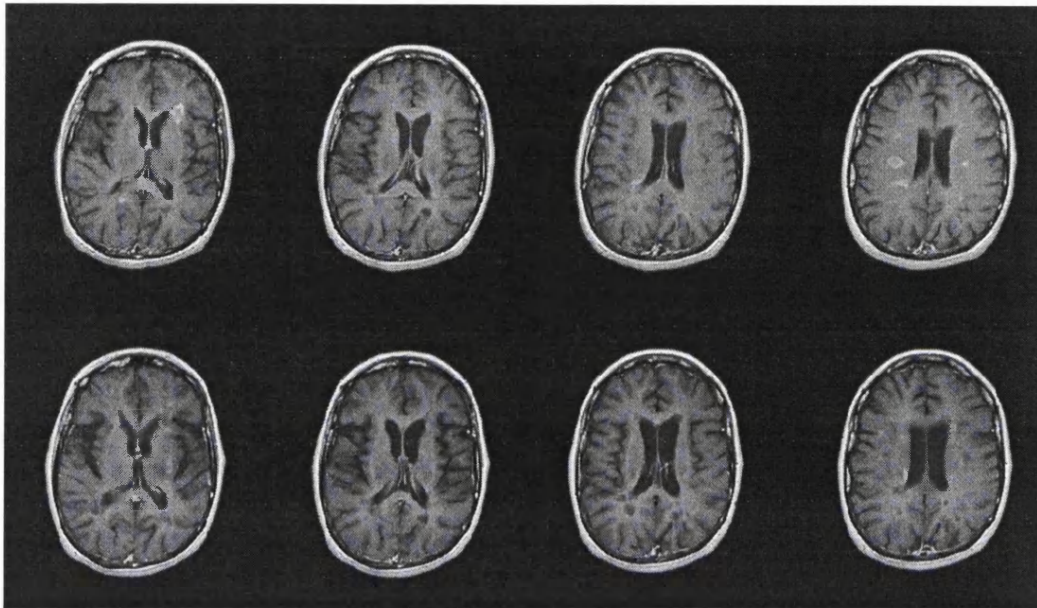
	Definite cerebral volume change	No definite volume change	p
Numbers	16	13	
Mean age (range)	38 (32-50)	39 (26-53)	0.7
Sex	8F, 8M	5M, 8F	0.8
Disease subtype	11 SP 5 RR	5 SP 8 RR	0.2
Mean disease duration (range)	9 years (2-29)	8 years (1-26)	0.4
Mean baseline EDSS: month 0 (range)	5.4 (3.5-7)	4.9 (2-7)	0.2
Mean exit EDSS (range)	6.6 (3-8)	5 (1-8.5)	< 0.01
Mean baseline cerebral volume (range)	298 mls (269-345)	309 mls (271-377)	0.18
Mean baseline T2 lesion load: month 0 (range)	53 mls (13-161)	32 mls (2-97)	0.06
Mean change in T2 lesion load [month 18] (range)	+ 6.3mls (-17 to +41)	+ 0.8 mls (-6 to +9)	0.31
Mean detected new gadolinium volume [months 0-9] (range)	6.7 mls (0.47-34)	4 mls (0.2-14)	0.6

Range for "definite cerebral volume change" = -2.3 to - 21 mls/year and for "no definite volume change" = -1.9 to +2.1 mls/year.

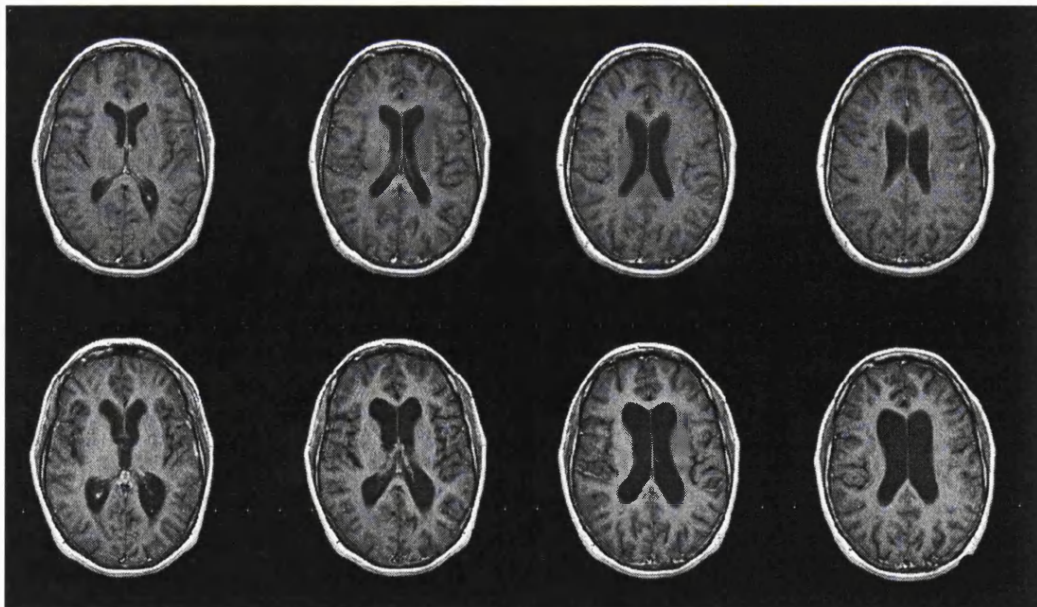
Patients in whom progressive atrophy was detected were more likely to have secondary progressive multiple sclerosis (11/16) and tended to have smaller brains at entry though this was not statistically significant. A significant change in EDSS score ($p < 0.05$) was seen in the group with progressive atrophy and this group had a slight tendency toward greater disability at baseline (mean EDSS 5.4 compared with 4.9 for the group without progressive atrophy, $p = 0.2$). These changes in EDSS were not accounted for by the acute effects of a relapse. Of the group in whom we detected progressive atrophy 8/16 had a sustained change in EDSS while in the group which did not have progressive atrophy only 2/13 had a sustained change. The 10 patients who had a sustained change in EDSS had a significantly higher rate of progressive atrophy when compared with the group without a sustained EDSS change (-6.4 mls/year compared with -1.8 mls/year respectively, $p < 0.05$). However both groups showed a significant change in cerebral volume from baseline ($p < 0.05$).

Baseline T2 lesion load, T2 lesion load changes (over 18 months) and gadolinium volumes (over 10 months) did not significantly correlate with progressive atrophy (mls/yr) but there was a trend suggesting a higher baseline lesion load ($p = 0.06$) in the group that developed progressive atrophy. As gadolinium volumes were only measured for the first 10 months we also examined their relationship to the development of atrophy between 0 and 12 months but no significant correlation was found. Development of marked atrophy was seen both in patients who had minimal gadolinium enhancement detected over the initial 10 months and those with intense activity (figure 19)

Figure 19: Development of atrophy.



Above are matched scans from month 0 (top row) and month 9 (bottom row). This patient with marked enhancement detected shows changes in the ventricles and sulci over a 9 month period. The volume of new gadolinium enhancement detected over month 0-9 was 34mls.



Above are matched scans from month 0 (top row) and month 18 (bottom row). This patient had minimal enhancement detected at month 0 (0.4 mls) and none during months 1-9, 12 and 18. There is marked dilation of the ventricles over 18 months with increased differentiation of the grey/white matter. The atrophy had evolved gradually with a graded increase evident at month 6 and 12.

Gadolinium volumes were significantly higher for the group that had a definite sustained change in EDSS ($p < 0.05$) and there were trends to suggest a higher baseline T2 lesion load and change in T2 lesion load in this group.

The mean rate of development of atrophy in those who received anti-CD4 antibodies was -3.6 mls/year and in those who received placebo was -3.1 mls per/year ($p = 0.77$).

4.4 Discussion

4.4 (a) Introduction

This was the first study to demonstrate progressive cerebral atrophy by serial MRI scanning in individual patients with multiple sclerosis. The results suggest that atrophy correlates with worsening disability and although it may be present in patients who do not have measurably increasing disability it progresses at a significantly slower rate than in those who do. These findings suggest that this measure is clinically relevant, gradable, objective and practical enough for inclusion in treatment trials. It may also have greater sensitivity in detecting clinically relevant changes than some currently used disability scales and MRI measures.

4.4 (b) Relationship of atrophy to disability

It seems unlikely that progressive cerebral atrophy is the primary cause of worsening motor disability as measured by the EDSS, in this regard changes in the spinal cord are likely to be more relevant. However it is at very least a process which runs in parallel with clinical disease progression and is therefore a poor prognostic sign. The opportunity to analyze the

relationship between cerebral atrophy and progressive cognitive impairment was not available as the only data available was from the Kurtzke functional system mental score, which is very limited and has poor reliability (Francis et al. 1991). In addition patients with significant cognitive impairment were excluded from the trial. Previous investigators have demonstrated a relationship between serial psychometry and change in MRI lesion load (Feinstein et al. 1993), hence future investigation with regard to atrophy will be of considerable interest.

4.4 (c) Measurement of cerebral atrophy.

The technique described is relatively simple to apply, has high serial reproducibility and is not time consuming. This particular slice prescription was chosen for a number of reasons. First, slices below the level of the velum interpositum commonly include orbital tissue which interferes with the extraction, necessitating extensive manual editing. Secondly the most rostral of the selected slices tends to be situated at the level of the roof of the lateral ventricles. Beyond this point the increasing convexity of the brain means that small changes in positioning lead to large changes in measured volume, reducing reproducibility. However in slices positioned through the ventricles even where the brain surface is becoming convex, there is little change in measured volume with repositioning: it appears that as the brain circumference gets smaller, so do the ventricles and hence the measured volume remains relatively constant (see figure 17) with small positioning changes. Thirdly this area is a very common site for disease activity and for the development of atrophy, evidenced both as ventricular and sulcal enlargement (see figure 19). Sensitivity to detect change is thus maximised.

Gadolinium enhanced T1 weighted scans were chosen for two reasons. Firstly the grey level of CSF is close to background and hence automatically thresholded out. Secondly this type of imaging forms an essential part of ongoing treatment trials in multiple sclerosis (Polman et al. 1995). Administration of gadolinium results in small amounts of sinus enhancement but this is consistent across time in any given patient. Ideally in future studies non gadolinium enhanced scans should be used and the technique could further be improved by volume acquisition. This would overcome repositioning errors, probably the major factor affecting reproducibility, and may allow segmentation of the white and grey matter as they would have better differentiation. The high reproducibility allows changes in individual patients to be categorised with some degree of confidence. However it is important to be aware that there may be a difference between short term reproducibility as defined in the study of patients scanned weekly and long term reproducibility when other factors need to be considered such as gradient drift and the effects of normal ageing.

4.4 (d) Pathological implications

In our patients we have seen that atrophy is the result of both ventricular and sulcal enlargement (figure 19) but the extent to which grey matter involvement contributes to this sulcal change is uncertain without formal measurement. The changes we have observed in most patients are diffuse and symmetrical (as in the spinal cord) but in some the ventricles are enlarged with a degree of asymmetry unexpected from normal biological variation, suggesting a focal pathology. Periventricular T1 hypointense lesions at the tips of the lateral ventricular horn were occasionally seen, the functional significance of which has been

discussed recently (van Walderveen et al. 1995) but direct evolution of a hypointense lesion to "atrophy" over this time period was not observed. It seems possible that these hypointense lesions may (in some cases) be an intermediate stage in the development of atrophy as current evidence suggests they have less tissue structure than lesions visualised by T2 weighted imaging only. Of importance, atrophy is only detectable by observing change at the borders of the brain and spinal cord with the CSF spaces. This suggests that the central nervous system responds to tissue destruction in a fluid manner, reorganising itself to fill areas devoid of tissue due to previous damage. If so, considerable tissue destruction may occur but will not be accounted for in the characteristics of a focal abnormality as previously discussed in chapter 1.

4.4 (e) Possible confounding factors

It is also important to be aware of other factors that may influence cerebral volume such as excessive alcohol intake (Ron et al. 1982), anorexia (Kohlmeyer et al. 1983), corticosteroid administration (Bentson et al. 1978) and acute dehydration (Mellanby and Reveley, 1982). None of the patients in the trial had evidence of severe dehydration, malnutrition or alcohol abuse as evidenced by clinical examination, normal blood urea and electrolytes, albumin and liver enzymes. Eight patients received intravenous methylprednisolone (1g daily for 3 days) and no steroids were given within 3 months of any of the measured timepoints. The rate of progressive atrophy in those patients who received steroids was not significantly different from those who did not. It is also possible that the anti-CD4 antibodies may have distorted the natural history of the development of atrophy either by influencing disease activity or by a direct effect on brain volume. This seems unlikely in view of the overall similarity between

treated and untreated groups. In addition there was no control group (as the imaging analysed was post gadolinium) and hence the contribution normal ageing over this time period is uncertain. A study using a similar technique to this and examining the effect of ageing from the third to the eighth decade (in a cross-sectional design) has quantified the cerebral volume represented in seven 5 mm slices with the most caudal slice just above the orbits (Pfefferbaum et al. 1994). An average decrease in cortical grey matter volume of 0.7 mls/year, stable cortical white matter volumes and an increase in ventricular CSF of 0.3 mls/yr was found. Given that the volume of brain examined in the earlier study is far greater than that represented in this technique it seems unlikely that normal ageing makes a significant difference to the findings. All serial studies would be subject to ageing effects and this would not influence the fact that atrophy develops at a significantly higher rate in those with worsening disability .

4.4 (f) Relationship to other MR parameters

The group who developed atrophy had a smaller cerebral volume at baseline (despite having proportionately more men). However this was not significant and may reflect the fact that this group was slightly more disabled at baseline and that the atrophic process was already established. The lack of strong relationship between atrophy and other MR measures of disease activity, such as gadolinium enhancing lesion volume, T2 lesion load or change in T2 lesion load is of particular interest. There are at least three possible reasons for this. First, the extent and duration of enhancement (indicating blood brain barrier breakdown) may not always result in the same degree of tissue destruction. Secondly we do not know the precise pathophysiology of atrophy and its temporal relationship to episodes of blood brain barrier

breakdown. Thirdly the relationship of enhancement over 10 months to the development of atrophy over 12 and 18 months was examined. It is possible that this is misleading and that the development of atrophy may be a response to events that have occurred some time before or after the period of scanning with gadolinium. Nevertheless, current opinion favours the view that the greater the activity (as evidenced by gadolinium enhancement) the worse the prognosis with regard to the development of disability. This is supported by a recent study suggesting that the frequency of gadolinium enhancing lesions detected over a six month period in a group of secondary progressive patients was predictive of increase in disability measured 5 years later (Losseff et al. 1996) and the fact that in the present study gadolinium volumes were significantly higher for those who developed a definite sustained EDSS change; a similar observation was made in a previous study (Smith et al. 1993). To detect gadolinium enhancement visually one needs sufficient contrast from surrounding tissues. Of interest, one of the patients illustrated in figure 19 displays a diffuse change in the grey-white matter differentiation over 18 months (Prof G du Boulay, personal communication) despite no focal enhancing lesions having been detected during months 1-9, month 12 and 18. One possible explanation for this is diffuse enhancement which would be not included in the measurement of gadolinium volumes.

Baseline T2 lesion load showed a strong trend ($p = 0.06$) towards increased volume in the group who subsequently developed atrophy. This trend was not seen for serial lesion load measurement and it is possible that the development of atrophy may interfere with this measurement, by changes in brain structure affecting repositioning and by "loss" of existing lesions which become part of the CSF spaces. However this is unlikely unless progressive atrophy is extreme, as seen in figure 19.

It is well recognised that patient's disability may progress without any detectable MRI activity (Kidd et al. 1996) and hence current MRI activity measures may not be reflecting or predicting all functionally relevant pathological change.

Progressive cerebral atrophy appears to be a common finding in this group selected for a treatment trial, it may be detected in individual patients over a short period of time and may appear at an early stage in the disease. In the present study early progressive atrophy was detected in 5 out of 13 relapsing-remitting patients with a mean disease duration of 7.2 years (range 2-12 years). Cerebral atrophy may develop at a rapid rate despite the static appearance of the patients measured disability and absent MR activity. The results suggest that the technique used to measure cerebral atrophy is objective and yields clinically relevant information of prognostic value.

Chapter 5: Conclusion

5.1 Practical uses of techniques to measure atrophy

Will the techniques described in this thesis have practical use in the assessment of putative treatments aimed at preventing disability in multiple sclerosis? Firstly it is important to be clear what is being assessed. MRI can be used in treatment trials to give insight into various aspects of the pathological process. For example, gadolinium enhancement tells us about blood brain-barrier breakdown (an early event) and atrophy tells us about loss of tissue (probably a late event). If a treatment had no effect on atrophy this might be because we have examined its effect over too short a time course. It must also be considered that the administration of an immune modulating agent may itself result in a decrease of brain volume if blood brain barrier breakdown ceases and inflammatory infiltration ceases. There is some preliminary evidence that this may indeed be the case (Dr J Frank, personal communication).

A convincing cross-sectional correlation has been demonstrated between spinal cord atrophy and disability. However it remains to be seen if serial monitoring of patients using the techniques described will show a definite relationship between progressive disability and worsening atrophy. Such studies are ongoing at present and the technique described in chapter 3 has been adopted in a longitudinal pan-European study of primary progressive MS and as a secondary outcome measure in an ongoing trial of beta-interferon beta 1a in primary progressive MS (Biogen).

It has also been demonstrated that progressive cerebral atrophy may be detected in most patients with relatively aggressive disease who were selected for a phase II treatment

trial over an 18 month period. In addition a subtype dependent effect was detected since there was a trend suggesting that the secondary progressive group developed more atrophy than the relapsing-remitting group. Hence in planning any future trial it will be necessary to bear these factors in mind. One advantage of the technique described is that it can be applied to 2D imaging and partly because of this it has been adopted as a secondary outcome measure for an ongoing trial of beta-interferon beta 1b in secondary progressive MS (Schering). Further advances could be made using volume acquisition and image registration and subtraction. At the time of writing one group has developed a highly promising technique with which it is possible to detect quite small changes on serial volume imaging (Fox et al. 1996). Another route forward to improve sensitivity would be to segment out the grey and white matter. Conventional spin echo achieves poor definition between the grey and white matter. The heavily T1 weighted volume acquisition described earlier achieves good differentiation of grey and white matter in the brain, such that pixel histograms show a clear bimodal distribution. By use of brain extraction followed by mathematical techniques to segment histograms of grey and white cerebral tissue, reproducible measurements on white matter alone could possibly be made.

5.2 Concluding remarks

The work described in this thesis aimed to investigate changes in the nervous system that were associated with or responsible for fixed functional deficit in MS; firstly by studying the spinal cord (in view of the clinical relationship between spinal cord dysfunction and motor

disability) in a cross sectional study and secondly by examining the evolution of such changes in the brain.

These studies demonstrate that atrophy is a process closely linked with disability, that it manifests both in the brain and spinal cord and that it may evolve independently of new disease activity as indicated by gadolinium enhanced MRI.

However although variations in the degree of atrophy explain a proportion of the variance in disability between patients, and in the development of disability in an individual patient, it is clear from both studies of the brain and spinal cord that patients may be disabled without obvious atrophy and that disability may evolve in the absence of progressive atrophic changes.

Disability and impairment are the final clinical manifestations of a disease process and may be brought about by many different underlying mechanisms. It is important to try to consider these mechanisms separately as they may operate independently. At a rudimentary level we can learn a great deal from the clinical observation that persistent impairment may result from an acute relapse, due to failure to recover from that relapse or to the process of chronic progression. It is possible that every episode of disease activity results in some damage, be it subclinical or not. We know that in acute relapses and perhaps to a certain degree at other times, functional impairment is associated with blood brain barrier breakdown and when this resolves function returns to a large extent although evidence of demyelination persists (Youl et al. 1991). Breakdown of the blood brain barrier coincides with inflammation and as discussed earlier it is likely that soluble factors (in addition to the physical consequences of demyelination) are partly responsible for impairment of function (Koller et al. 1996; Moreau et al. 1996). Various mechanisms may underlie recovery: resolution of inflammation and insertion of new sodium channels are important early mechanisms (Moll

et al. 1991; Youl et al. 1991). Remyelination does occur and may be extensive (Prineas et al. 1993b), although conclusive evidence that restoration of conduction by remyelination in MS is lacking.

However “chronic progression” as observed clinically in primary and secondary progressive MS, behaves completely differently from acute relapsing-remitting disease. Here we observe a slow insidious deterioration (although superimposed relapses sometimes occur during the secondary progressive phase). Atrophy is likely to contribute particularly to this insidious process as it is a common feature of progressive MS, whether relapses are occurring or not and it evolves in the absence of new gadolinium enhancement.

We have characterised and quantified a process closely linked to the advancement of disability, but does the development of atrophy represent a process in which progressive neurodegeneration occurs as a result of previous inflammatory insults, or is this an independent process? If the former is true, then it may be the case that the same factors that are toxic to myelin or the oligodendrocyte are also toxic to axons, and/or that oligodendrocyte function is necessary to support and nourish the axon. In lesions that develop during the progressive phase of the disease demyelination is often associated with complete and selective loss of oligodendrocytes unlike plaques that develop during the first or second bout (Lassmann et al. 1994). However, how can we explain the observation that atrophy evolves in the absence of new disease activity as measured by gadolinium enhanced MRI? One could postulate that this could arise from a primary oligodendropathy and some pathological reports have suggested the existence of this in some MS lesions (Lucchinetti et al. 1996). Alternatively could there be a process that contributes to atrophy of the nervous system some time after an inflammatory insult but not necessarily related to the degree of that insult?

Of great interest with regard to this latter hypothesis is a recently observed correlation between atrophy and diffuse abnormality of the spinal cord in MS. This diffuse abnormality has been detected on proton density weighted sagittal images of the spinal cord in progressive MS (Lycklama a Nijeholt et al. 1996) and changes the whole appearance of the cord. The abnormality is not present or as extensive on T2 weighted images and it correlates with the presence of atrophy and disability. These imaging characteristics are most suggestive of astrogliosis, as experimental gliosis has been shown to increase proton density and prolong T1 without marked change in T2 (Barnes et al. 1988). I have observed a similar diffuse abnormality on the heavily weighted T1 scans acquired to study atrophy and quantification of this change has shown a correlation between the degree of this change (on the T1 spinal cord images) and atrophy and disability (Losseff et al. 1997).

Gliosis is a relatively neglected feature of MS pathology. It may be extensive and is in part responsible for the abnormal signal seen on MRI (McDonald, 1986). Astrocytic gliosis is a well described phenomenon of a range of insults to the CNS (Duchen, 1992) including MS (Adams, 1977) and may be driven by cytokines such as TNF α and IL-6 (Balasingam et al. 1994). Interestingly gliosis may evolve over months following a static insult (Long et al. 1973) and a glial scar may appear as a contracted area. Could this diffuse abnormality to some extent be indicative of underlying gliosis? If so, could gliosis be more than an epiphenomenon? Most importantly could it be in part responsible for progressive insidious dysfunction that commonly occurs in MS, such as can be seen in a limb that becomes contracted and useless due to the formation of scar tissue following a burn? Further study of this hypothesis will be challenging. The next step will be to serially examine the relationship between atrophy and MRI changes suggestive of gliosis. In parallel with this, it will be important to ascertain if progressive gliosis, (which can occur following a static insult) could

produce worsening functional impairment as seen in MS. This and further multiparametric serial MR studies may go some way towards unravelling the relationships between pathology (inflammation, demyelination, gliosis, axonal loss) and disability in MS.

Bibliography

Abbas, A.K. (1987) Warner-Lambert/Parke-Davis award lecture. Cellular interactions in the immune response. The roles of B lymphocytes and interleukin-4. *Am J Pathol* **129**, 25-33.

Acheson, E.D. (1977) Epidemiology of multiple sclerosis. *Brit Med Bul* **33**, 9-14.

Adams, C.W.M. (1977) Pathology of multiple sclerosis: progression of the lesion. *Brit Med Bul* **33**, 15-20.

Adams, C.W., Poston, R.N., Buk, S.J., Sidhu, Y.S. and Vipond, H. (1985) Inflammatory vasculitis in multiple sclerosis. *J Neurol Sci* **69**, 269-283.

Adams, R.D. and Kubik, C.S. (1952) The morbid anatomy of the demyelinating diseases. *Am J Med* **12**, 510-546.

Arnold, D.L., Matthews, P.M., Francis, G.S., O'Connor, J. and Antel, J.P. (1992) Proton magnetic resonance spectroscopic imaging for metabolic characterization of demyelinating plaques. *Ann Neurol* **31**, 235-241. (Abstract)

Arnold, D.L., Riess, G.T., Matthews, P.M., Francis, G.S., Collins, D.L., Wolfson, C. and Antel, J.P. (1994) Use of proton magnetic resonance spectroscopy for monitoring disease progression in multiple sclerosis. *Ann Neurol* **36**, 76-82.

Arnold, D.L., Fu, L., De Stefano, S., Narayanan, S., Matthews, P.M., Francis, G.S. and Antel, J.P. (1996) . Imaging of axonal damage in multiple sclerosis: Relation to MRI appearance, clinical disability and clinical course. *Neurology* **46 (Suppl)**, 481. (Abstract)

Balasingam, V., Tejada Berges, T., Wright, E., Bouckova, R. and Yong, V.W. (1994) Reactive astrogliosis in the neonatal mouse brain and its modulation by cytokines. *J Neurosci* **14**, 846-856.

Barkhof, F., Thompson, A.J., Hodgkinson, S., van Oosten, B., Lai, M., Polman, C.H., McLeod, J., Rudge, P., Moseley, I.F., Ader, H. and Miller, D.H. (1997) Double-blind, placebo-controlled, MR monitored exploratory trial of chimeric anti-CD4 antibodies in MS. *Neurology* (In Press)

Barnes, D., McDonald, W.I., Landon, D.N. and Johnson, G. (1988) The characterization of experimental gliosis by quantitative nuclear magnetic resonance imaging. *Brain* **111**, 83-94.

Barnes, D., Munro, P.M., Youl, B.D., Prineas, J.W. and McDonald, W.I. (1991) The longstanding MS lesion. A quantitative MRI and electron microscopic study. *Brain* **114**, 1271-1280.

Barson, A.J. and Sands, J. (1977) Regional and segmental characteristics of the human adult spinal cord. *J Anat* **123**, 797-803.

Beaulieu, C. and Allen, P.S. (1994) Some magnetisation transfer properties of water in myelinated and nonmyelinated nerves. *Proceedings of The Society of Magnetic Resonance* **1**, 169.

Bentson, J., Reza, M., Winter, J. and Wilson, G. (1978) Steroids and apparent cerebral atrophy on computed tomography scans. *J Comput Assist Tomog.* **2**, 16-23.

Bielschowsky, M. (1903) Zur histologie der multiplen sklerose. *Neur Zbl* 770.

Blatter, D.D., Bigler, E.D., Gale, S.D., Johnson, S.C., Anderson, C.V., Burnett, B.M., Parker, N., Kurth, S. and Horn, S.D. (1995) Quantitative volumetric analysis of brain MR: normative database spanning 5 decades of life. *Am J Neuroradiol* **16**, 241-251.

Bloch, F., Hansen, W.W. and Packard, M.E. (1946) Nuclear induction. *Physics Reviews* **69**, 127.

Brandt, E.R., Mackay, I.R., Hertzog, P.J., Cheetham, B.F., Sherritt, M. and Bernard, C.C. (1993) Molecular detection of interferon-alpha expression in multiple sclerosis brain. *J Neuroimmunol* **44**, 1-5.

British Standards Institution (1979) Precision of test methods I: Guide for the determination and reproducibility for a standard test method (*BS 5497, part 1*), London: British Standards Institution.

Brownell, B. and Hughes, J.T. (1962) The distribution of plaques in the cerebrum in multiple sclerosis. *J Neurol Neurosurg Psychiatry* **25**, 315-320.

Charcot, M. (1868) Histologie de le sclerose en plaques. *Gaz Hop Paris* **141**, 554-555, 557-558.

Comi, G., Filippi, M., Martinelli, V., Sirabian, G., Visciani, A., Campi, A., Mammi, S., Rovaris, M. and Canal, N. (1993) Brain MRI imaging correlates of cognitive impairment in multiple sclerosis. *J Neurol Sci* **115 (Suppl)**, 66-73.

Compston, D.A.S., Kellar Wood, H., Robertson, N., Sawcer, S. and Wood, N.W. (1995) Genes and susceptibility to multiple sclerosis. *Acta Neurol Scand* **161(Suppl)**, 43-51.

Cruveilhier, J. (1829) Anatomie pathologique du corps humain. 2. Livraison 52, Plate 2 Paris: Bailliere.

Davie, C.A., Hawkins, C.P., Barker, G.J., Brennan, A., Tofts, P.S., Miller, D.H. and McDonald, W.I. (1993) Detection of myelin breakdown products by proton magnetic resonance spectroscopy. *Lancet* **341**, 630-631.

Davie, C.A., Hawkins, C.P., Barker, G.J., Brennan, A., Tofts, P.S., Miller, D.H. and McDonald, W.I. (1994) Serial proton magnetic resonance spectroscopy in acute multiple sclerosis lesions. *Brain* **117**, 49-58.

Davie, C.A., Barker, G.J., Webb, S., Tofts, P.S., Thompson, A.J., Harding, A.E., McDonald, W.I. and Miller, D.H. (1995) Persistent functional deficit in multiple sclerosis and autosomal dominant cerebellar ataxia is associated with axon loss. *Brain* **118**, 1583-1592.

Dawson, J.W. (1916) The histology of disseminated sclerosis. *Trans R Soc Edin* **50**, 517-740.

Dean, G. and Kurtzke, J.F. (1971) On the risk of multiple sclerosis according to age at immigration to South Africa. *Br Med J* **3**, 725-729.

Dousset, V., Grossman, R.I., Ramer, K.N., Schnall, M.D., Young, L.H., Gonzalez-Scarano, F., Lavi, E. and Cohen, J.A. (1992) Experimental allergic encephalomyelitis and multiple sclerosis: Lesion characterization with magnetization transfer imaging. *Radiology* **182**, 483-491.

Duchen, L.W. (1992) General pathology of neurons and neuroglia. In: Adams, J.H. and Duchon, L.W. (Eds.) *Greenfield's Neuropathology*, 5th edn. pp. 1-68. London: Edward Arnold.

Ebers, G.C., Sadovnick, A.D., Risch, N.J. and the Canadian Collaborative Study Group (1995) A genetic basis for familial aggregation in multiple sclerosis. *Nature* **377**, 150-151.

Eldenstein, W.A., Hutchison, J.M.S., Johnson, G. and Redpath, T. (1980) Spin warp NMR imaging and applications to human whole-body imaging. *Proceedings of The Society of Magnetic Resonance* **1**, 170.

Esiri, M.M. and Morris, C.S. (1991) Immunocytochemical study of macrophages and microglial cells and extracellular matrix components in human CNS disease. 2. Non-neoplastic diseases. *J Neurol Sci* **101**, 59-72.

Fazekas, F., Offenbacher, H., Fuchs, S., Schmidt, R., Niederkorn, K., Horner, S. and Lechner, H. (1988) Criteria for an increased specificity of MRI interpretation in elderly subjects with suspected multiple sclerosis. *Neurology* **38**, 1822-1825.

Feinstein, A., Ron, M. and Thompson, A. (1993) A serial study of psychometric and magnetic resonance imaging changes in multiple sclerosis. *Brain* **116**, 569-602.

Filippi, M., Horsfield, M.A., Morrissey, S.P., MacManus, D.G., Rudge, P., McDonald, W.I. and Miller, D.H. (1994) Quantitative brain MRI lesion load predicts the course of clinically isolated syndromes suggestive of multiple sclerosis. *Neurology* **44**, 635-641.

Filippi, M., Campi, A., Colombo, B., Martinelli, V., Pereira, C. and Comi, G. (1995a) A spinal cord MRI study of benign and secondary progressive multiple sclerosis. *Proceedings of The Society of Magnetic Resonance* **1**, 277.

Filippi, M., Horsfield, M.A., Bressi, S., Martinelli, V., Baratti, C., Reganati, P., Campi, A., Miller, D.H. and Comi, G. (1995b) Intra- and inter-observer agreement of brain MRI lesion volume measurements in multiple sclerosis. A comparison of techniques. *Brain* **118**, 1601-1612.

Filippi, M., Paty, D.W., Kappos, L., Barkhof, F., Compston, D.A., Thompson, A.J., Zhao, G.J., Wiles, C.M., McDonald, W.I. and Miller, D.H. (1995c) Correlations between changes in disability and T2-weighted brain MRI activity in multiple sclerosis: a follow-up study. *Neurology* **45**, 255-260.

Fontaine, B., Seilhean, D., Tourbah, A., Daumas Duport, C., Duyckaerts, C., Benoit, N., Devaux, B., Hauw, J.J., Rancurel, G. and Lyon Caen, O. (1994) Dementia in two histologically confirmed cases of multiple sclerosis: one case with isolated dementia and one case associated with psychiatric symptoms. *J Neurol Neurosurg Psychiatry* **57**, 353-359.

Fox, N., Freeborough, P.A. and Rossor, M.N. (1996) Visualization and quantification of rates of atrophy in Alzheimers disease. *Lancet* **348**, 94-97.

Fralix, T.A., Ceckler, T.L., Wolff, S.D., Simon, S.A. and Balaban, R.S. (1991) Lipid bilayer and water proton magnetization transfer effect of cholesterol. *Magn Reson Med* **18**, 214-223.

Francis, D.A., Bain, P., Swan, A.V. and Hughes, R.A.C. (1991) An assessment of disability rating scales used in multiple sclerosis. *Arch Neurol* **48**, 299-301.

Frisen, L. and Hoyt, W.F. (1974) Insidious atrophy of retinal nerve fibers in multiple sclerosis. Fundoscopic identification in patients with and without visual complaints. *Arch Ophthalmol* **92**, 91-97.

Gass, A., Barker, G.J., Kidd, D., Thorpe, J.W., MacManus, D., Brennan, A., Tofts, P.S., Thompson, A.J., McDonald, W.I. and Miller, D.H. (1994) Correlation of magnetization transfer ratio with clinical disability in multiple sclerosis. *Ann Neurol* **36**, 62-67.

Gawne-Cain, M.L., Rovaris, M., Wang, L. and Miller, D.H. (1996a) A comparison of conventional and fast spin-echo sequences for the measurement of lesion load in multiple sclerosis using a semiautomated contour technique. *Proceedings of The Society of Magnetic Resonance* **1**, 170.

Gawne-Cain, M.L., O'Riordan, J.I. and Miller, D.H. (1996b) Comparison of fast FLAIR and CSE for detection of MS lesions in the brain. *Proceedings of The Society of Magnetic Resonance* **1**, 551.

Gawne-Cain, M.L., Webb, S.L., Tofts, P.S. and Miller, D.H. (1996c) The effect of repositioning inaccuracies on intracranial MS lesion volume measurements. *Proceedings of The Society of Magnetic Resonance* **1**, 534.

Ghatak, N.R., Hirano, A., Lijtmaer, H. and Zimmerman, H.M. (1974) Asymptomatic demyelinated plaque in the spinal cord. *Arch Neurol* **30**, 484-486.

Goodkin, D.E. (1991) EDSS reliability. *Neurology* **41**, 332.

Goodkin, D.E., Ross, J.S., Medendorp, S.V., Konecni, J. and Rudick, R.A. (1992) Magnetic resonance imaging lesion enlargement in multiple sclerosis. Disease-related activity, chance occurrence, or measurement artifact? *Arch Neurol* **49**, 261-263.

Greenfield, J.G. and King, L.S. (1936) Observations on the histopathology of the cerebral lesions in disseminated sclerosis. *Brain* **59**, 445-456.

Grimaud, J., Lai, M., Thorpe, J., Adeleine, P., Plummer, D., Barker, G., Wang, L., Tofts, P.S., McDonald, W.I. and Miller, D.H. (1997) Quantification of MRI lesion load in multiple sclerosis: a comparison of three computer-assisted techniques. *Mag Res Image* (In Press)

Gross, K.R., Tomberg, T.A., Kokk, A.A. and Kaasik, A.E. (1993) [The prognosis of multiple sclerosis: computed tomographic comparisons]. *Zh Nevropatol Psikhiatr Im S S Korsakova* **93**, 32-35.

Guttman, L. (1973) *Spinal cord injuries: Comprehensive management and research*, Oxford: Blackwell Scientific Publications.

Hageleit, U., Will, C.H. and Seidel, D. (1987) Automated measurements of cerebral atrophy in multiple sclerosis. *Neurosurg Rev* **10**, 137-140.

Hart, M.N., Fabry, Z., Love Homan, L., Keiner, J., Sadewasser, K.L. and Moore, S.A. (1992) Brain microvascular smooth muscle and endothelial cells produce granulocyte macrophage colony-stimulating factor and support colony formation of granulocyte-macrophage-like cells. *Am J Pathol* **141**, 421-427.

Hawkins, C.P., Mackenzie, F., Tofts, P., du Boulay, E.P. and McDonald, W.I. (1991) Patterns of blood-brain barrier breakdown in inflammatory demyelination. *Brain* **114**, 801-810.

Hobart, J., Lamping, D. and Thompson, A.J. (1996) Evaluating neurological outcome measures: the bare essentials. *J Neurol Neurosurg Psychiatry* **60**, 127-130.

Holmes, J., Madgwick, T. and Bates, D. (1995) The cost of multiple sclerosis. *Br J Med Econ* **8**, 181-193.

Huber, S.J., Paulson, G.W., Shuttleworth, E.C., Chakeres, D., Clapp, L.E., Pakalnis, A., Weiss, K. and Rammohan, K. (1987) Magnetic resonance imaging correlates of dementia in multiple sclerosis. *Arch Neurol* **44**, 732-736.

Isaac, C., Li, D.K., Genton, M., Jardine, C., Grochowski, E., Palmer, M., Kastrukoff, L.F., Oger, J. and Paty, D.W. (1988) Multiple sclerosis: a serial study using MRI in relapsing patients. *Neurology* **38**, 1511-1515.

Katz, D., Taubenberger, J.K., Cannella, B., McFarlin, D.E., Raine, C.S. and McFarlin, H.F. (1993) Correlation between magnetic resonance imaging findings and lesion development in chronic active multiple sclerosis. *Ann Neurol* **34**, 661-669.

Kermode, A.G., Thompson, A.J., Tofts, P., MacManus, D.G., Kendall, B.E., Kingsley, D.P., Moseley, I.F., Rudge, P. and McDonald, W.I. (1990) Breakdown of the blood-brain barrier precedes symptoms and other MRI signs of new lesions in multiple sclerosis. Pathogenetic and clinical implications. *Brain* **113**, 1477-1489.

Kesselring, J., Miller, D.H., Robb, S.A., Kendall, B.E., Moseley, I.F., Kingsley, D., du Boulay, E.P. and McDonald, W.I. (1990) Acute disseminated encephalomyelitis. MRI findings and the distinction from multiple sclerosis. *Brain* **113**, 291-302.

Khoury, S.J., Guttmann, M.D., Orav, E.J., Hohol, M.J., Ahn, S.S., Hsu, L., Kikinis, R., Mackin, G.A., Jolesz, F.A. and Weiner, H.L. (1994) Longitudinal MRI in multiple sclerosis: Correlation between disability and lesion burden. *Neurology* **44**, 2120-2124.

Kidd, D., Thorpe, J.W., Thompson, A.J., Kendall, B.E., Moseley, I.F., MacManus, D.G., McDonald, W.I. and Miller, D.H. (1993) Spinal cord MRI using multi-array coils and fast spin echo. II. Findings in multiple sclerosis. *Neurology* **43**, 2632-2637.

Kidd, D., Thompson, A.J., Kendall, B.E., Miller, D.H. and McDonald, W.I. (1994) Benign form of multiple sclerosis: MRI evidence for less frequent and less inflammatory disease activity. *J Neurol Neurosurg Psychiatry* **57**, 1070-1072.

Kidd, D., Thorpe, J., Barker, G.J., McDonald, W.I., Miller, D.H. and Thompson, A.J. (1996) MRI dynamics of the brain and spinal cord in progressive multiple sclerosis. *J Neurol Neurosurg Psychiatry* **60**, 15-19.

Kohlmeyer, K., Lehmkuhl, G. and Poutska, F. (1983) Computed tomography of anorexia nervosa. *Am J Neuroradiol* **4**, 437-438.

Koller, H., Buchholz, J. and Siebler, M. (1996) Cerebrospinal fluid from multiple sclerosis patients inactivates neuronal Na⁺ current. *Brain* **119**, 457-463.

Kurtzke, J.F. and Berlin, L. (1954) The effects of isoniazid on patients with multiple sclerosis: preliminary report. *Am Rev Tuberc* **70**, 577-592.

Kurtzke, J.F. (1955) A new scale for evaluating disability in multiple sclerosis. *Neurology* **5**, 580-583.

Kurtzke, J.F., Beebe, G.W., Nagler, B., Kurland, L.T. and Auth, T.L. (1977) Studies on the natural history of multiple sclerosis-8. Early prognostic features of the later course of the illness. *J Chronic Dis* **30**, 819-830.

Kurtzke, J.F. (1983) Rating neurologic impairment in multiple sclerosis: an expanded disability status scale (EDSS). *Neurology* **33**, 1444-1452.

Lai, H.M., Davie, C.A., Gass, A., Barker, G.J., Webb, S.L., Tofts, P.S., Thompson, A.J., McDonald, W.I. and Miller, D.H. (1997) Serial magnetisation transfer ratios in gadolinium enhancing lesions in multiple sclerosis. *J Neurol* (In Press)

Languino, L.R., Plescia, J., Duperray, A., Brian, A.A., Plow, E.F., Geltosky, J.E. and Altieri, D.C. (1993) Fibrinogen mediates leukocyte adhesion to vascular endothelium through an ICAM-1-dependent pathway. *Cell* **73**, 1423-1434.

Lassmann, H., Rossler, K., Zimprich, F. and Vass, K. (1991) Expression of adhesion molecules and histocompatibility antigens at the blood-brain barrier. *Brain Pathol* **1**, 115-123.

Lassmann, H., Suchanek, G. and Ozawa, K. (1994) Histopathology and the blood cerebrospinal fluid barrier in multiple sclerosis. *Ann Neurol* **36 (Suppl)**, 42-46.

Lauterbur, P.C. (1973) Image formation by induced local interactions: examples employing nuclear magnetic resonance. *Nature* **242**, 190-191.

Lexa, F.J., Grossman, R.I. and Rosenquist, A.C. (1994) MR of Wallerian degeneration in the feline visual system: Characterization by magnetization transfer rate with histopathologic correlation. *Am J Neuroradiol* **15**, 201-212.

Lightman, S., McDonald, W.I., Bird, A.C., Francis, D.A., Hoskins, A., Batchelor, J.R. and Halliday, A.M. (1987) Retinal venous sheathing in optic neuritis. Its significance for the pathogenesis of multiple sclerosis. *Brain* **110**, 405-414.

Loizou, L.A., Rolfe, E.B. and Hewazy, H. (1982) Cranial computed tomography in the diagnosis of multiple sclerosis. *J Neurol Neurosurg Psychiatry* **45**, 905-912.

Long, D.M., Maxwell, R.E. and French, L.A. (1973) The effects of glucosteroids upon cold-induced brain edema. III. Prevention of gliosis following brain edema. *J Neuropath Exp Neurol* **32**, 245-255.

Losseff, N.A., Kingsley, D.P.E., McDonald, W.I., Miller, D.H. and Thompson, A.J. (1996) Clinical and magnetic resonance imaging predictors of disability in primary and secondary progressive multiple sclerosis. *Multiple Sclerosis* **1**, 218-222.

Losseff, N.A., Miller, D.H., McDonald, W.I. and Thompson, A.J. (1997) T1 hypointensity, disability and atrophy of the spinal cord in multiple sclerosis. *J Neurol Neurosurg Psychiatry* (Abstract in press).

Lucchinetti, C.F., Bruck, W., Rodriguez, M. and Lassmann, H. (1996) Distinct patterns of multiple sclerosis pathology indicates heterogeneity in pathogenesis. *Brain Pathol* **6**, 259-274.

Lycklama a Nijeholt, G.J., Barkhof, F., Scheltens, P., Castelijns, J.A., Uitdehaag, B.M.J., van Waesberghe, J.H.T.M., Jongen, P.J.H., Hommes, O.R., Polman, C.H. and Valk, J. (1996) Multiple sclerosis in the spinal cord: Relevance of diffuse abnormality on magnetic resonance images. *J Neurol* **243**, (Suppl) 32. (Abstract)

MacFadyen, D.J., Drance, S.M., Douglas, G.R., Airaksinen, P.J., Mawson, D.K. and Paty, D.W. (1988) The retinal nerve fibre layer, neuroretinal rim area, and visual evoked potentials in MS. *Neurology* **38**, 1353-1358.

McCarron, R.M., Wang, L., Cowan, E.P. and Spatz, M. (1991) Class II MHC antigen expression by cultured human cerebral vascular endothelial cells. *Brain Res* **566**, 325-328.

McDonald, W.I. (1963) The effects of experimental demyelination on conduction in peripheral nerve: a histological and electrophysiological study. II: Electrophysiological observations. *Brain* **86**, 501-524.

McDonald, W.I. and Sears, T.A. (1970) The effects of experimental demyelination on conduction in the central nervous system. *Brain* **93**, 583-598.

McDonald, W.I. (1976) Conduction in the optic nerve. *Trans. ophthal. Soc. U. K.* **96**, 352-354.

McDonald, W.I. (1986) The mystery of the origin of multiple sclerosis. *J Neurol Neurosurg Psychiatry* **49**, 113-123.

Mellanby, A.R. and Reveley, M.A. (1982) Effects of acute dehydration on computerized tomographic assessment of cerebral density and ventricular volume. *Lancet* **2**, 874.

Miller, D.H., Kendall, B.E., Barter, S., Johnson, G., MacManus, D.G., Logsdail, S.J., Ormerod, I.E. and McDonald, W.I. (1988a) Magnetic resonance imaging in central nervous system sarcoidosis. *Neurology* **38**, 378-383.

Miller, D.H., Ormerod, I.E., McDonald, W.I., MacManus, D.G., Kendall, B.E., Kingsley, D.P. and Moseley, I.F. (1988b) The early risk of multiple sclerosis after optic neuritis. *J Neurol Neurosurg Psychiatry* **51**, 1569-1571.

Miller, D.H., Hornabrook, R.W. and Purdie, G. (1992) The natural history of multiple sclerosis: a regional study with some longitudinal data. *J Neurol Neurosurg Psychiatry* **55**, 341-346.

Miller, D.H., Albert, P.S., Barkhof, F., Francis, G., Frank, J.A., Hodgkinson, S., Lublin, F.D., Paty, D.W., Reingold, S.C. and Simon, J. (1996) Guidelines for the use of magnetic resonance techniques in monitoring the treatment of multiple sclerosis. *Ann Neurol* **39**, 6-16.

Moll, C., Mourre, C., Lazdunski, M. and Ulrich, J. (1991) Increase of sodium channels in demyelinated lesions of multiple sclerosis. *Brain Research* **556**, 311-316.

Moreau, T., Coles, A., Wing, M., Issacs, J., Hale, G., Waldmann, H. and Compston, D.A. (1996) Transient increase in symptoms associated with cytokine release in patients with multiple sclerosis. *Brain* **119**, 225-237.

Morrisey, S.P., Miller, D.H., Kendall, B.E., Kingsley, D.P., Kelly, M.A., Francis, D.A., MacManus, D.G. and McDonald, W.I. (1993) The significance of brain magnetic resonance imaging abnormalities at presentation with clinically isolated syndromes suggestive of multiple sclerosis. A 5-year follow-up study. *Brain* **116**, 135-146.

Mumford, C.J., Wood, N.W., Kellar Wood, H., Thorpe, J.W., Miller, D.H. and Compston, D.A. (1994) The British Isles survey of multiple sclerosis in twins. *Neurology* **44**, 11-15.

Myers, L.S., Ellison, G.W. and Leake, B.D. (1993) Reliability of the Disability Status Scale. *Neurology* **43 (Suppl 2)**, 204.

Namerow, N.S. and Thompson, L.R. (1969) Plaques, symptoms, and the remitting course of multiple sclerosis. *Neurology* **19**, 765-766.

Newcombe, J., Hawkins, C.P., Henderson, C.L., Patel, H.A., Woodroffe, M.N., Hayes, G.M., Cuzner, M.L., MacManus, D., du Boulay, E.P. and McDonald, W.I. (1991) Histopathology of multiple sclerosis lesions detected by magnetic resonance imaging in unfixed postmortem central nervous system tissue. *Brain* **114**, 1013-1023.

Noseworthy, J.H., Paty, D.W. and Ebers, G.C. (1984) Neuroimaging in multiple sclerosis. *Neurol Clin* **2**,759-777.

Noseworthy, J.H., Vandervoort, M.K., Wong, C.J., Ebers, G.C. and the Canadian Cooperative Multiple Sclerosis Study Group (1990) Interrater variability with the expanded disability status scale (EDSS) and functional systems (FS) in a multiple sclerosis clinical trial. *Neurology* **40**, 971-975.

Noseworthy, J.H. (1994) Clinical scoring methods for multiple sclerosis. *Ann Neurol* **36** (Suppl), 80-85.

O'Riordan, J.I., McDonald, W.I. and Miller, D.H. (1996) The prognostic significance of brain MRI in clinically isolated syndromes suggestive of demyelination- a 10 year follow up. *J Neurol Neurosurg Psychiatry* **61**, 214. (Abstract)

Oppenheimer, D.R. (1978) The cervical cord in multiple sclerosis. *Neuropathol Appl Neurobiol* **4**, 151-162.

Ormerod, I.E., Miller, D.H., McDonald, W.I., du Boulay, E.P., Rudge, P., Kendall, B.E., Moseley, I.F., Johnson, G., Tofts, P.S., Halliday, A.M., Bronstein, A.M., Scaravilli, F., Harding, A.E., Barnes, D. and Zilkha, K.J. (1987) The role of NMR imaging in the assessment of multiple sclerosis and isolated neurological lesions; a quantitative study. *Brain* **110**, 1579-1616.

Ozawa, K., Suchanek, G., Breitschopf, H., Bruck, W., Budka, H., Jellinger, K. and Lassmann, H. (1994) Patterns of oligodendroglia pathology in multiple sclerosis. *Brain*. **117**, 1311-1322.

Paty, D.W., Oger, J.J.F., Kastrukoff, L.F., Hashimoto, S.A., Hooge, J.P., Eisen, A.A., Eisen, K.A., Purves, S.J., Low, M.D., Brandeys, V., Robertson, W.D. and Li, D.K.B. (1988) MRI in the diagnosis of MS: a prospective study with comparison of clinical evaluation, evoked potentials, oligoclonal banding and CT. *Neurology* **38**, 180-185.

Paty, D.W., Koopmans, R.A., Ken Redekop, W., Oger, J.J.F., Kastrukoff, L.F. and Li, D.K.B. (1992) Does MRI activity rate predict the clinical course of MS. *Neurology* **42** (Suppl 3), 427.

Paty, D.W. and Li, D.K. (1993) Interferon beta-1b is effective in relapsing-remitting multiple sclerosis. II. MRI analysis results of a multicenter, randomized, double-blind, placebo-controlled trial. UBC MS/MRI Study Group and the IFNB Multiple Sclerosis Study Group. *Neurology* **43**, 662-667.

Pfefferbaum, A., Mathalon, D.H., Sullivan, E.V., Rawles, J.M., Zipursky, R.B. and Lim, K.O. (1994) A quantitative magnetic resonance imaging study of changes in brain morphology from infancy to late adulthood. *Arch Neurol* **51**, 874-887.

Polman, C.H., Dahlke, F., Thompson, A.J., Ghazi, M., Kappos, L., Miltenburger, C. and Pozilli, C. (1995) Interferon beta-1b in secondary progressive multiple sclerosis - outline of the clinical trial. *Multiple Sclerosis* **1** (Suppl 1), 51-54.

Poser, C.M., Paty, D.W., Scheinberg, L., McDonald, W.I., Davis, F.A., Ebers, G.C., Johnson, K.P., Sibley, W.A., Silberberg, D.H. and Tourtellotte, W.W. (1983) New diagnostic criteria for multiple sclerosis: guidelines for research protocols. *Ann Neurol* **13**, 227-231.

Powell, H.C. and Lampert, P.W. (1983) Pathology of multiple sclerosis. *Neurol Clin.* **1**, 631-644.

Prineas, J.W. and Connell, F. (1978) The fine structure of chronically active multiple sclerosis plaques. *Neurology* **28**, 68-75.

Prineas, J.W., Barnard, R.O., Revesz, T., Kwon, E.E., Sharer, L. and Cho, E.S. (1993a) Multiple sclerosis. Pathology of recurrent lesions. *Brain* **116**, 681-693.

Prineas, J.W., Barnard, R.O., Revesz, T., Kwon, E.E., Sharer, L. and Cho, E.S. (1993b) Multiple sclerosis. Pathology of recurrent lesions. *Brain* **116**, 681-693.

Purcell, E.M., Torrey, H.C. and Pound, R.V. (1946) Resonance absorption by nuclear magnetic moments in a solid. *Physics Reviews* **69**, 37-38.

Rao, S.M., Glatt, S., Hammeke, T.A., McQuillen, M.P., Khatri, B.O., Rhodes, A.M. and Pollard, S. (1985) Chronic progressive multiple sclerosis. Relationship between cerebral ventricular size and neuropsychological impairment. *Arch Neurol* **42**, 678-682.

Rao, S.M., Leo, G.J., Haughton, V.M., St Aubin-Faubert, P. and Bernardin, B.S. (1989) Correlation of magnetic resonance imaging with neuropsychological testing in multiple sclerosis. *Neurology* **39**, 161-166.

Rao, S.M., Leo, G.J., Bernardin, L. and Unverzagt, F. (1991a) Cognitive dysfunction in multiple sclerosis. I. Frequency, patterns, and prediction. *Neurology*. **41**, 685-691.

Rao, S.M., Leo, G.J., Ellington, L., Nauertz, T., Bernardin, L. and Unverzagt, F. (1991b) Cognitive dysfunction in multiple sclerosis. II. Impact on employment and social functioning. *Neurology*. **41**, 692-696.

Revesz, T.R., Kidd, D., Thompson, A.J., Barnard, R.O. and McDonald, W.I. (1994) A comparison of the pathology of primary and secondary progressive multiple sclerosis. *Brain* **117**, 759-765.

Risch, N. (1990) Linkage strategies for genetically complex traits. I. Multilocus models. *Am J Hum Genet* **46**, 222-228.

Ron, M.A., Acker, W., Shaw, G.K. and Lishman, W.A. (1982) Computerized tomography of the brain in chronic alcoholism: a survey and follow-up study. *Brain* **105**, 497-514.

Runmarker, B. and Andersen, O. (1993) Prognostic factors in a multiple sclerosis incidence cohort with twenty five years follow up. *Brain* **116**, 117-134.

Sadovnick, A.D., Ebers, G.C., Wilson, R.W. and Paty, D.W. (1992) Life expectancy in patients attending multiple sclerosis clinics. *Neurology*. **42**, 991-994.

Schluesener, H.J., Sobel, R.A., Linington, C. and Weiner, H.L. (1987) A monoclonal antibody against a myelin oligodendrocyte glycoprotein induces relapses and demyelination in central nervous system autoimmune disease. *J Immunol* **139**, 4016-4021.

Schubert, D.S. and Foliart, R.H. (1993) Increased depression in multiple sclerosis patients: A meta-analysis. *Psychosomatics* **34**, 124-130.

Schumacher, G.A., Beebe, G.W., Kibler, R.F., Kurland, L.T., Kurtzke, J.F., McDowell, F., Nagler, B., Sibley, W.A., Tourtellotte, W.W. and Willmon, T.L. (1965) Problems of experimental trials of therapy in multiple sclerosis. *Ann N Y Acad Sci* **122**, 552-568.

Selmaj, K., Raine, C.S., Cannella, B. and Brosnan, C.F. (1991) Identification of lymphotoxin and tumor necrosis factor in multiple sclerosis lesions. *J Clin Invest* **87**, 949-954.

Shaw, P.J., Smith, M.N., Ince, P.G. and Bates, D. (1987) Chronic periphlebitis retinae in multiple sclerosis. A histopathological study. *J Neurol Sci* **77**, 147-152.

Smith, M.E., Stone, L.A., Albert, P.S., Frank, J.A., Martin, R., Armstrong, M., Maloni, H., McFarlin, D.E. and McFarland, H.F. (1993) Clinical worsening in multiple sclerosis is associated with increased frequency and area of gadopentetate dimeglumine-enhancing magnetic resonance imaging lesions. *Ann Neurol* **33**, 480-489.

Sobel, R.A. and Kuchroo, V.K. (1992) The immunopathology of acute experimental allergic encephalomyelitis induced with myelin proteolipid protein. T cell receptors in inflammatory lesions. *J Immunol* **149**, 1444-1451.

Stewart, W.A., Hall, L.D. and Berry, K. (1986) Magnetic resonance imaging (MRI) in multiple sclerosis (MS): Pathological correlation studies in eight cases. *Neurology* **36**, 320

The IFNB Multiple Sclerosis Study Group and the University of British Columbia MS/MRI Analysis Group (1995) Interferon beta-1b in the treatment of multiple sclerosis: Final outcome of the randomized controlled trial. *Neurology* **45**, 1277-1285.

Thompson, A.J., Kermode, A.G., MacManus, D.G., Kendall, B.E., Kingsley, D.P.E., Moseley, I.F. and McDonald, W.I. (1990) Patterns of disease activity in multiple sclerosis: clinical and magnetic resonance imaging study. *Br Med J* **300**, 631-634.

Thompson, A.J., Kermode, A.G., Wicks, D., MacManus, D.G., Kendall, B.E., Kingsley, D.P. and McDonald, W.I. (1991) Major differences in the dynamics of primary and secondary progressive multiple sclerosis. *Ann Neurol* **29**, 53-62.

Thompson, A.J., Miller, D., Youl, B., MacManus, D., Moore, S., Kingsley, D., Kendall, B., Feinstein, A. and McDonald, W.I. (1992) Serial gadolinium-enhanced MRI in relapsing/remitting multiple sclerosis of varying disease duration. *Neurology* **42**, 60-63.

Thorpe, J.W., Kidd, D., Kendall, B.E., Tofts, P.S., Barker, G.J., Thompson, A.J., MacManus, D.G., McDonald, W.I. and Miller, D.H. (1993) Spinal cord MRI using multi-array coils and fast spin echo. I. Technical aspects and findings in healthy adults. *Neurology* **43**, 2625-2631.

Thorpe, J.W., Barker, G.J., Jones, S.J., Losseff, N.A., MacManus, D.G., Webb, S., Mortimer, C., Tofts, P.S., McDonald, W.I. and Miller, D.H. (1995) Magnetisation transfer ratios and transverse magnetisation decay curves in optic neuritis: correlation with clinical findings and electrophysiology. *J Neurol Neurosurg Psychiatry* **59**, 487-492.

Thorpe, J.W., Kidd, D., Moseley, I.F., Kendall, B., Thompson, A.J., MacManus, D., McDonald, W.I. and Miller, D.H. (1996) Serial gadolinium enhanced MRI of the brain and spinal cord in early relapsing-remitting multiple sclerosis. *Neurology* **46**, 373-378.

Tofts, P.S., Barker, G.J., Simmons, A., MacManus, D.G., Thorpe, J., Gass, A. and Miller, D.H. (1994) Correction of nonuniformity in images of the spine and optic nerve from fixed receive-only surface coils at 1.5 T. *J Comput Assist Tomogr* **18**, 997-1003.

Tofts, P.S., Barker, G.J., Filippi, M., Gawne-Cain, M.L. and Lai, M. (1996) An oblique cylinder contrast-adjusted (OCCA) phantom to measure the accuracy of brain lesion volume estimation schemes in multiple sclerosis. *Proceedings of The Society of Magnetic Resonance* **1**, 553.

Tomiak, M.M., Rosenblum, J.D., Prager, J.M. and Metz, C.E. (1994) Magnetisation transfer: a potential method to determine the age of multiple sclerosis lesions. *Am J Neuroradiol* **15**, 1508-1569.

Traugott, U. and Lebon, P. (1988) Multiple sclerosis: involvement of interferons in lesion pathogenesis. *Ann Neurol* **24**, 243-251.

Ulrich, J. and Groebke-Lorenz, W. (1976) The optic nerve in multiple sclerosis. A morphological study with retrospective clinico-pathological correlations. *J Neuropath Exp Neurol* **3**, 149-159.

van Walderveen, M.A., Barkhof, F., Hommes, O.R., Polman, C.H., Tobi, H., Frequin, S.T. and Valk, J. (1995) Correlating MRI and clinical disease activity in multiple sclerosis: relevance of hypointense lesions on short-TR/short-TE (T1-weighted) spin-echo images. *Neurology* **45**, 1684-1690.

Weinshenker, B.G., Bass, B., Rice, G.P.A., Noseworthy, J., Carriere, W., Baskerville, J. and Ebers, G.C. (1989a) The natural history of multiple sclerosis: a geographically based study.

1. Clinical course and disability. *Brain* **112**, 133-146.

Weinshenker, B.G., Bass, B., Rice, G.P., Noseworthy, J., Carriere, W., Baskerville, J. and Ebers, G.C. (1989b) The natural history of multiple sclerosis: a geographically based study.

2. Predictive value of the early clinical course. *Brain* **112**, 1419-1428.

Weinshenker, B.G., Rice, G.P., Noseworthy, J.H., Carriere, W., Baskerville, J. and Ebers, G.C. (1991) The natural history of multiple sclerosis: a geographically based study. 3.

Multivariate analysis of predictive factors and models of outcome. *Brain* **114**, 1045-1056.

Weinshenker, B.G. (1994) Natural history of multiple sclerosis. *Ann Neurol* **36 (Suppl)**, 6-11.

Whitaker, J.N., Kachelhofer, R.D., Bradley, E.L., Burgard, S., Layton, B.A., Reder, A.T., Morrison, W., Zhao, G.J. and Paty, D.W. (1995) Urinary myelin basic protein like material as a correlate of the progression of multiple sclerosis. *Ann Neurol* **38**, 625-632.

Wicks, D.A.G., Tofts, P.S., Miller, D.H., Du Boulay, G.H., Feinstein, A., Sacares, P.R., Harvey, I., Brenner, R. and McDonald, W.I. (1992) Volume measurement of multiple sclerosis lesions with magnetic resonance images. *Neuroradiology* **34**, 475-479.

Willoughby, E.W., Grochowski, E., Li, D.K., Oger, J., Kastrukoff, L.F. and Paty, D.W. (1989) Serial magnetic resonance scanning in multiple sclerosis: a second prospective study in relapsing patients. *Ann Neurol* **25**, 43-49.

Wolff, S.D. and Balaban, R.S. (1989) Magnetisation transfer contrast (MTC) and tissue water proton relaxation in vivo. *Magn Res Med* **10**, 135-144.

World Health Organisation (1990) International classification of impairments, disabilities and handicaps, Geneva: World Health Organisation.

Wucherpfennig, K.W., Newcombe, J., Li, H., Keddy, C., Cuzner, M.L. and Hafler, D.A. (1992) T cell receptor alpha-V beta repertoire and cytokine gene expression in active multiple sclerosis lesions. *J Exp Med* **175**, 993-1002.

Yoo, D.S., Lemieux, L., Arridge, S.R. and Tofts, P.S. (1995) Segmentation of skull contours in MR head images. *Proceedings of The Society of Magnetic Resonance* **2**, 707.

Youl, B.D., Turano, G., Miller, D.H., Towell, A.D., MacManus, D.G., Moore, S.G., Jones, S.J., Barrett, G., Kendall, B.E., Moseley, I.F., Tofts, P.S., Halliday, A.M. and McDonald, W.I. (1991) The pathophysiology of acute optic neuritis: an association of gadolinium leakage with clinical and electrophysiological deficits. *Brain* **114**, 2437-2450.

Young, I.R., Hall, A.S., Pallis, C.A., Legg, N.J., Bydder, G.M. and Steiner, R.E. (1981) Nuclear magnetic resonance imaging of the brain in multiple sclerosis. *Lancet* **318**, 1063-1066.

Appendix

The Expanded Disability Status Scale (EDSS) and Functional Systems (FS) scores

Functional systems

PYRAMIDAL FUNCTIONS

- 0 normal
- 1 abnormal signs without disability
- 2 minimal disability
- 3 mild or moderate paraparesis or hemiparesis
- 4 marked paraparesis or hemiparesis; moderate quadriparesis; monoplegia
- 5 quadriplegia

CEREBELLAR FUNCTIONS

- 0 normal
- 1 abnormal signs without disability
- 2 mild ataxia
- 3 moderate truncal or limb ataxia
- 4 severe ataxia, all limbs
- 5 unable to perform coordinated movements due to ataxia

BRAIN STEM FUNCTIONS

- 0 normal
- 1 signs only
- 2 moderate nystagmus or other mild disability
- 3 severe nystagmus, marked extraocular weakness, or moderate disability of other cranial nerves
- 4 marked dysarthria or other marked disability
- 5 inability to swallow or speak

SENSORY FUNCTIONS

- 0 normal
- 1 vibration or figure-writing decrease only, in one or two limbs
- 2 mild decrease in touch or pain or position sense, and/or moderate decrease in vibration sense in one or two limbs; or vibratory (c/s figure-writing) decrease alone or in three or four limbs
- 3 moderate decrease in touch or pain or position sense, and/or essentially lost vibration in one or two limbs; or mild decrease in touch or pain and/or moderate decrease in all proprioceptive tests in three or four limbs

4 marked decrease in touch or pain or loss of proprioception, alone or combined, in one or two limbs; or moderate decrease in touch or pain and/or severe proprioceptive decrease in more than two limbs

5 loss (essentially) of sensation in one or two limbs; or moderate decrease in touch or pain and/or loss of proprioception for most of the body below the head

6 sensation essentially lost below the head

BOWEL AND BLADDER FUNCTIONS

0 normal

1 mild urinary hesitancy, urgency or retention

2 moderate urinary hesitancy, urgency or retention of bowel or bladder, or rare urinary incontinence

3 frequent urinary incontinence

4 in need of almost constant catheterisation

5 loss of bladder function

6 loss of bladder and bowel function

VISUAL (OR OPTIC) FUNCTIONS

0 normal

1 scotoma with visual acuity (corrected) better than 20/30

2 worse eye with scotoma with maximal visual acuity (corrected) of 20/30 to 20/59

3 worse eye with large scotoma, or moderate decrease in fields, but with maximal visual acuity (corrected) of 20/60 to 20/99

4 worse eye with marked decrease of fields and maximal visual acuity (corrected) of 20/100 to 20/200; grade 3 plus maximal acuity of better eye of 20/60 or less

5 worse eye with maximal visual acuity (corrected) less than 20/200; grade 4 plus maximal acuity of better eye of 20/60 or less

6 grade 5 plus maximal visual acuity of better eye of 20/60 or less

CEREBRAL OR MENTAL FUNCTIONS

0 normal

1 mood alteration only

2 mild decrease in mentation

3 moderate decrease in mentation

4 marked decrease in mentation (chronic brain syndrome - moderate)

5 dementia or chronic brain syndrome - severe or incompetent

OTHER FUNCTIONS

0 none

1 any other neurologic findings attributed to MS

Expanded disability status scale (EDSS)

- 0 Normal neurologic exam (all grade 0 in FS; cerebral grade 1 acceptable)
- 1.0 No disability, minimal signs in one FS
- 1.5 No disability, minimal signs in more than one FS
- 2.0 Minimal disability in one FS (one FS grade 2, others 0 or 1)
- 2.5 Minimal disability in two FS (two FS grade 2, others 0 or 1)
- 3.0 Moderate disability in one FS (one FS grade 3, others 0 or 1), or mild disability in three or four FS (three/four FS grade 2, others 0 or 1) though fully ambulatory
- 3.5 Fully ambulatory but with moderate disability in one FS (grade #) and one or two FS grade 2; or two FS grade 3; or five FS grade 2 (others 0 or 1)
- 4.0 Fully ambulatory without aid, self sufficient, up and about some 12 hours a day despite relatively severe disability consisting of one FS grade 4 (others 0 or 1), or combinations of lesser grades exceeding limits of previous steps. Able to walk without aid or rest some 500 meters.
- 4.5 Fully ambulatory without aid, up and about much of the day, able to work a full day, may otherwise have some limitation of full activity or require minimal assistance, characterised by relatively severe disability, usually consisting of one FS grade 4 (others 0 or 1), or combinations of lesser grades exceeding limits of previous steps. Able to walk without aid or rest for some 300 meters.
- 5.0 Ambulatory without aid or rest for some 200 meters; disability severe enough to impair full daily activities (eg to work a full day without special provisions). Usual FS equivalents are one grade 5 alone, others 0 or 1; or combinations of lesser grades usually exceeding specifications for step 4.0.
- 5.5 Ambulatory without aid or rest for about 100 meters; disability severe enough to preclude full daily activities. Usual FS equivalents are one grade 5 alone, others 0 or 1; or combinations of lesser grades usually exceeding specifications for step 4.0.
- 6.0 Intermittent or unilateral constant assistance (cane, crutch or brace) required to walk about 100 meters with or without resting. Usual FS equivalents are combinations with more than two FS grades 3+.
- 6.5 Constant bilateral assistance (canes, crutches or braces) required to walk about 20 meters without resting. Usual FS equivalents are combinations with more than two FS grade 3+.

- 7.0 Unable to walk beyond 5 meters even with aid, essentially restricted to wheelchair; wheels self in standard wheelchair and transfers alone; up and about in wheelchair some 12 hours a day. Usual FS equivalents are combinations with more than one FS grade 4+; very rarely, pyramidal grade 5 alone.
- 7.5 Unable to take more than a few steps; restricted to a wheelchair; may need aid in transfer; wheels self but cannot carry on in standard wheelchair a full day; may require motorised wheelchair. Usual FS equivalents are combinations with more than one FS grade 4+.
- 8.0 Essentially restricted to bed or chair or perambulated in wheelchair; but may be out of bed itself much of the day; retains many self-care functions; generally has effective use of arms. Usual FS equivalents are combinations, generally grade 4+ in several systems.
- 8.5 Essentially restricted to bed much of the day; has some effective use of the arm(s); retains some self-care functions. Usual FS equivalents are combinations, mostly grade 4+ in several systems.
- 9.0 Helpless bed patient; can communicate and eat. Usual FS equivalents are combinations, mostly grade 4+ in several systems.
- 9.5 Totally helpless bed patient; unable to communicate effectively or eat/swallow. Usual FS equivalents are combinations, almost all grade 4+.
- 10 Death due to MS.